GEOTHERMAL GRADIENT AND ITS ROLE ON INDUCED SEISMICITY IN RATON BASIN, COLORADO AND NEW MEXICO

By

Katherine Pfeiffer

B.S., Texas Christian University, 2016

A thesis submitted to the

Faculty of the Graduate School of the

University of Colorado in partial fulfillment

of the requirement for the degree of

Master of Science

Department of Geology

2018

This thesis entitled:

Geothermal Gradient and its role on induced seismicity in Raton Basin, Colorado and New Mexico

Written by Katherine Pfeiffer

has been approved for the Department of Geology

Shemin Ge, Department Chair

Paul Weimer

Anne Sheehan

Date

The final copy of this thesis has been examined by the signatories, and we find that both and content and the form meet acceptable presentation standards of scholarly work in the above mentioned discipline.

ABSTRACT

Pfeiffer, Katherine (M.S., Geological Sciences)

Geothermal Gradient and its role on Induced Seismicity in Raton Basin, Colorado and New Mexico

Thesis directed by Shemin Ge

Raton Basin, in southeastern Colorado and northern New Mexico, is known for coal bed methane (CBM) production. Raton Basin also has been a site of wastewater injection, a byproduct of the CMB production since the 1990s. Raton Basin has experienced an increase in earthquakes since wastewater injection began with over 130 $M \geq 3$ events between 1990 and 2016. Seismicity has been attributed to anthropogenic causes because of a significant increase since 2001 following commencement of wastewater disposal. The largest earthquake is a moment magnitude (M_w) 5.3 in 2011. Peer-reviewed studies have attributed the increase in earthquakes to pore pressure increase due to injection. However, other studies have presented the possibility of a naturally high geothermal gradient to the increase in earthquake activity. The average geothermal gradient is 49 °C/km and may also be the cause of seismicity in the Basin. The goal of this study was to assess if there is a spatial relationship between wastewater injection wells, seismicity, and the geothermal gradient. Cool wastewater has the ability to change the stress of the warmer rocks in the subsurface, thus leading to failure.

I hypothesized that injection wells in areas with a higher geothermal gradient would have a stronger correlation with earthquakes. Results of coupled fluid and heat transport modeling do not show a clear correlation between the role of the geothermal gradient in induced seismicity from wastewater injection. Modeling results show a temperature change of a few degrees °C at an observation point 100 m away from the disposal wells. This temperature change is at the same depth of disposal. The modeling results indicate most fluid moves laterally and thus the temperature decrease does not reach the depths at which earthquakes are occurring.

ACKNOWLEDGMENTS

Thank you to my family, friends, and mentors throughout graduate school for their constant support. Thank you to my committee for your time and advice: Shemin Ge, Anne Sheehan, and Paul Weimer. A special thanks to Shemin Ge for her patience and guidance throughout my thesis - this thesis would not have been possible without your mentorship. Thank you for helping me with modeling issues, taking time to discuss my research, and editing my work. Anne and Paul, thank you for teaching engaging classes that challenged me and made me a better geoscientist. Becky Simon and Megan Brown were a large part of my thesis development. Thank you for always being available to discuss my thesis and for endless coffee runs that got us out of the office. Thank you to all the other graduate students at CU Boulder for making my time here unforgettable. My family provided unwavering support throughout my thesis. Thank you to my mom for the hours of editing you put towards this thesis. I appreciate your love and encouragement. Thank you to my dad and sisters for taking many stressed out phone calls over the past few years. Thank you to Hal Macartney and Paul Morgan for providing data on both bottom hole temperatures and wastewater disposal temperatures – both of which were imperative to my modeling. Lastly, thank you to the University of Colorado Department of Geological Sciences for funding my Master's and facilitating a community of support.

Table of Contents

LIST OF FIGURES

LIST OF TABLES

1. INTRODUCTION

Induced seismicity has been gaining notoriety throughout the United States during the past few decades due to the sharp increase in the number of midcontinent earthquakes. In fact, during the past decade there has been a six-fold increase in earthquakes in this region [*Zhang et al.*, 2013]. Since the 1920s, pumping fluids in and out of the subsurface has been recognized to potentially cause earthquakes [*Hubbert and Rubey*, 1959, *Folger and Tiemann*, 2015, *Foulger et al.*, 2017]. Colorado, as well as Texas and Oklahoma, are at the forefront of this issue as they are actively producing a large amount of oil and gas, which requires disposal of large amounts of wastewater from hydraulic fracturing. Disposal has statistically correlated to increases in seismicity [*Folger and Tiemann*, 2015, *Foulger et al.*, 2017]. The prominent increase in the number of earthquakes in these regions has been attributed to the disposal of wastewater. Wastewater - water that is unsuitable for agricultural or drinking water use - is a byproduct of natural gas and oil extraction [*Rubinstein and Mahani*, 2015]. One way to dispose of this produced wastewater is to inject it back into deep formations in the subsurface.

Studies have shown that pore pressure may increase with the injection of these fluids [*Rubinstein et al.*, 2014, *Weingarten et al.*, 2015, *Nakai et al.,* 2017]. The migration of pore pressure increase to faults has allowed for seismicity. In the fault zone, the effective stress and the frictional resistance may be lowered, allowing faults to slip [*Hubbert and Rubey*, 1959; *Rubinstein et al.*, 2014]. The shock wave produced from fault slippage has the potential to reach the surface and cause damage to infrastructure if sufficiently large [*Folger and Tiemann*, 2015]. However, there is an ongoing debate in some regions as to the cause of the seismicity, with experts pointing to other potential causes. Raton Basin, in southern Colorado, is an example of such an area (Figure 1). The most widely expressed alternative to injection-induced seismicity is the depth at the occurrence of the earthquakes relative to the injection depth. Specifically, a majority of the earthquake locations in the Raton Basin are traced to the crystalline basement rock, with locations ranging from 0.5 to 7 km below the injection well depths (Figure 2) [*Weingarten et al.*, 2015]. In addition, Raton Basin is being explored as a potential geothermal resource because of its high temperature gradient [*Macartney and Morgan*, 2011]. Elevated temperatures in the subsurface can change fluid properties such as viscosity and hydraulic conductivity and allow them to migrate more easily [*De Simone et al.,* 2013]. We explore whether the link to seismicity could be due to the ease at which the pore pressure is able to migrate to faults and result in fault slippage as well as thermal contrast that results in thermo-elastic effects.

For this study, temperature and fluid flow were modeled in Raton Basin to see if there is a spatial relationship between injection wells, seismicity, and geothermal activity as well as to further understand the physics of induced seismicity.

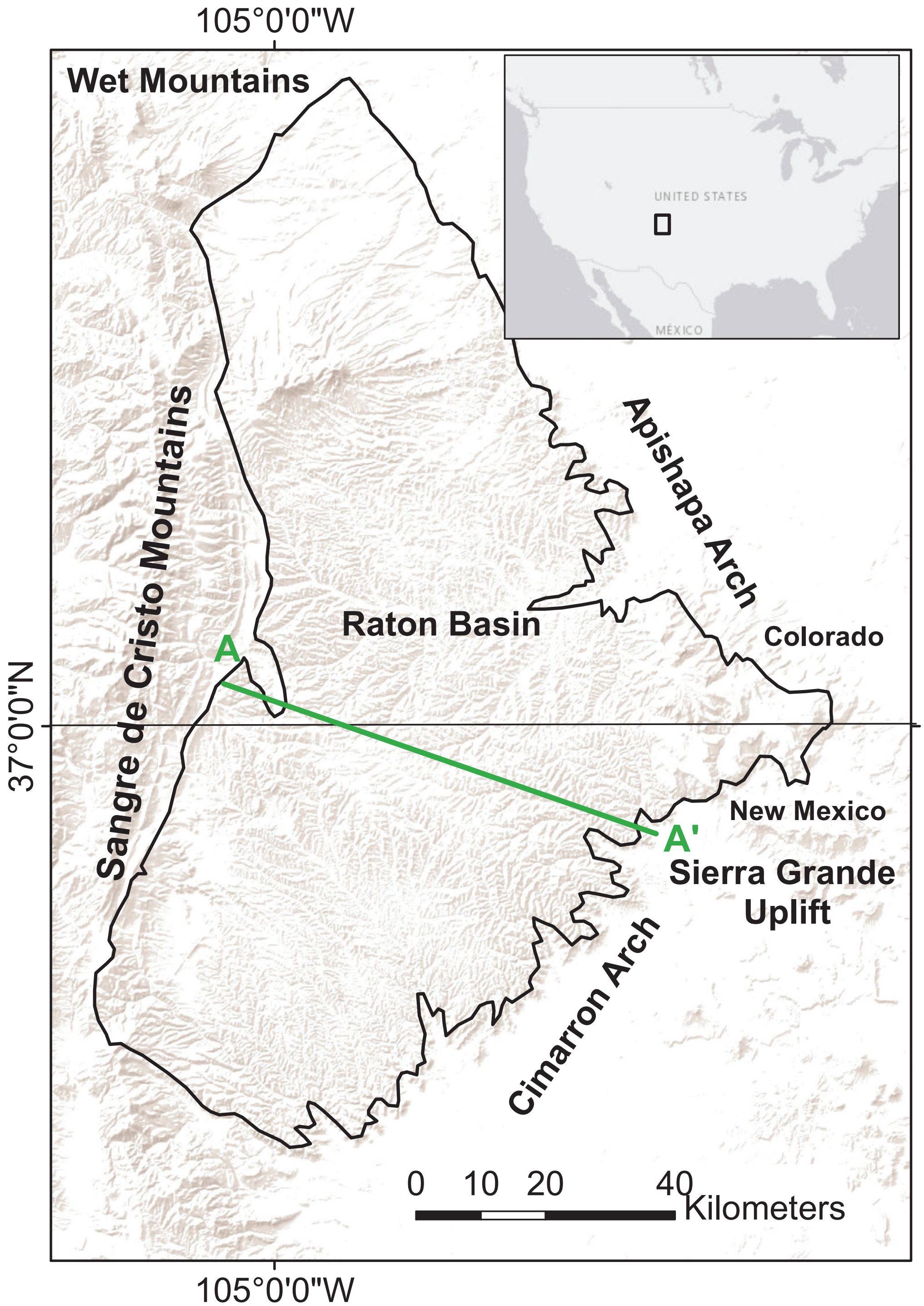

Figure 1. Outline of Raton Basin with structural features. A to A' shows the cross section line that is represented in Figure 6.

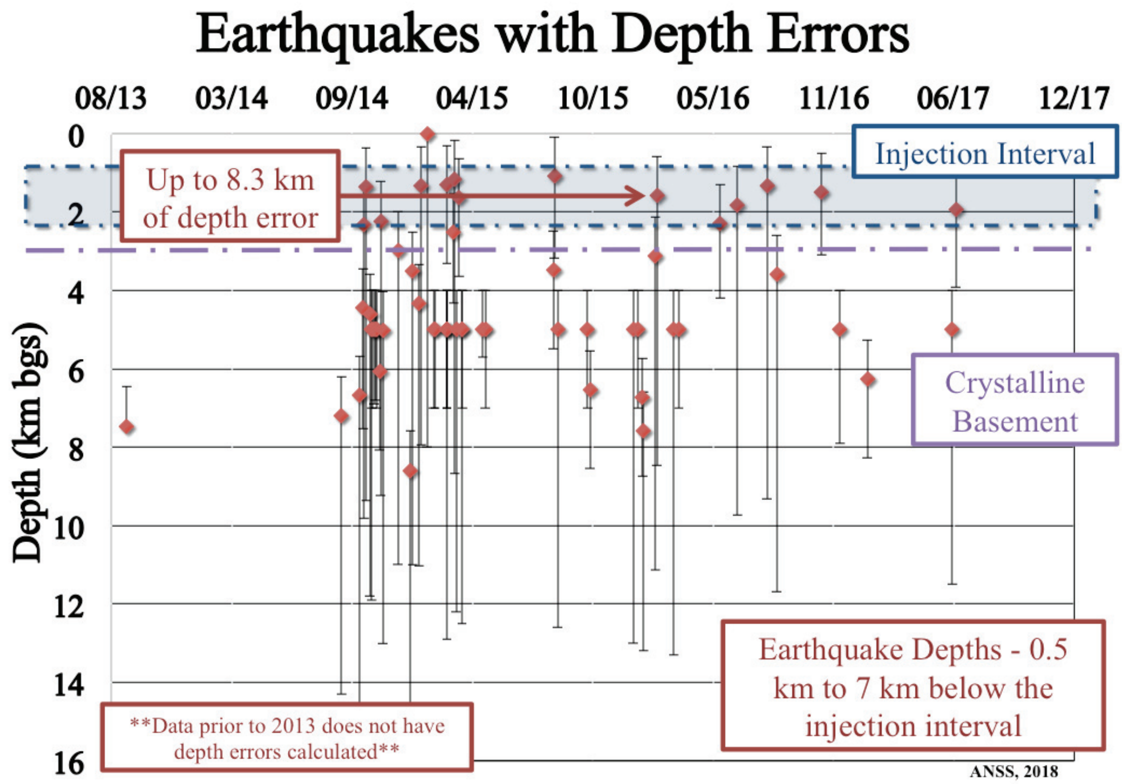

Figure 2. Epicenter depths for Earthquakes in Raton Basin from 2013 – 2017. Error bars represent the vertical depth error for epicenters in the USGS Catalog. The injection interval is shown in blue. The start of the crystalline basement is shown in purple [ANSS, 2018].

2. BACKGROUND

2.1 Study Site

Raton Basin is an asymmetrical synclinal basin (Figure 1 and 5). The Basin is approximately delineated by the outcrop of the Cretaceous Trinidad Formation and is estimated to be approximately 2,200 mi^2 (5,698 km^2) (Table 1). Originally explored by Stephen Long in his Great Plains Expedition, the Basin was later commercially mined for coal from 1870 to 2002 [*Osterhourt et al.*, 2015]. As a result of a change in mining practices in the 1970's, implemented by the U.S. Bureau of Mines, coal bed methane (CBM) became more popular. This change involved extracting the methane before mining coal to improve mine safety. Since the early 1990s, companies produce CBM from the Upper Cretaceous aged formations (Table 1). A byproduct of this CBM production is wastewater due to the dewatering procedure. Methane is adsorbed into the coal macerals so the coal seam has to be depressurized to be produced. Macerals are organic components of coal. As you pump water from the well you decrease the pressure which allows methane to desorb from the coal and flow as gas state to the surface [*Weingarten*, 2015]. Wastewater injection began in 1994 on the Colorado side of Raton Basin and 1999 on the New Mexico side, while potential injection driven seismicity began in 2001 [*Weingarten*, 2015]. Few seismic events were present in the Basin prior to 2001 [ANSS, 2016]. Wastewater in Raton is injected primarily into the Dakota Formation, a 68-m thick sandstone that lies approximately 1,500 m below the surface (Table 1) [*Geldon,* 1989, *COGCC*, 2016, *Weingarten*, 2015].

2.2 Geology

For this study, the boundary of Raton Basin, as defined by the outcrop of the Trinidad Formation, is approximately 130 km long north - south and 60 km wide east - west. The Basin is an asymmetrical syncline with steeply dipping beds along its western limb and much shallower dips along the eastern limb adjacent to the Great Plains region [*Baltz*, 1965; *Topper*, 2011] (Figure 5). Elevations range from 4,000 ft (1,219 m) in the east to 11,000 ft (3,352 m) in the west. Laramide faulting and thrusting during the Paleocene, approximately 70 - 55 my ago, resulted in uplift of the western beds to their current position. The Basin is bounded to the west by the Sangre de Cristo Mountains (Figure 1) and the western edge is heavily deformed by thrust faults and several major folds (Figure 3) [*Baltz,* 1965]. As a result, Precambrian crystalline rocks are juxtaposed against Lower Permian sedimentary rocks [*Nelson et al.*, 2013; *Baltz,* 1965]. The north plunging axis, the La Veta syncline, runs parallel to the Sangre de Cristo (Figure 3) [*Baltz,* 1965]. The southern extension of the Wet Mountains is the northern boundary of the Basin

(Figure 1). To the north, the north-south trending Wet Mountains split into two different branches, the Apishapa and Greenhorn (Figure 3). The northern extension plunges east and southeast, known as the Apishapa Uplift and the Apishapa Arch forms the northeast boundary of Raton Basin. The southern spur, known as the Greenhorn Nose, plunges south into the Basin (Figure 3). Raton Basin is separated to the south from the Las Vegas sub-basin by an interbasinal arch, known as the Cimarron Arch. The Las Animas Uplift forms the eastern extent of Raton Basin. The Sierra Grande Uplift in northeastern New Mexico also bounds Raton Basin to the east, and is known as the Sierra Grande Arch [*Baltz,* 1965].

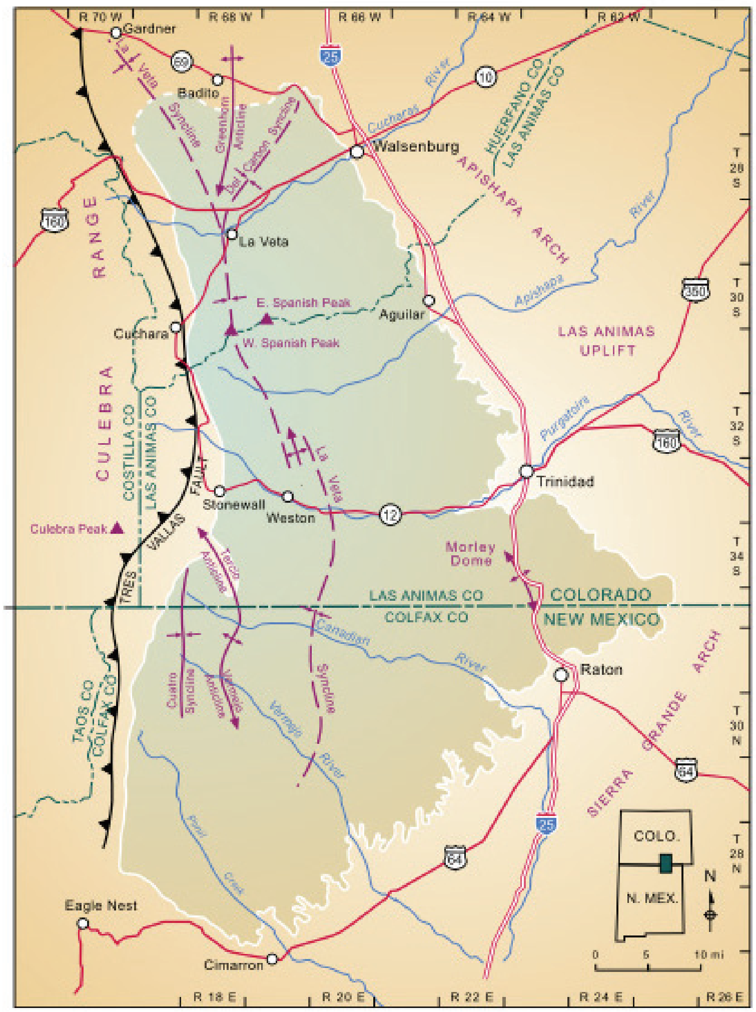

Figure 3. Raton Basin with structural components, rivers, and county lines [Topper, 2011].

The tectonic history of Raton Basin can be divided into four different events [*Bohlen*, 2012]. Uplift of Raton's crystalline basement rocks occurred in the PreCambrian Era. The formation of the Ancestral Rocky Mountains during the Pennsylvanian and Permian resulted in widespread uplift and tilted block faulting in Colorado. The formation of the Ancestral Rocky Mountains in the early Pennsylvanian originally formed Raton Basin [*Bohlen,* 2012]. The present - day configuration of Raton Basin was formed during the third phase of tectonic activity, the Laramide Orogeny, during the late Cretaceous through the Early Eocene.

The San Juan Mountains, located to the 230 miles west of Raton Basin, formed during the volcanic period from the Oligocene to Miocene [*Bohlen*, 2012]. This volcanic activity shaped the present day landscape. There were up to 18 late Tertiary magmatic events. Later east – west extensional tectonic activity formed the Rio Grande Rift [*Carlton*, 2006]. Post Laramide uplift and dike eruptions led to the creation of the nearby Spanish Peaks (Figure 5) [*Bohlen*, 2012]. The Spanish Peaks, located in Huerfano County, Colorado, reach heights up to 13,000 ft (3,962 m) and were intruded 22 Ma (Figure 3) [*Abbott et al.,* 1983]. Radial dikes extend from the Spanish Peaks throughout northern Raton and form wall – like features due to differential erosion [*Geldon*, 1989]. In addition, other Tertiary – aged intrusions have formed dikes in the northern portion of the Basin while sills are prominent in the southern and central regions. The dates for these intrusions range from approximately 32 to 25 Ma (Oligocene to Miocene). During the Miocene to Pleistocene, basin and range block faulting depressed the San Luis Mountains and Rio Grande Valleys [*Gabelman,* 2005]. The boundaries of Raton Basin, specifically, the Wet Mountains, Apishapa Arch, and Las Animas and Sierra Grande Uplifts were formed during the Tertiary [*Baltz*, 1965]. Uplift and erosion of the Sangre de Cristo Mountains continued during the Pliocene, which led to a number of formations being deposited in the Basin.

The heat flow anomaly in Colorado is the result of intrusive igneous activity and is the second most areally extensive heat flow anomaly in the U.S. (Figure 4) [*Sares et al.*, 2009]. Heat flow at the edge of the Basin is approximately 100 mW/m^2 while at the center of the Basin it is 200 mW/m^2 [*Viegas et al.*, 2012]. The mean heat flow is estimated to be between 115 and 165 mW/m^2, which is significantly higher than the High Plains average of 60 – 80 mW/m^2 [*Morgan*, 2009].

The oldest sedimentary rocks present in the area range in age from the Mississippian to Permian [*Osterhourt et al.*, 2015]. The Pennsylvanian to Early Permian was marked by sediment fill from uplift of the San Luis Valley, which lies to the West of Raton Basin. These sediments are known as the Sangre de Cristo Formation. Table 1 shows a stratigraphic column of Raton Basin. The Sangre de Cristo Formation (PRsc) sits above the crystalline basement and is a 1,000 m thick sandstone unit (Figure 5, 6). The Triassic – Permian unit, known as the Dockum Group, is 125 m thick and consists of sandstones and shales. The Triassic Period was tectonically quiet in the region, resulting in the deposition of shallow marine and terrestrial sediment [*Osterhourt et al.*, 2014]. The Jurassic aged Morrison (Jmra) and Entrada (Je) Formations are shale, limestone, and sandstone units that are approximately 150 m thick in total. During the Late Cretaceous to Paleocene, the Sevier and Laramide Orogenies contributed to the accumulation of sediment in the Basin, known as the Dakota and Purgatoire Formations [*Osterhourt et al.*, 2014]. The Dakota (Kd) and Purgatoire (Kp) are the main targets for injection due to their permeable sandstone lithology and greater depth. Most injection wells target the Dakota Formation to dispose wastewater, but the Purgatoire, Morrison, Entrada and Dockum formations are also included in the screened injection well interval.

Era	Period	Formation (Members)	Lithology	Average Thickness (m)	Hydrologic Unit (modeled thickness - m)
Cenozoic	Tertiary	Poison Canyon	Sandstone, Conglomerate, Shale	381	Not Modeled
Mesozoic	Upper Cretaceous	Raton	Shale, Siltstone, Sandstone, Coal	304	Not Modeled
		Vermejo	Shale, Siltstone, Sandstone, Coal	49	Not Modeled
		Trinidad	Sandstone, Shale	40	Not Modeled
	Mid Cretaceous	Pierre Shale	Shale	600	1 (600 m)
		Niobrara (Smokey Hills and Fort Hays)	Limestone, Chalk, Sandy Shale	300	2 (300 m)
	Early Cretaceous	Benton (Carlile Shale, Codell, Greenhorn, and Graneros)	Sandstone, Limestone, Shale	100	3 (100 m)
		Dakota	Sandstone	70	4 (1,300 m)
		Purgatoire	Sandstone, Shale	30	4
	Jurassic	Morrison	Shale, Limestone, Sandstone	109	4
		Entrada	Sandstone	36	4
	Triassic-Permian	Dockum	Sandstone, Shale	125	4
Palaeozoic	Permian-Pennsylvanian	Sangre de Cristo	Sandstone	1000	5 (1,000 m)
	Precambrian	Crystalline Basement	Gneiss, Schist, Granite		6 (1,700 m)

Table 1. Stratigraphic column in Raton Basin. Coal bed methane production occurs in the Trinidad, Raton, and Vermejo Formations (shown by red box). Disposal of wastewater occurs in the Dakota, Purgatoire, Morrison, Entrada, and Dockum Formations (shown by orange box). [*Geldon,* 1989; *Bohlen*, 2012; *Osterhourt et al.*, 2015; *Weingarten*, 2015]

The retreating Western Interior Seaway during the Cretaceous also created the environments in which the Benton through Raton Formations were deposited [*Baltz*, 1965]. The Benton (Kb) is Early Cretaceous in age and sits above the Dakota Sandstone (Kd). It is composed of relatively thin sandstone, limestone, and shale [*Geldon*, 1989]. Average thickness of Benton Formation in Raton Basin is 100 m [*Weingarten*, 2015]. The Niobrara (Kn) is a 300 m thick limestone, chalk, and sandy shale unit [*Geldon*, 1989; *Weingarten*, 2015]. The Mid – Cretaceous aged Pierre Shale and Niobrara Formations are found extensively throughout Colorado. The Pierre Shale (Kpn) is a shale unit that is 600 m thick in Raton Basin [*Weingarten*, 2015].

The 40 m thick Trinidad Formation (Kt) is composed of sandstone deposits from regressive beach and shelf deposits [*Billingsley*, 1997]. The Vermejo (Kv) and Raton (TKr) formations produce 98% of the CBM for Raton Basin [*Osterhourt et al.*, 2014]. These Upper Cretaceous aged units are composed of shale, siltstone, sandstone, and coal. The overlying Raton Formation is thicker with an average thickness of 300 m while the underlying Vermejo Formation is approximately 50 m thick [*Geldon*, 1989].

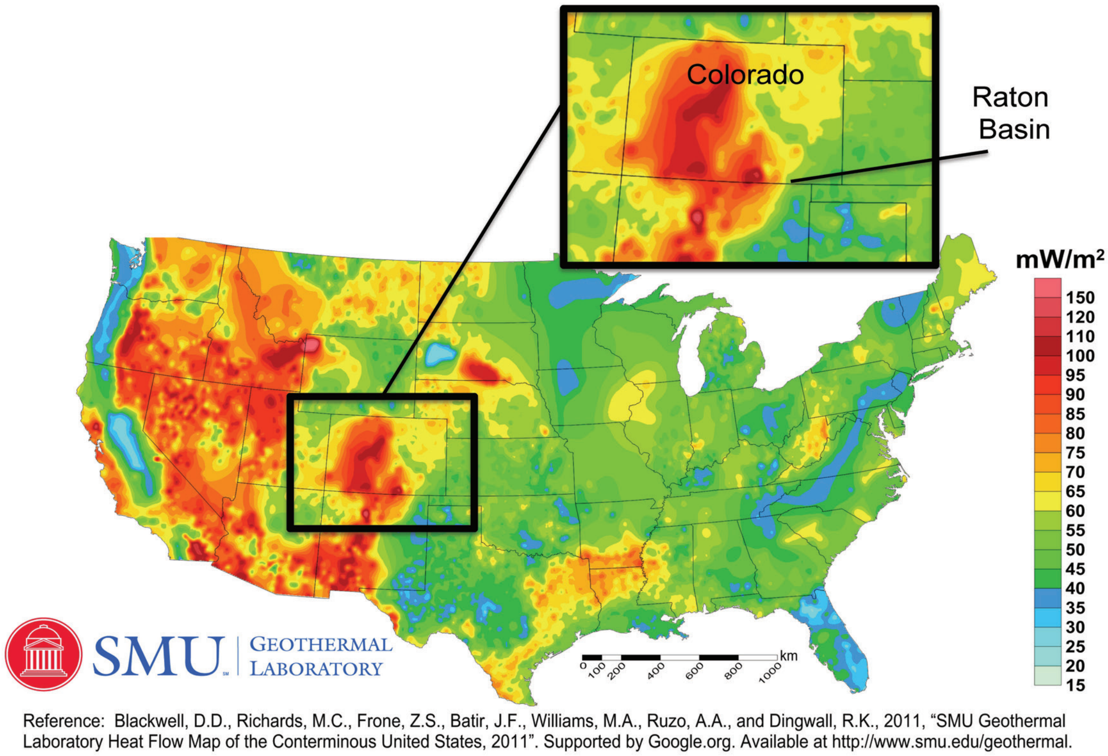

Figure 4. Heat flow map of the United States. Colorado is shown with a zoomed in view with the black box [Blackwell, 2011]

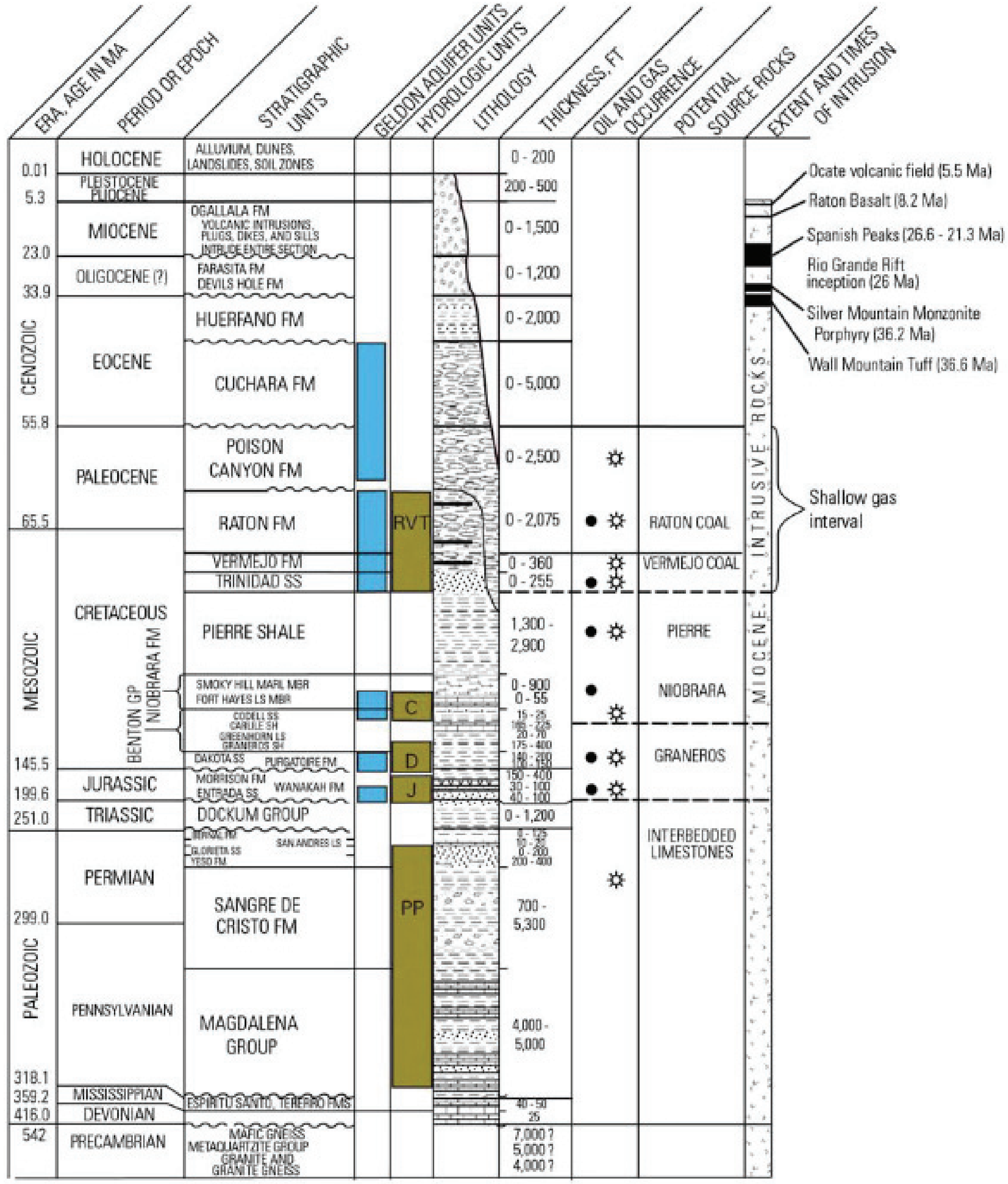

Figure 5. Stratigraphic Column, Petroleum Systems, and Intrusions [Higley, 2005].

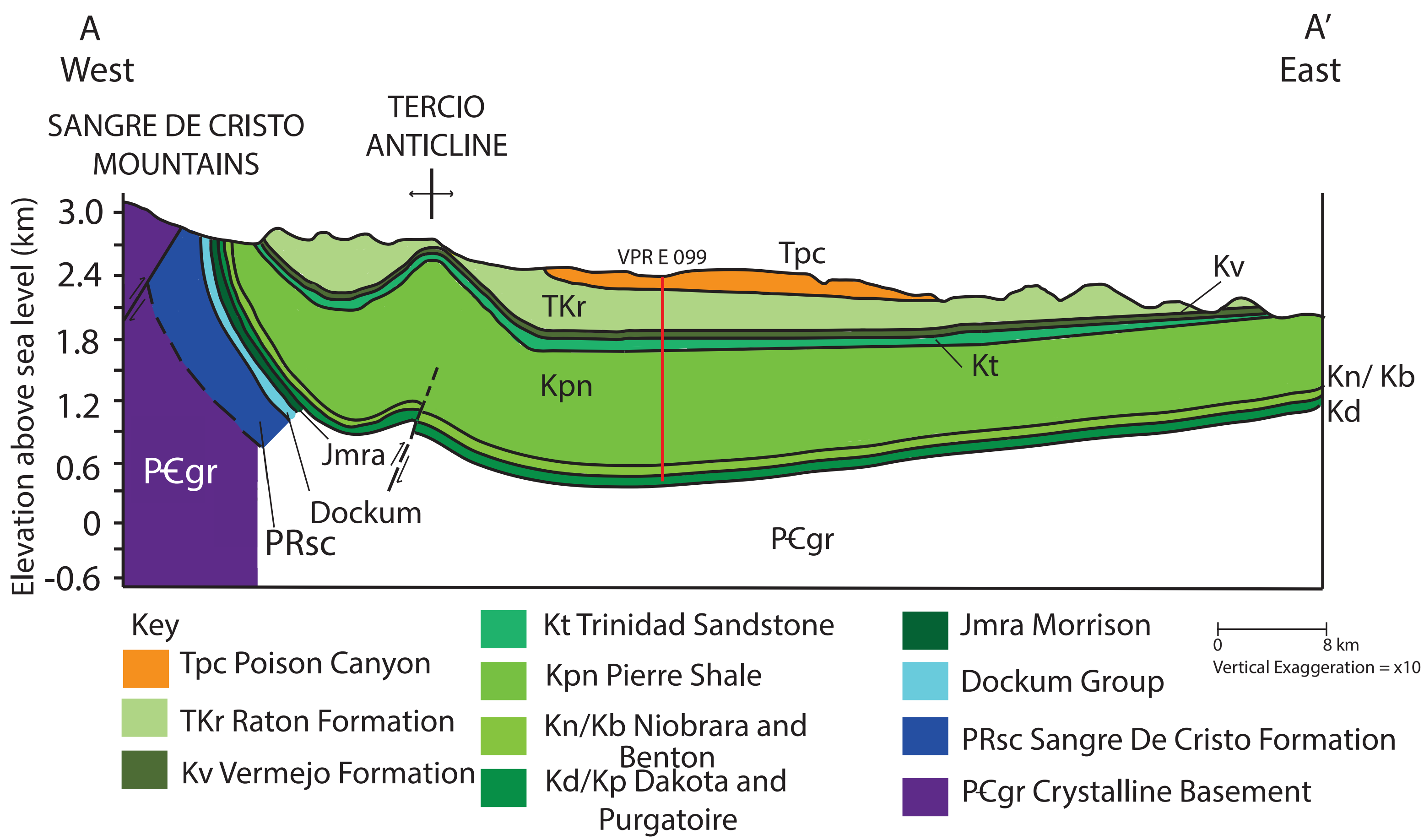

Figure 6. Cross section of Raton Basin. A majority of injection occurs in the Kd (Dakota Sandstone) with seismicity occurring at depths from 3 – 5 km below ground surface in the crystalline basement. VPR E 099 is an injection well in the basin and is shown injecting into the Dakota. Modified from Stevens et al., 1992

2.3 Hydrogeology

Groundwater recharge to bedrock aquifers in the Raton Basin occurs due to precipitation in the upland areas to the west and seepage from alluvium in stream valleys [*Geldon*, 1989]. The Purgatoire and Apishapa Rivers are the primary rivers and both are tributaries of the Arkansas River (Figure 3) [*Geldon*, 1989]. Approximately 90% of the CBM production in Raton Basin is within the Purgatoire River watershed located in Las Animas County, Colorado (Figure 3) [*Topper*, 2011].

The groundwater of the central Raton Basin moves regionally from west to east with local flow being intercepted by stream divides to local valleys (Figure 7) [*Geldon*, 1989]. Therefore, subsurface flow is north and south inward towards the Purgatoire River drainage. Groundwater flows down dip in the western side of the basin, and up dip in the east, following the synclinal structure of the basin. The movement of groundwater plays a role in the distribution of Raton's geothermal gradient. The average geothermal gradient in Raton Basin is 49 ± 12 °C/km [*Morgan and Witcher*, 2011]. The highest geothermal gradients are located on the east - central side of the Basin beneath the Purgatoire River drainage (Figure 8). There is a negative correlation between the geothermal gradient and elevation (depth below ground surface (bgs)), which is interpreted as groundwater flow down dip in the west and up dip in the east (Figure 9). This groundwater movement results in thermal convection, which explains the lateral distribution of the geothermal gradient in Raton Basin. This pattern is seen in wells deeper than 1,150 m as well as shallower. Heat transport by groundwater convection extends to depths of at least 2 km in Raton Basin [*Morgan*, 2009].

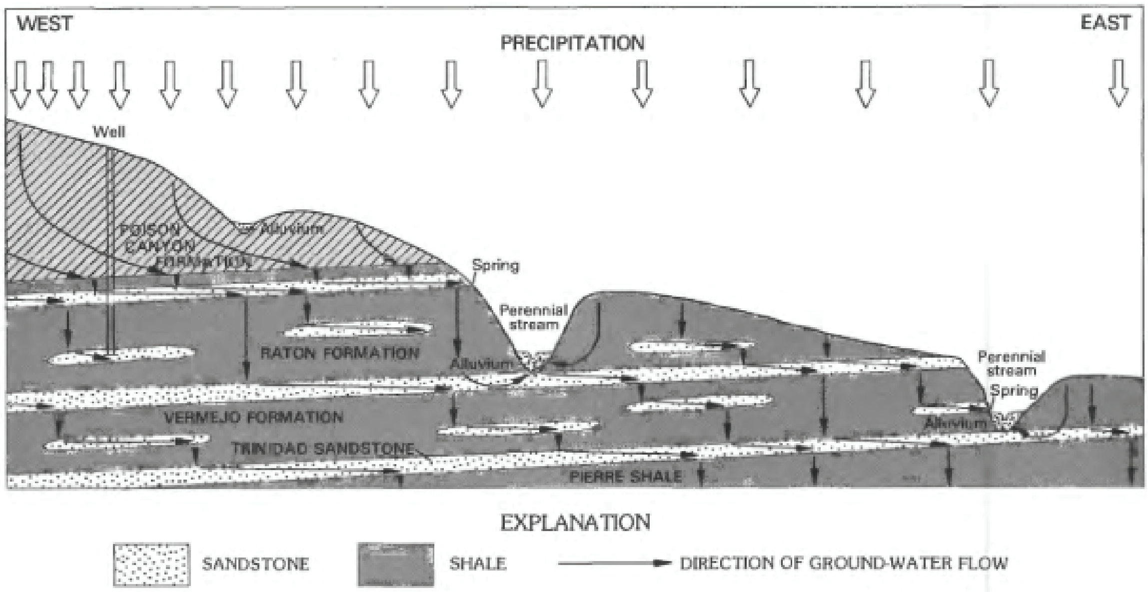

Figure 7. Groundwater flow from west to east in Raton Basin [Geldon, 1989].

There is a projected temperature of 149 °C at 2,438.4 m (300°F at a depth of 8,000 ft) over 960 km^2 (350 mi^2) in Raton Basin. It is worth noting that there is a negative correlation between geothermal gradient and elevation in Raton Basin, which means the deepest part of the Basin, to the West, has a lower geothermal gradient then the eastern part of Raton Basin [*Morgan*, 2009] (Figure 6). This has been attributed to thermal convection from groundwater. Heat transport by groundwater convection extends to depths of at least 609 ft (2,000 m) [*Morgan*, 2009].

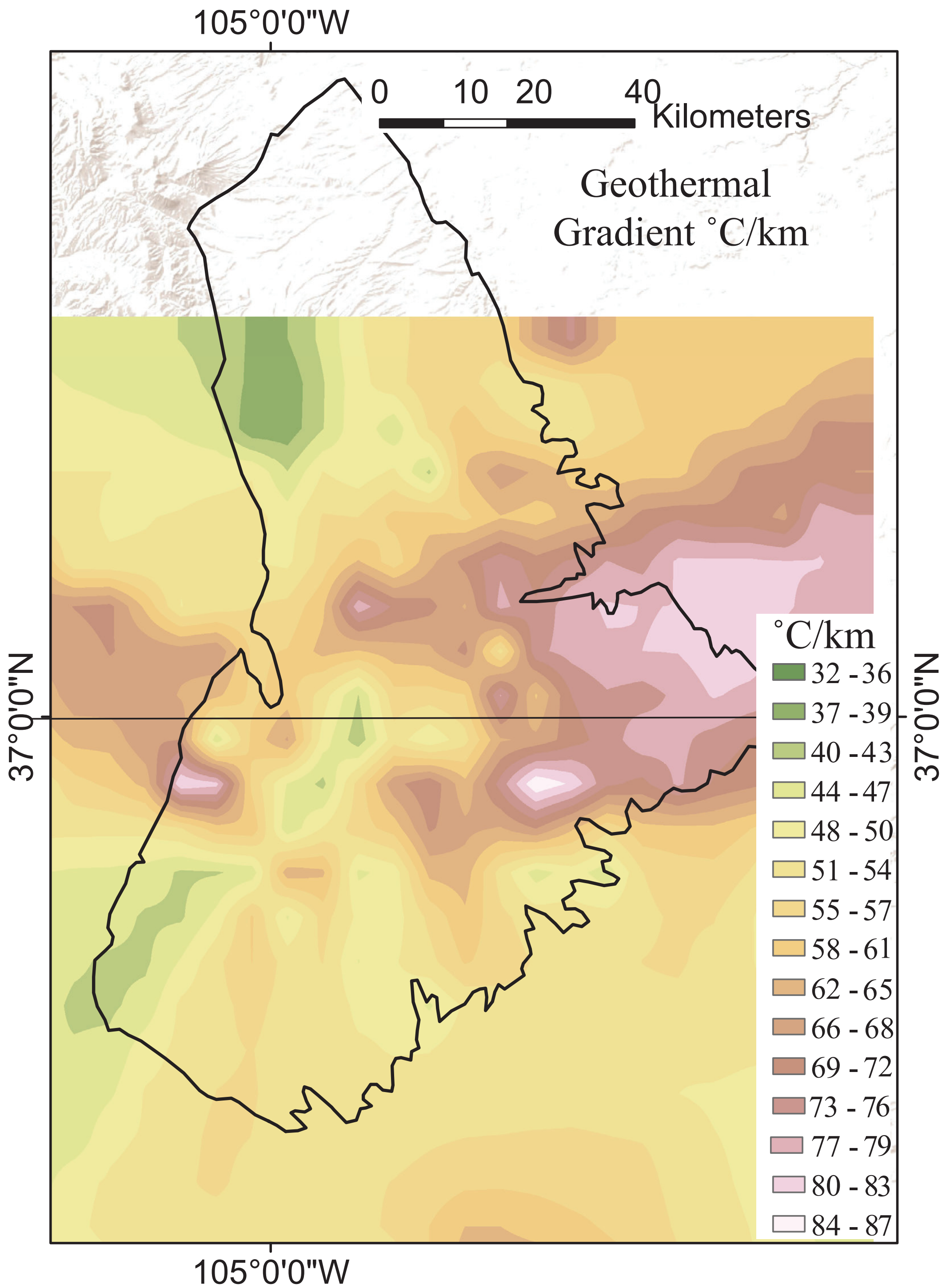

Figure 8. Geothermal Gradient of Raton Basin from BHT measurements [COGCC, 2016, *Kelley*, 2015 and *Kelley*, 2011, National Geothermal Data System, 2017, and *Morgan*, personal comm.].

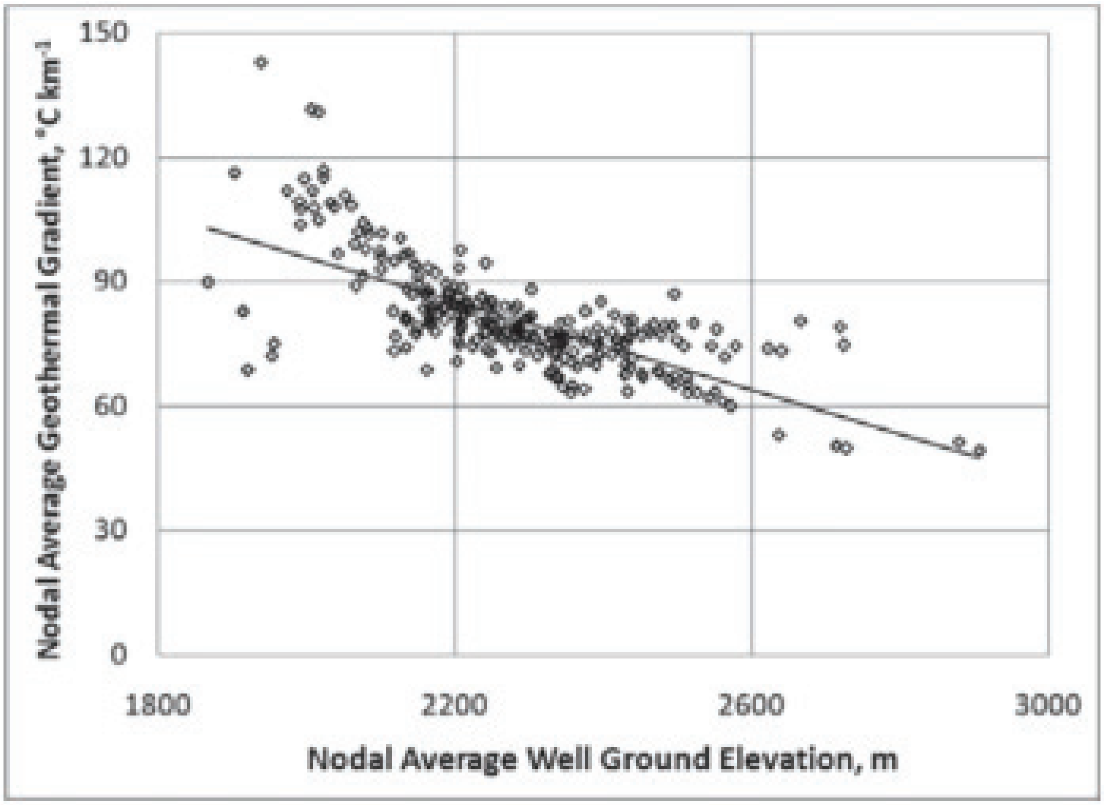

Figure 9. Geothermal Gradient vs. Elevation in Raton Basin. There is a negative correlation between elevation and geothermal gradient, meaning higher elevations have lower geothermal gradients [*Morgan*, 2011].

The Raton Basin, like many other basins in the area such as the San Luis and Denver Julesburg Basin, is hydrostatically underpressured as discovered by drill- stem tests conducted from 1956 – 1982 [*Belitz and Bredehoeft*, 1988; *Nelson et al.*, 2013]. Underpressured reservoirs have pressures well below normal values of hydrostatic and lithostatic pressures. The underpressure in Raton Basin is thought to be caused by uplift, erosion, and equilibration of fluid pressure to atmospheric pressure where the formations crop out [*Nelson et al.*, 2013]. Underpressure developed as strata were exposed to Earth's surface by uplift and erosion. Strata allowed for equilibrium of pore pressure in the formation with atmospheric pressure. Low permeability Pierre Shale, Niobrara, and Benton formations and limited up-gradient outcrops and faults in the subsurface restrict recharge. Most induced seismicity across the country has been attributed to change in pore pressures due to disposal [*Rubinstein et al*., 2015]. However, because Raton Basin is hydrostatically underpressured, wastewater is gravity fed into the disposal wells, meaning that fluid is drained down the well without any added pressure [*Barnhart et al.*, 2014]. Of the 21 wells on the Colorado side, 5 have been injected under pressure at one point in time (Table 2) [*Rubinstein et al.,* 2014].

2.4 Coal-bed methane

The coal industry was prominent in the region until 2002 when it was no longer economically viable to mine [*Hoffman and Brister*, 2003]. Raton Basin was divided into two major coalfields, the Trinidad Coal Field and Walsenburg Coal Field named after their respective towns [*Tremain*, 1980]. The local Spanish Peaks igneous complex and associated intrusions contributed to the elevated coal rank in the area as high heat flow elevated the geothermal gradient (49± 12 °C/km) [*Carlton*, 2006; *Morgan and Witcher*, 2011]. The natural gas from the coal beds is thermogenic in origin, meaning it contains a higher percentage of non-methane hydrocarbon at higher pressure, temperature, and greater depth [*Baltz*, 1965]. Methane gas is generated from thermal alteration or maturation of the interbedded coals and carbonaceous shale in the area [*Dolly and Meissner*, 1977].

The extraction of methane occurs after water is pumped out of coal seams to lower the water pressure, which in turn allows the methane to desorb, i.e. be released from the coal seam. The methane then coalesces and bubbles into the pumped water [*Weingarten*, 2015]. The Raton and Vermejo formations produce 98% of the CBM in Raton Basin [*Osterhourt et al.*, 2015] (Table 1). Most the production takes place in Las Animas County, CO with a total number of 2,771 producing wells (Figure 3). The total number of producing CBM wells in Raton Basin is approximately 3,500 [*COGCC*, 2016].

2.5 Wastewater Disposal

Wastewater is a byproduct of natural gas, oil, and CBM production. The formation brine, also known as produced water or wastewater, is ancient groundwater that has been trapped in the same pore spaces as hydrocarbons [*Rubinstein and Mahani*, 2015]. This salty water is produced during oil and gas extraction. Formation water typically contains dissolved minerals or other materials that make it unsuited for agricultural or human uses [*Rubinstein and Mahani*, 2015].

Wastewater injection typically takes place in high-permeability formations that are deeper than the producing formations, which is the case in the Raton Basin as the Dakota Formation is located deeper than the CBM producing formations (Table 1). The wastewater injection is typically isolated from the fluid from both drinking-water aquifers and oil and gas producing reservoirs [*Rubinstein and Mahani*, 2015].

Wastewater injection wells are known as Class II wells, as defined in the Underground Injection Control Program (UIC) in association with the Safe Drinking Water Act [*EPA*, 2018]. Class II injection well depths in Raton Basin range from 1,250 m to 2,100 m [*COGCC*, 2016 - Appendix]. Most wells target the Dakota Formation, but the underlying Purgatoire, Morrison, Entrada and Dockum Formations are also included in the injection interval [*COGCC*, 2016 - Table 1 and Figure 6]. Wastewater disposal began in 1994 in the Colorado portion of the Basin and expanded into New Mexico in 1999 (Table 2). Disposal volume began to increase significantly in 2001. There were ten disposal wells in 2001, which increased to 21 in 2002 [*Viegas et al.*, 2012]. As of December 2016, there are 28 active disposal wells and more than 3,000 CBM producing wells [*COGCC*, 2016; NMOCD, 2016]. Of the 28 disposal wells, 22 are located within the Purgatoire River field in Las Animas County, CO and the other six are in the Raton Coal Field in Colfax County, NM (Figure 3). It is worth noting that the disposal well information for the New Mexico portion of the Basin is unavailable prior to June 2006. Six wells have injected waster as opposed to gravity disposal from 1999 – 2016 (Table 2).

Table 2. Raton Basin Salt Water Disposal Well Information, New Mexico and Colorado. Wells that have injected under pressure at one time are shown by *. Wells are that outside of the basin outline are marked with ~ .

Well Name	Disposal Start Date	Years Active	Average Disposal Rate (bbl/month)	Maximum Disposal Rate (bbl/month)	Cumulative Disposal Volume (barrels)
Jarosa 32-33 WD	May-07	2007-2016	149,187	334,640	17,305,692
SouthPaw	Apr-09	2009-2016	124,516	282,880	12,451,600
Cottontail Pass Disposal 32-33	Nov-94	1999-2016	76,945	448,374	16,543,178
Cimarron 32-18 WD	Jan-01	2005-2016	29,910	157,207	4,247,178
Ferminia	Sep-07	2007-2016	65,894	146,789	7,380,101
Sawtooth	4/1/00	2000-2016	45,942	131,967	9,234,370
La Garita	Aug-01	2001-2016	29,648	203,122	548,914
San Pablo 11-4 WD	Dec-14	2014-2016	138,232	249,592	4,976,383
Weston 24-23 A WD	Jan-04	2004-2016	93,723	211,903	14,620,852
Long Canyon 43-12 WD	Apr-01	2004-2016	81,908	166,039	15,480,652
Apache Canyon 19-10*	Jan-95	1999-2016	46,012	265,405	9,892,512
Apache Canyon 10-3*	Jan-95	1999-2016	14,960	69,382	3,231,394
VPR C 204 WDW	Mar-12	2012-2016	145,839	230,500	6,854,448
Garcia (EPA) 1-WD ~	Jan-99	1999-2016	1,240	4,800	262,948
PCW	Jul-97	1999-2016	115,823	327,572	25,017,857
Wild Boar	Aug-00	1999-2016	118,928	491,058	23,428,799
Hill Ranch Deep	Jul-05	2005-2016	17,090	67,081	2,358,403
Beardon	Jan-01	2001-2016	67,316	593,835	12,386,139
Polly	Jul-09	2009-2015	4,014	74,285	389,438
Del Agua	Jul-05	2005-2012	107,767	196,239	9,160,226
Lopez Canyon SWD*	Sep-10	2010-2016	6,236	33,871	461,434
VPR A 007	Jun-06	2006-2016	82,195	237,672	10,438,782
VPR C 39	May-00	2000-2016	115,757	356,826	21,993,787
VPR C 14*	Sep-99	1999-2002	84,416	378,554	17,474,060
VPR A 182*	Jun-06	2006-2016	324,903	485,190	41,262,655
VPR A 500	Jun-08	2006-2016	125,620	228,404	12,938,869
VPR B 027	Jun-06	2006-2016	63,260	115,768	8,033,957
VPR D 025	Jun-06	2006-2016	181,534	714,590	23,054,880
VPR A 042	Jun-06	2006-2016	126,944	387,704	16,121,901
VPR E 099*	Jun-06	2006-2016	258,602	367,588	32,842,506

2.6 Seismicity

Induced seismicity has been a focus of scientific research for the past few decades [*Ellsworth,* 2013; *Rubinstein and Mahani*, 2015]. At least 50% of the 4.5 magnitude (M) or larger earthquakes in the interior of the U.S. during the past decade are in areas with injection induced seismicity [*van der Elst et al.*, 2013]. There are a number of ways in which fluid injection can cause earthquakes. The most widely researched includes the increase of pore-fluid pressure along a fault, which lowers the effective stress resulting in fault failure. The Mohr – circle can be used to explain the reduced angle of internal friction [Figure 10 – *Brown*, 2018, *Rubinstein and Mahani*, 2015]. Deformation may occur when fluids are compressed within pore spaces resulting in poro-elastic effects [*Rubinstein and Mahani*, 2015; *Foulger et al.*, 2017]. Poroelasticity deals with the interaction of fluid flow and solids deformation within a porous medium. An external load affects the volume fraction of pores. Fluid-filled pores experience an increase in pressure due to this mechanical stress of pumping in wastewater. This leads to fluid migration. The pore volume is changed which shifts the solid material and causes deformation [Comsol, 2017]. Thermoelastic deformation, specifically compressions, may result when cool fluid is injected into a much warmer rock [*De Simone et al.*, 2013; *Gaucher et al.*, 2015].

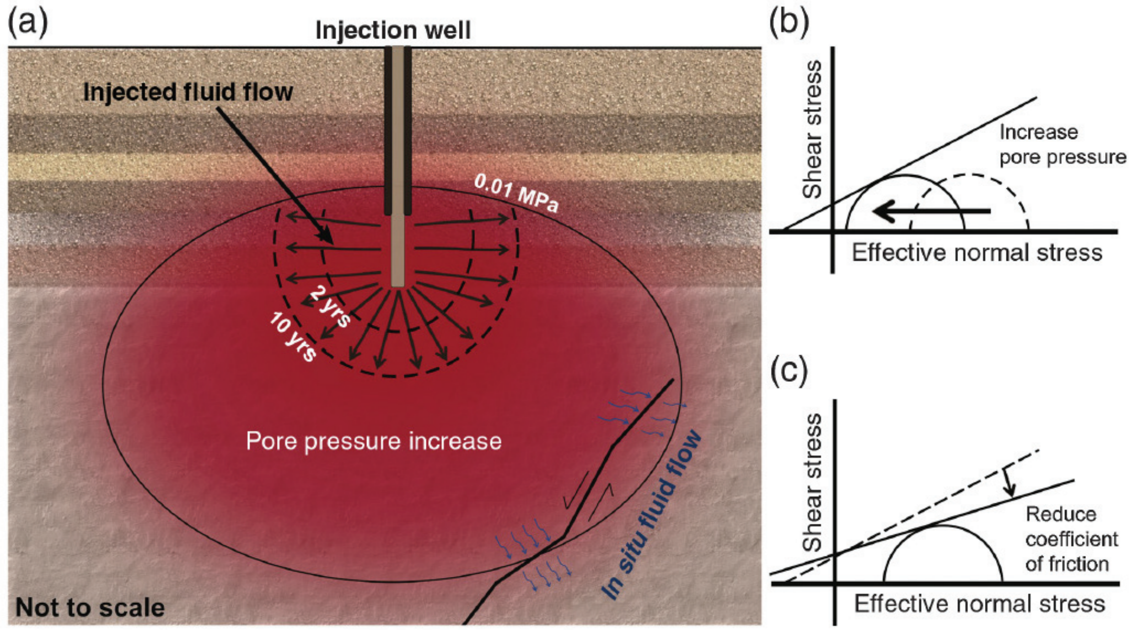

Figure 10. Conceptual figure of the mechanisms of fluid induced seismicity. a) Red area is pore pressure increase from disposal with a contour of 0.01MPa after 10 years. The dashed lines are the area that injected fluid flow reaches after 2 years of injection and 10 years. A fault is shown in the solid black line with blue arrows representing in situ fluid flow near the fault. b) Mohr – Coulomb diagram triggering via pore pressure increase along a pre – existing fault that is optimally oriented. c) Mohr – Coulomb showing induced seismicity from reduction of coefficient of friction from in situ fluid flow caused by injection induced seismicity pore pressure gradient [Brown, 2018].

In the United States, there are approximately 35,000 active wastewater disposal wells. However, only a few dozen wells have been proven to induce earthquakes [*Rubinstein and Mahani*, 2015]. The issue of fluid injection induced earthquakes was first documented in Colorado during the 1960s [*Evans*, 1966]. Rocky Mountain Arsenal (RMA), located in northeastern Denver, was the site of chemical waste disposal into the subsurface with a single injection well. Fluids were injected into the heavily fractured Precambrian metamorphic rocks. As a result of injecting a large amount of liquid waste (approximately 4.7 Mbbl), RMA experienced earthquakes that were unknown to the area prior to injection. In fact, prior to 1962 the Denver area had not experienced a noticeable earthquake since November 7, 1882 [*Evans*, 1966]. A total of 710 earthquakes were recorded in the Denver area from March 1962 to October 1965, with a majority of epicenters within five miles of the RMA injection well [*Evans*, 1966]. Other seismic events were located at distances greater than 10 km and at depths greater than four km from the RMA's well [*Rubinstein and Mahani*, 2015].

In the case of Raton Basin, the injection interval includes the Dakota, Purgatoire, Dockum, and Entrada formations, and the majority of wastewater is injected into the Dakota. In contrast to the RMS, fluids are not dumped directly into Precambrian basement rock. An increase in the injection of produced wastewater began in 1999 in Raton Basin with seismicity beginning in 2001 (Figure 11). In 1999 there were 22.9 million barrels (3,640,809 m^3) of wastewater produced, increasing to 119 million barrels (1.89×10^7 m^3) in 2007 [*Topper*, 2011]. The closest known active faults are within the Quaternary sediments present in the western part of the Basin [*Rubinstein et al.*, 2014]. There are a number of faults in the crystalline basement, with some cutting into the permeable overlying sedimentary layers (Figure 6).

Historical and instrumental data show that the increase in seismicity in Raton Basin is temporally correlated to wastewater injection [*Rubinstein et al.*, 2014; *Barnhart et al.*, 2014; *Meremonte et al.*, 2002]. Between 1972 and 2001 only one $M \geq 4$ earthquake occurred in the area. However, between August 2001 and 2013 there were 12 $M \geq 4$ recorded earthquakes in the Raton Basin [*Rubinstein et al.*, 2014]. Moment magnitude (M) is a measurement of the earthquake size or energy. It is similar to the Richter magnitude but is more accurate in describing the size of earthquakes [*Folger and Tiemann*, 2015].

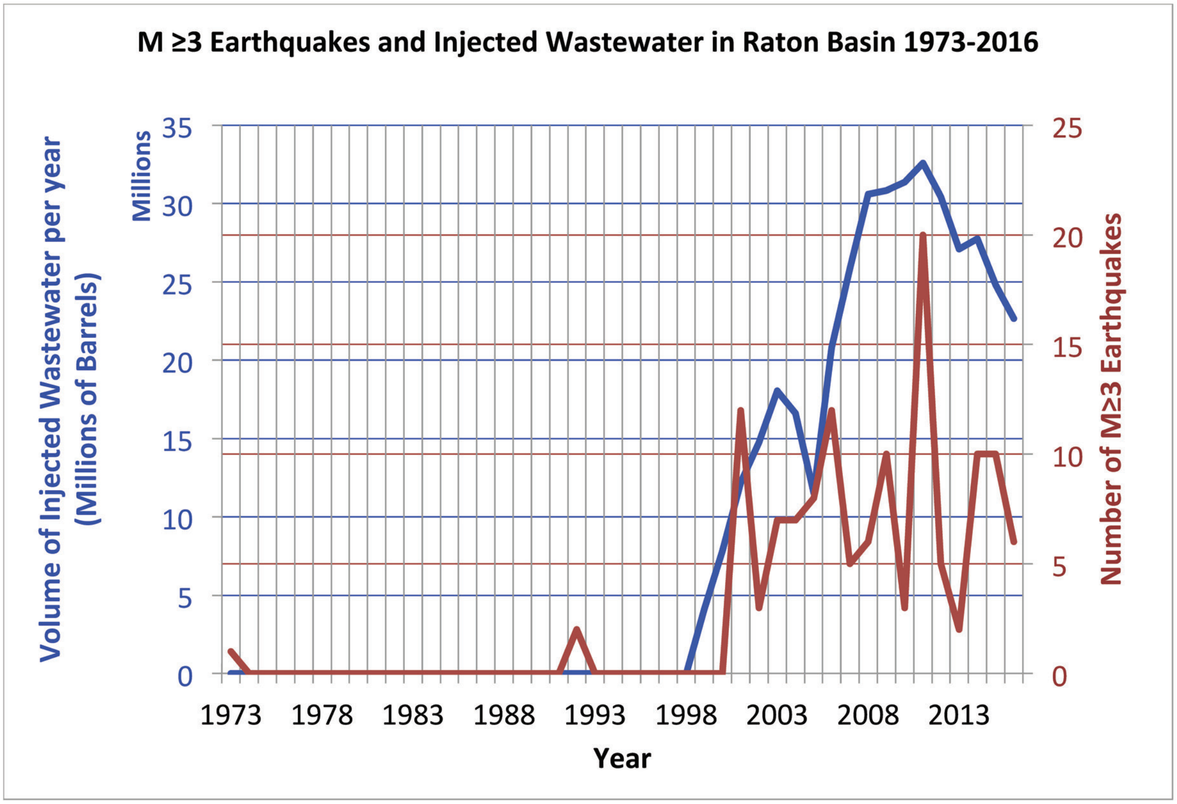

Figure 11. Earthquakes M ≥ 3 and Volume of Injected Wastewater in Raton Basin from 1973 and 2016 [COGCC, 2016; ANSS, 2016]

The largest earthquake occurred on August 23, 2011 when a M_w 5.3 earthquake damaged buildings in the town of Trinidad, CO [*Viegas et al.*, 2012; *Barnhart et al.*, 2014] (Figure 13). Approximately 41 million barrels (approximately 4.9 million m^3) of wastewater was injected from two disposal wells (VPR C 39 and VPR C 14 – Figure 24) before the earthquake, which is enough water to fill 1,960 Olympic sized swimming pools and seven times the total amount disposed of at RMA in 4 years [*Rubinstein et al.*, 2014]. The United States Geological Survey (USGS) located 584 aftershocks between the August 23rd event and December 15th, 2011 (Figure 14) [*Barnhart et al.*, 2014]. These series of earthquakes are referred to as an earthquake swarm. Raton has had two major earthquake swarms in the same area in 2001 and 2011. Meremonte et al. [2002] discovered a spatial correlation between the location of brine reinjection from CBM and the earthquake swarm in August 2001. A majority of the events were recorded within five km of active disposal wells [*Meremonte et al.*, 2002]. Rubinstein et al. [2014] noted that seismicity tended to occur within two km of high volume and high injection rate wells. Weingarten et al. [2015] defined high rate injection wells as having injection rates greater than 300,000 barrels/ month, which is higher than the injection rates in Raton Basin. Viegas et al. [2012] showed that wells do not have to cross a fault to trigger an earthquake and may be up to six km away from the epicenter.

Most induced seismicity has been attributed to changes in pore pressure because of the injection pressure at which the wastewater is disposed. However, Raton Basin is hydrostatically underpressured so the wastewater is gravity fed in the disposal wells [*Barnhart et al.*, 2014]. Although, studies have shown that even though the Basin is underpressured, pore pressure may still increase due to wastewater disposal [*Weingarten et al.*, 2015]. However, Seismic events have occurred prior to the commencement of wastewater injection in the Basin suggesting natural causes, such as ambient tectonic activity. For example, earthquakes in 1966 and 1973 in Raton Basin are two examples attributed to tectonic activity [*COGCC*, 2016] (Figure 11).

There are differences between induced seismicity in geothermal reservoirs versus wastewater disposal. Geothermal reservoirs will stimulate reservoirs on purpose in order to create permeable rock that allows fluid to flow. Therefore, they are at aiming to reduce rocks strength and therefore microseismicity. Wastewater disposal areas are not aiming to stimulate permeability, as they are already disposing in formations with high permeability and porosity. In addition, the location of geothermal reservoirs and disposal sites are different. Geothermal reservoirs are normally in tectonically active areas that are more prone to seismicity, unlike the center of continents where wastewater disposal occurs [*Majer et al*. 2007].

The mechanisms for induced seismicity in geothermal reservoirs and wastewater disposal are similar. Pore pressure increase is observed from both disposal wells and geothermal injection wells. Geothermal reservoirs add another component that wastewater disposal sites do not – production. Water is also withdrawn from the reservoir, which can create volume changes and affect the failure (Figure 12) [*Majer et al*. 2007].

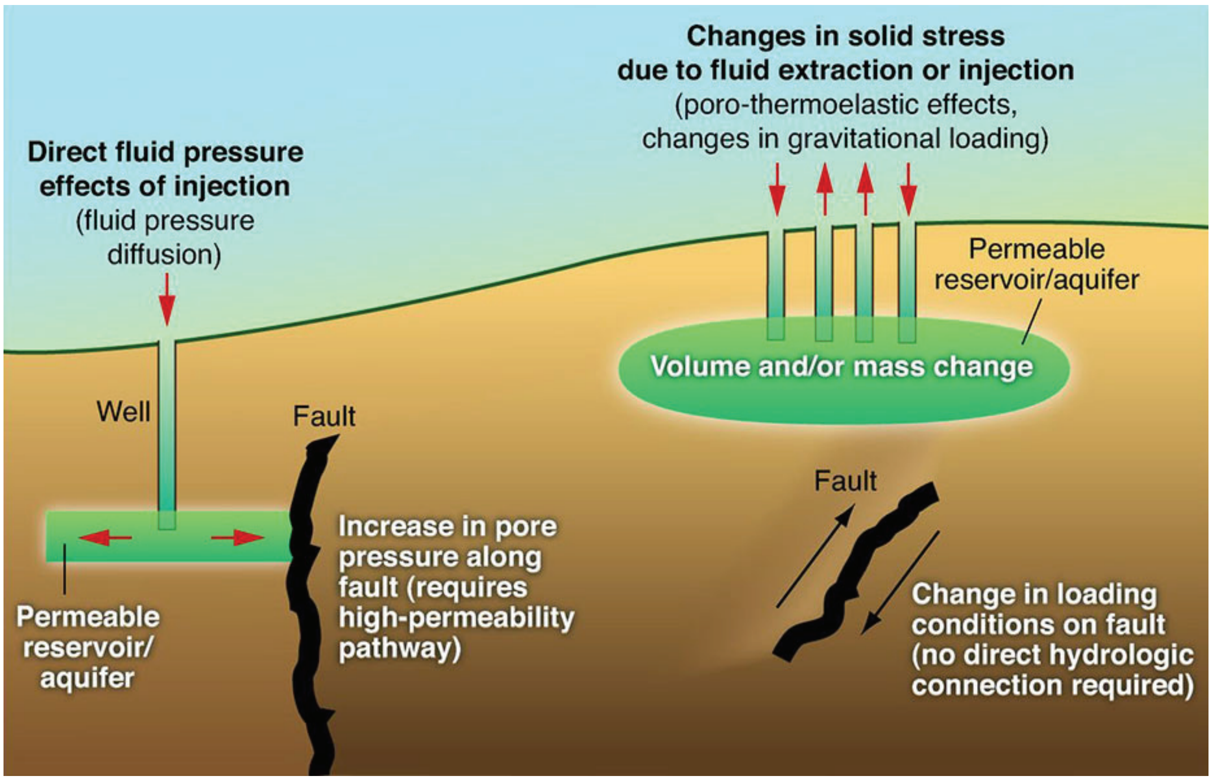

Figure 12. Mechanisms for induced seismicity. Wastewater disposal is illustrated on the left into a permeable reservoir while enhanced geothermal reservoirs are illustrated with the mass/volume change in a reservoir [*Ellsworth et al.*, 2003].

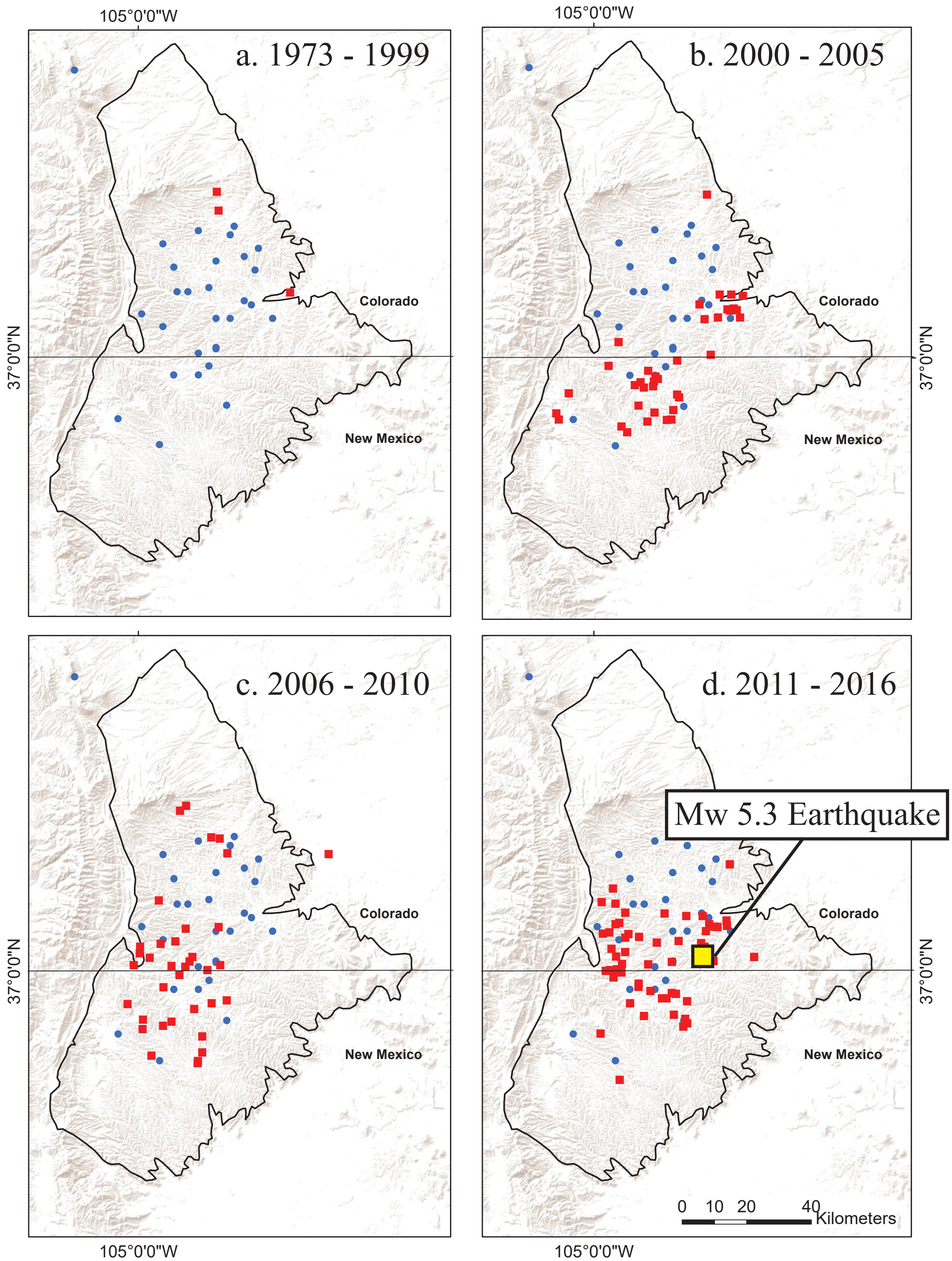

Figure 13. Map showing M ≥ 3 Earthquakes in Raton Basin (red squares) though time. Injection wells are shown in blue. The Mw 5.3 earthquake is shown in yellow [COGCC, 2016; ANSS, 2016].

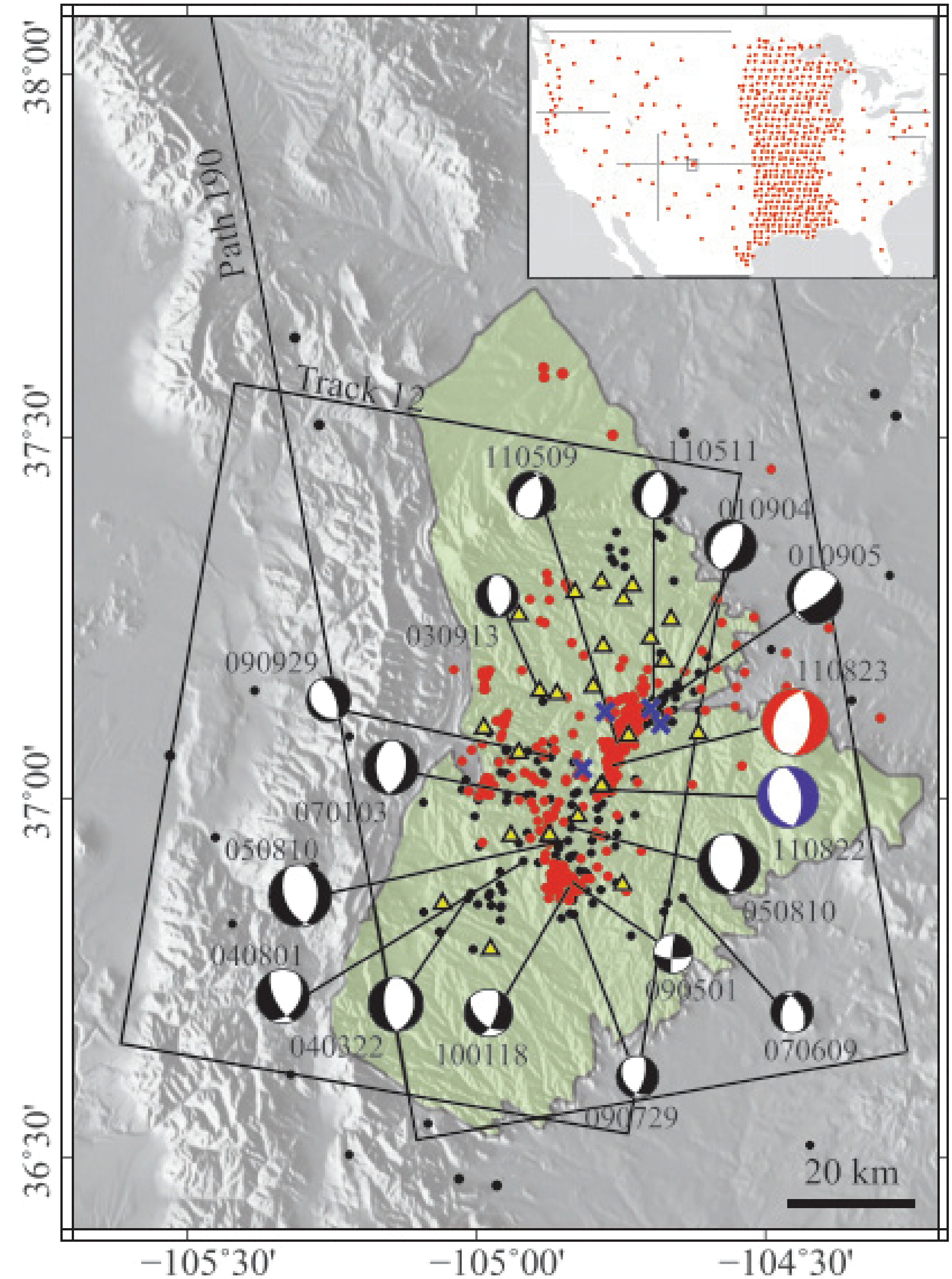

Figure 14. Regional moment tensors for seismicity in Raton Basin. Black dots are seismicity prior to the 2011 Trinidad earthquake (shown as the red moment tensor). Red dots are seismicity that Rubinstein et al. 2014 located. Blue crosses are temporary seismometers that the USGS deployed after the 2011 Mw 5.3 earthquake. Yellow triangles are the wastewater injection wells. Black outlined boxes are spatial extends for InSAR. [*Barnhart et al.,* 2014.]

2.7 Geothermal Gradient and Enhanced Geothermal Systems

There is much debate about the causes of the recent seismicity in Raton Basin. The Raton Basin has an average geothermal gradient of 49 ± 12°C/km, which is much higher than the average for the western United States (34°C/km) [*Morgan and Witcher*, 2011*; Nathenson and Guffanti*, 1988]. Although some studies have shown a spatial and temporal correlation between wastewater injection and seismicity, no unanimity as to the origin of the Basin's seismic activity has been reached [*Rubinstein et al.*, 2014; *Barnhart et al.*, 2014; *Meremonte et al.*, 2002] (Figure 11). Most research into thermal effects on induced seismicity is focused on Enhanced Geothermal Systems (EGS) [*Foulger et al.,* 2017, *Gaucher et al.*, 2015, *Brodsky et al.,* 2013]. EGS are reservoirs in areas of high geothermal gradients that are stimulated by either hydraulic fracturing, water injection, or chemical stimulation to extract heated water for energy production [*Gaucher et al.*, 2015, *Majer et al*. 2007]. Water is injected into the fractured rocks in the subsurface, which is then heated by surrounding warm rock, and is then extracted in separate producing wells (Figure 15). The goal is to enhance and create permeable pathways for fluids to flow. This process creates microearthquakes (M < 3) in most cases, but some larger earthquakes have taken place, such as the M 4.6 that occurred in The Geysers field in northern California in the 1980s [*Majer et al*. 2007, *U.S. DOE*, 2006].

The injection of cool water into much warmer rock results in thermal contraction and thus rock failure [*De Simone et al.,* 2013]. The temperature difference between the injected water, at atmospheric conditions at the surface, and hot geothermal reservoir causes thermal contraction of the fracture surfaces, which affects the in situ stress state [*Majer et al*., 2007] The higher temperature of Raton Basin, along with wastewater injection of fluids that are significantly colder than the surrounding rock, could lead to thermal contraction. Temperature variation affects fluid viscosity and deforms the rock mass thermoelasticity [*Holtzman et al.*, 2018]. Hydrologic parameters, such as porosity and permeability, can be changed due to stress and strain due to increased water pressure. Increased fluid pressure extends father into fractured zones than in surrounding rock due to larger contrasts in the hydraulic conductivity. Temperature decrease lowers the total stress in addition to the effect stress by the thermo-elastic effect. This can then lead to tensile or shear failure [*Brodsky et al*., 2013; *De Simone et al.,* 2013; *Gaucher et al.*, 2015].

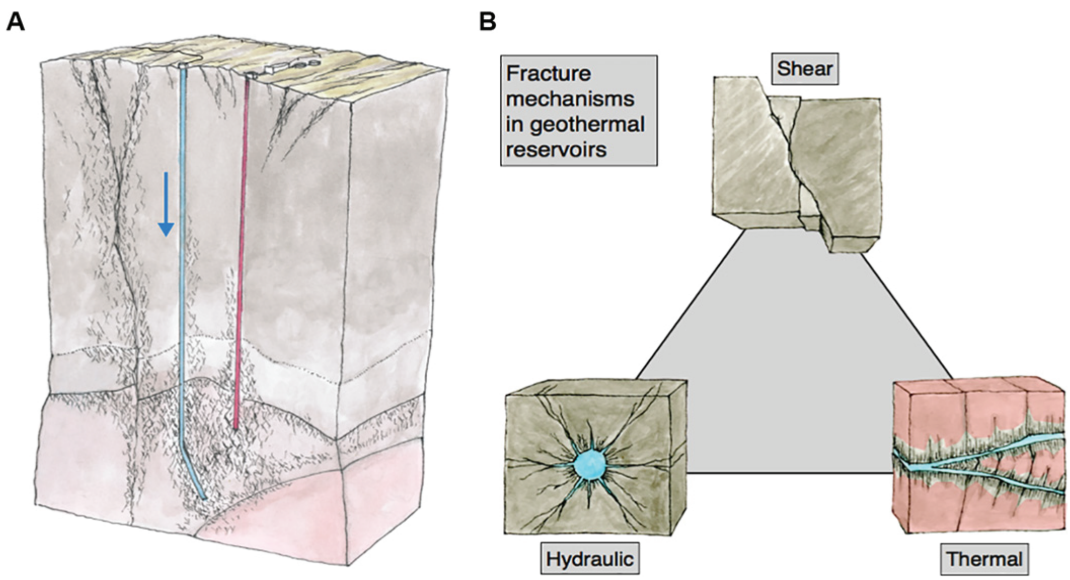

Figure 15. Mechanisms for Induced seismicity in EGS [*Holtzman*, 2018].

Elevated temperatures enhance the hydraulic conductivity and allow for fluids to migrate more easily [*Weingarten*, 2015]. Contraction and expansion of rock, resulting from temperature changes in both rock and fluids, create poro-thermoelasticity effects, driving changes in porosity, intrinsic permeability and hydraulic conductivity [*De Simone et al.*, 2013; *Gaucher et al.*, 2015]. Temperature decreases in rock due to cooler water injection, combined with an increase in pore pressure, can potentially cause rock failure due to the lowering of the effective normal stress, as can be shown by a Mohr circle [*De Simone et al.*, 2013; *Gaucher et al.*, 2015] (Figure 5, *Rubinstein et al.,* 2015). In addition to contraction, expansion of rock due to higher temperatures can cause pore pressure to increase due to confinement.

In order to address the relationship between the geothermal gradient and seismicity in Raton Basin, modeling with performed. Prior to modeling, multiple datasets were collected from a variety of sources. Disposal well information was collected from state websites for both New Mexico and Colorado. Secondly, geothermal data were collected from bottom hole temperatures. Pioneer Natural Resources provided wastewater disposal temperature while formation lithologies and parameters were collected from literature. Lastly, earthquake locations were collected from publically available earthquake catalogs.

3. DATA ACQUISITION and ANALYSIS

3.1 Injection Wells

Wastewater injection well information was for Raton Basin. The Colorado Oil and Gas Conservation Commission (COGCC) database provided injection rates, locations, current status, and dimensions for the injection wells on the Colorado side of the Basin [COGCC, 2016 - Appendix]. The New Mexico injection well information was collected from the New Mexico – Oil Conservation Division (NMOCD) [NMOCD, 2016]. Well logs from disposal wells and producing wells also provided top and bottom depths of formations and porosity in the Basin. In 2001, there were 10 injection wells, which increased to 21 in 2002 [*Viegas et al.*, 2012]. As of December 2016, there are 28 active injection wells (Table 2) [*COGCC*, 2016; NMOCD, 2016]. Note that injection well data prior to 2006 are not available for New Mexico injection wells and thus New Mexico injection rates were not included from 1999 to 2006 in the model study described later in this thesis.

3.2 Geothermal data

Bottom Hole Temperatures (BHT) data from the bottom of the producing CBM and disposal wells in the area were collected [*Kelley*, 2015 and *Kelley*, 2011, National Geothermal Data System, 2017, and *Morgan*, personal comm.]. This allows calculation of the spatially varying geothermal gradient (Figure 7). BHT are typically corrected because the measurement is taken within a few hours of drilling, which results in inaccurate temperatures due to drilling fluid convecting heat into or out of the hole [*Morgan*, 2009]. BHT are corrected using a standard correction equation to eliminate discrepancies between the temperatures recorded during drilling and days after drilling was completed. We corrected the BHT data using the following equation [*Kelley*, 2015].

$$BHT_{corrected}\ °C = BHT_{uncorrected}\ °C + 0.0056125 \text{ x Depth (m)} + 3.369$$

The COGCC provided BHT for Colorado side, while New Mexico Bureau of Geology and Mineral Resources through The National Geothermal Data Systems (NGDS) provided BHT data for the New Mexico side [*Kelley*, 2011; *Kelley*, 2015; *COGCC*, 2016,]. In total, 1,627 BHT data measurements were used to interpolate the geothermal gradient spatially for the model in this study.

3.3 Injection Temperature

The surface temperature of disposed wastewater was provided by Pioneer Natural Resources, a main operator in Raton Basin. The average temperature is 20°C. The temperatures were sampled between 2000 and 2014 at surface disposal tanks at different times of the year (Figure 16). These tanks store the wastewater before it is transported for disposal in the subsurface [Macartney, personal comm.].

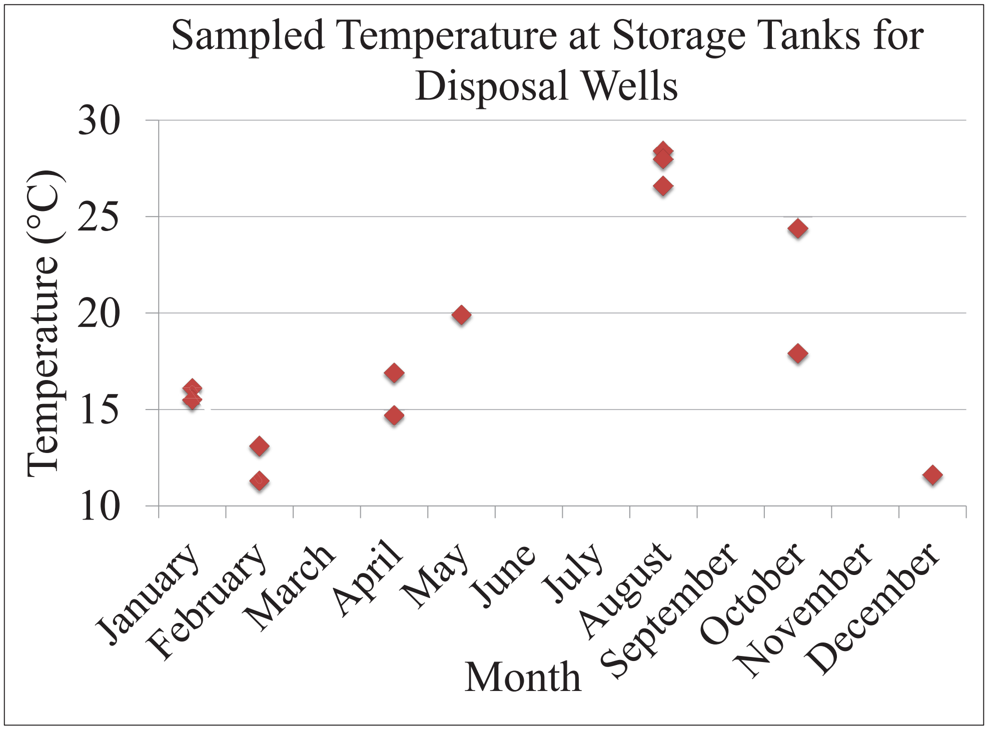

Figure 16. Wastewater temperature recorded at storage tanks on the surface prior to injection. There were collected from 2000 – 2014. Appendix has the years that each were sampled. [Pioneer Natural Resources; McCartney, personal communication]

3.4 Formation Geology

Formation lithologies were used to estimate porosity and permeability for the model. Porosity values for the injection intervals were taken from various injection well logs from the COGCC [*COGCC*, 2016]. Permeability from core and outcrop provided permeability values for formations [Bohlen, 2012; COGCC, 2016]. Literature values were also used when describing the hydraulic parameters of the different model layers, which varied due to lithology differences. These include density (kg/m^3), wet heat conductivity (saturated heat conductivity) (W/m -°C), specific heat of the rock (J/kg -°C), pore compressibility (1/Pa), and pore expansivity (1/°C) [Robertson, 1988 - Appendix].

The CBM producing formations - Raton, Vermejo, and Trinidad - have an average porosity of 14% and permeability ranging from <0.1- 28.5 millidarcys (md) (1 x10^{-16} m^2- 2.81x10^{-14} m^2) [*Dolly and Meissner*, 1977] (Table 1). These formations are not modeled in this study because they shallower then the depths that wastewater injection is occurring. The Pierre Shale, Niobrara and Benton Formations act as a confining layer to the underlying injection interval because of their low permeability. These formations' permeability ranges from 0.00475 md – 0.4 md (4x10^{-18} m^2 to 4x10^{-16} m^2) and restrict upward migration of groundwater from the injection interval into overlying formations. Porosities in the injection interval range from 5 to 16% with permeability ranging from 2 to 20 md (1.97x10^{-15} m^2 – 1.97x10^{-14} m^2 [*COGCC*, 2016]). Parameters used in the numerical modeling to represent these formations are discussed in Chapter 4.

3.5 Earthquakes

Earthquake locations and magnitudes in Raton Basin from 1973 to 2016 are shown in Figure 17. Earthquake data were collected from the Advanced National Seismic System (ANSS), which is operated by the United States Geological Survey (USGS) [*ANSS*, 2016]. Only earthquakes $M \geq 3$ were examined because that is the magnitude at which humans can feel the effects at the surface. In total, this catalog has recorded 142 $M \geq 3$ earthquakes in Raton Basin from January 1999 to April 2018, of which 130 of the 142 occurred from January 1999 to December 2016. Seismicity is on going in Raton Basin with the most recent earthquake (as of June 17, 2018) a M 3.5 occurred on February 25th 2018. Depths of seismicity epicenter from ground surface range from 3 to 6 km and thus primarily occur in the crystalline basement. Fault locations can be assumed from the locations of earthquakes as earthquakes highlight the location of preexisting faults.

Other earthquake logs were examined to compare depth uncertainty. These include Rubinstein et al. [2014], Barnhart et al., [2014], Meremonte et al., [2002], and Nakai et al., [2017]. The limitations and future work section (5.1) addresses the comparisons between these catalogs with the ANSS. Most earthquake epicenters are located within the crystalline basement in these catalogs with depths ranging from 4 – 6 km and uncertainties of up to 15 km [Nakai et al., 2017; Rubinstein et al., 2014]. These catalogs focus on certain earthquake sequences such as 2001 and 2011 and utilize temporary seismic arrays. Therefore, the relocations have less error in these events. In addition, a number of seismic models contribute to depth locations and associated errors [Rubinstein et al., 2014, Barnhart et al., 2014].

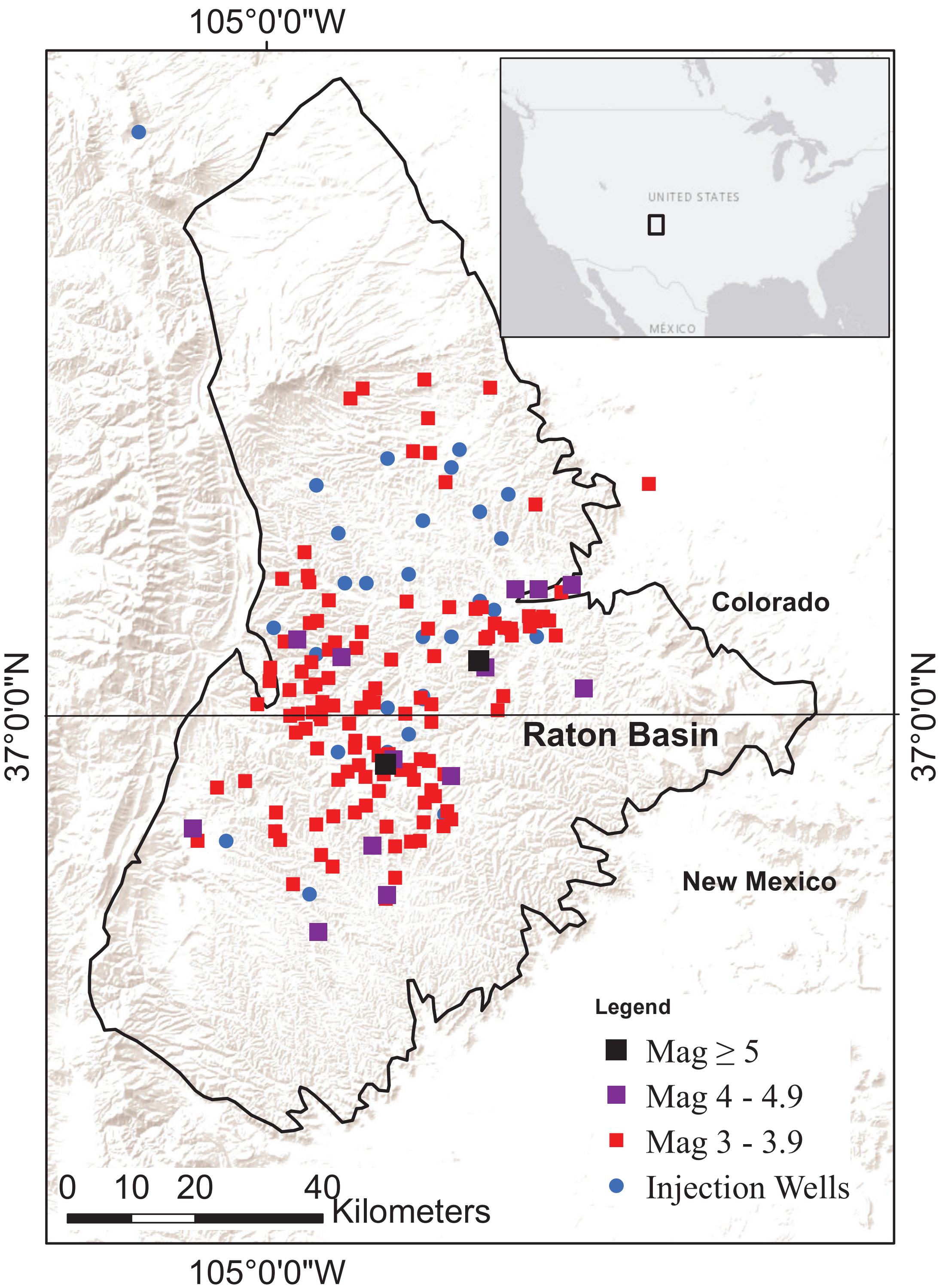

Figure 17. Wastewater disposal wells and earthquakes in Raton Basin. Earthquakes M 3 – 3.9 are shown by red squares. M 4 – 4.9 are purple squares and M ≥ 5 are black squares. Disposal wells are shown by blue squares.

4. GROUNDWATER FLOW and GEOTHERMAL MODELING

4.1 Objective

The scientific question addressed here is whether a spatial relationship exists between earthquakes, the injection wells, and the geothermal gradient. By using a coupled heat and fluid model, the objective is to determine if areas of high geothermal gradient, specifically the east central area, correspond to a change in earthquake activity (Figure 8). The hypothesis is that wells in high geothermal gradient areas have higher correlation with earthquake occurrence. Modeling was done to determine if any temperature contrasts due to cooler wastewater has the ability to reach the basement.

4.2 Numerical Model and Governing Equations

The Transport Of Unsaturated Groundwater and Heat (TOUGH2) code models pore pressure and temperature in three dimensions [*Pruess et al.,* 2012; Thunderhead Engineering, 2016]. TOUGH2 solves mass and energy balance equations while simulating non-isothermal multiphase flow in fractured and porous media. It was developed at the Lawrence Berkley National Laboratory and is written in FORTRAN77. TOUGH2 uses the integral finite difference method and simulates fluid and heat transfer in porous media. It uses a linear triangulation algorithm to interpolate between temperature data points and has been used in geothermal reservoir studies. PetraSim is the graphical interface that TOUGH2 is run in.

4.2.1 Mathematic Model

The mass and energy balance equation that is solved in TOUGH2 is

$$\frac{d}{dt}\int_{V_n} M^{\kappa}\, dV_n = \int_{\Gamma_n} F^{\kappa} \cdot n\, d\Gamma_n + \int_{V_n} q^{\kappa}\, dV_n \tag{1}$$

The integration is over an arbitrary subdomain V_n of the flow system. Γ_n is the boundary of the closed surface. M is the accumulation term and represents the mass or energy per volume. κ is the heat or fluid component. F symbolizes the mass or heat flux. q are the sinks and sources. η is the normal vector on surface element $d\Gamma_n$ pointing inward into V_n [*Pruess et al.,* 2012].

The mass accumulation is expressed as

$$M^{\kappa} = \phi \sum_{\beta} S_{\beta}\rho_{\beta} X_{\beta}^{\kappa} \quad (2)$$

κ is the total mass component obtained by summing over the fluid phases (β = liquid, gas, and non – aqueous phase liquids). ϕ is porosity. S_{β} is the saturation of phase β or the fraction of pore volume occupied by phase β. ρ_{β} is the density of phase β. X_{β}^{κ} is the mass fraction of component κ present in phase β [*Pruess et al.,* 2012].

Heat accumulation term in a multiphase system is:

$$M^{N\kappa+1} = (1-\phi)\rho_R C_R T + \phi \sum_{\beta} S_{\beta}\rho_{\beta}\, u_{\beta} \quad (3)$$

ρ_R grain density. N is the mass components (water, air, H2, solutes). C_R is the specific heat of the rock. T is temperature. u_{β} is specific internal energy in phase β [*Pruess et al.,* 2012].

Advective mass flux is sum over phases. Individual phase fluxes are given by a multiphase version of Darcy's law:

$$F_{\beta} = \rho_{\beta} u_{\beta} = -k\,\frac{k_{r\beta}\rho_{\beta}}{\mu_{\beta}}\,(\nabla P_{\beta} - \rho_{\beta}\mathrm{g}) \quad (4)$$

u_{β} is the Darcy velocity (volume flux) in the phase β. k is the absolute permeability. $k_{r\beta}$ is the relative permeability to phase β. μ_{β} is viscosity. P_{β} is the fluid pressure in phase β, which is the sum of pressure of a reference phase (usually taken to be the gas phase) and the capillary pressure. g is vector of gravitational acceleration.

Heat flux includes conductive and convective components

$$F^{N\kappa+1} = -\lambda\nabla T + \sum_{\beta} h_{\beta} F_{\beta} \quad (5)$$

λ is thermal conductivity. h_β is specific enthalpy in phase β.

4.3 Model Setup and Boundary Conditions

4.3.1 Domain and Discretization

I created a three dimensional coupled fluid and heat transport model to simulate pore pressure and temperature in Raton Basin from January 1999 to December 2016. The model domain extends 110 km north - south and 100 km east - west. Model depths range from 0.5 km (top of the confined aquifer) to 5 km (Figure 18). The Sangre de Cristo Mountains act as the western boundary; the Sierra Grande Uplift and Apishapa and Cimarron Arches mark the eastern, north, and south boundaries of Raton Basin (Figure 1). A spatially varying polygonal grid with refinement around injection wells in the horizontal direction allowed for finer grid dimensions in the injection interval in the vertical direction.

The model top is marked by the no flow boundary of the Pierre Shale, which has an average depth of 0.5 km bgs. The model extends into the crystalline basement to a total depth of 5 km. The average crystalline basement depth starts at 3.3 km bgs. The modeled Pierre Shale, Niobrara, and Benton Formations act as a confining layer to upward flow (Figures 6,18). Six hydrologic units were modeled with varying thicknesses to represent different lithologies in Raton Basin (Figure 18, 19).

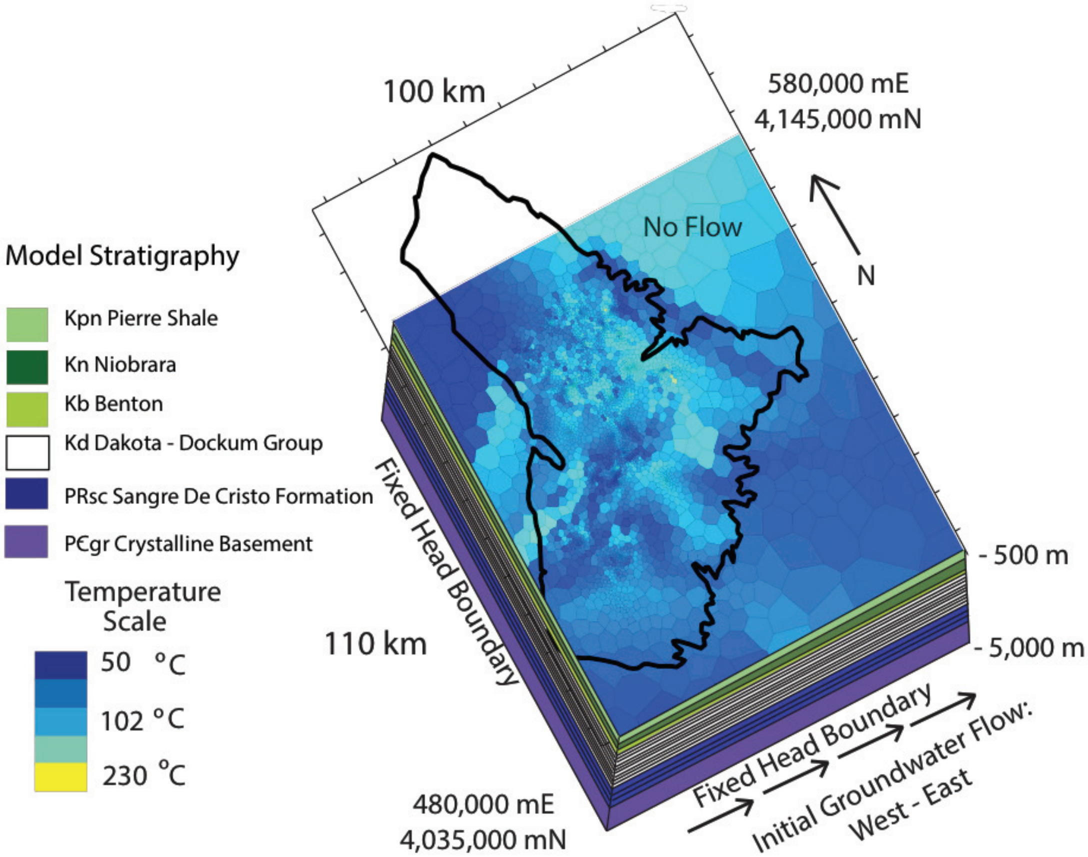

Figure 18. Domain and Boundary Conditions for the model. Plan view shows the model grid with Raton Basin's outline with the black line. The grid is refined around the disposal wells. The temperature for the top of the Dakota Formation is shown and interpolated from the Bottom Hole Temperature data points. Cross section view shows the layers of the model. UTM (mE and mN) was used as the coordinate system in the model.

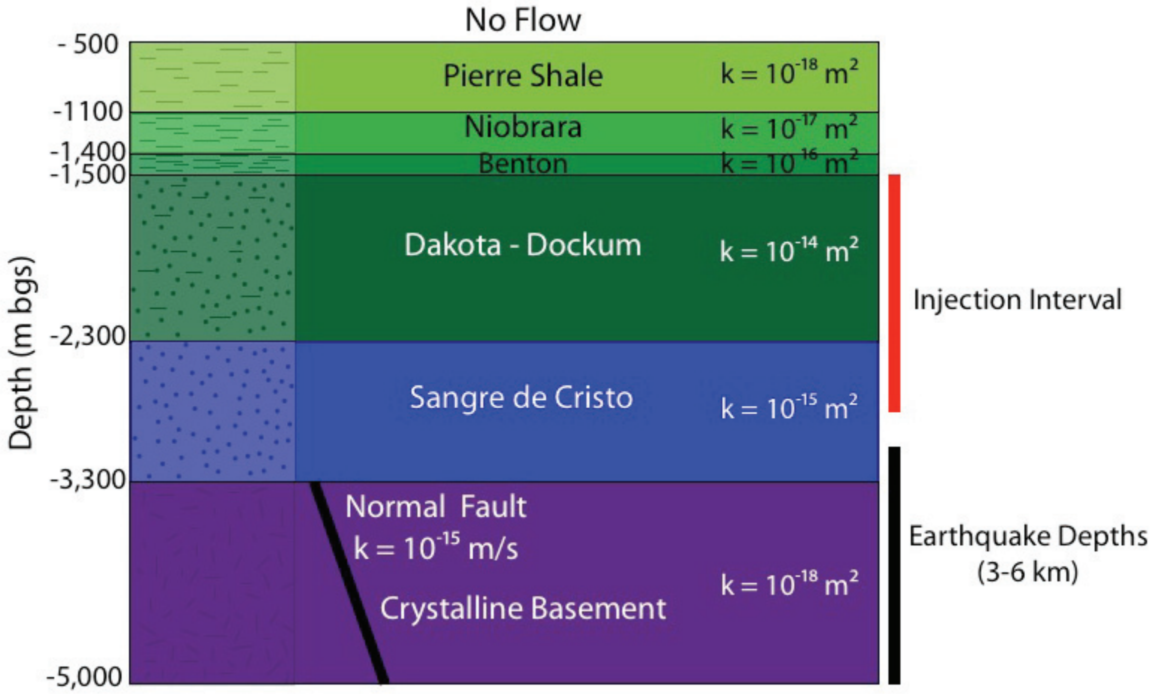

Figure 19. The six hydrogeologic units in the TOUGH2 model. Lithologies are shown and vary from shale, sandstone, and gneiss/granite in the crystalline basement. Permeability values are shown for each layer [*Geldon*, 1989; *Bohlen*, 2013, *Weingarten*, 2015]

4.3.2 Boundary and Initial Conditions

Fixed head boundaries are used on all boundaries of the domain. Drillstem test data from Nelson et al. [2013] provided the hydraulic head values in the Dakota Formation. These were used to determine the initial conditions for pressure in the Basin and it reflects overall groundwater flow from west to east (Figure 20 and 21). Pressure values equivalent to approximately 1,772 m of head (17.37 MPa) are shown on the western side of the Basin at a depth of 1,500 m while 1,547 m of head (15.16 MPa) is found on the eastern boundary of the Basin (Figure 20). The top is a zero flux boundary because the permeability values used in the top confining layers (Pierre Shale – Benton) are two to four orders of magnitude less than the injection interval (Figure 19). The boundaries of the model are far enough from injection wells that there will be little boundary effect on the model results.

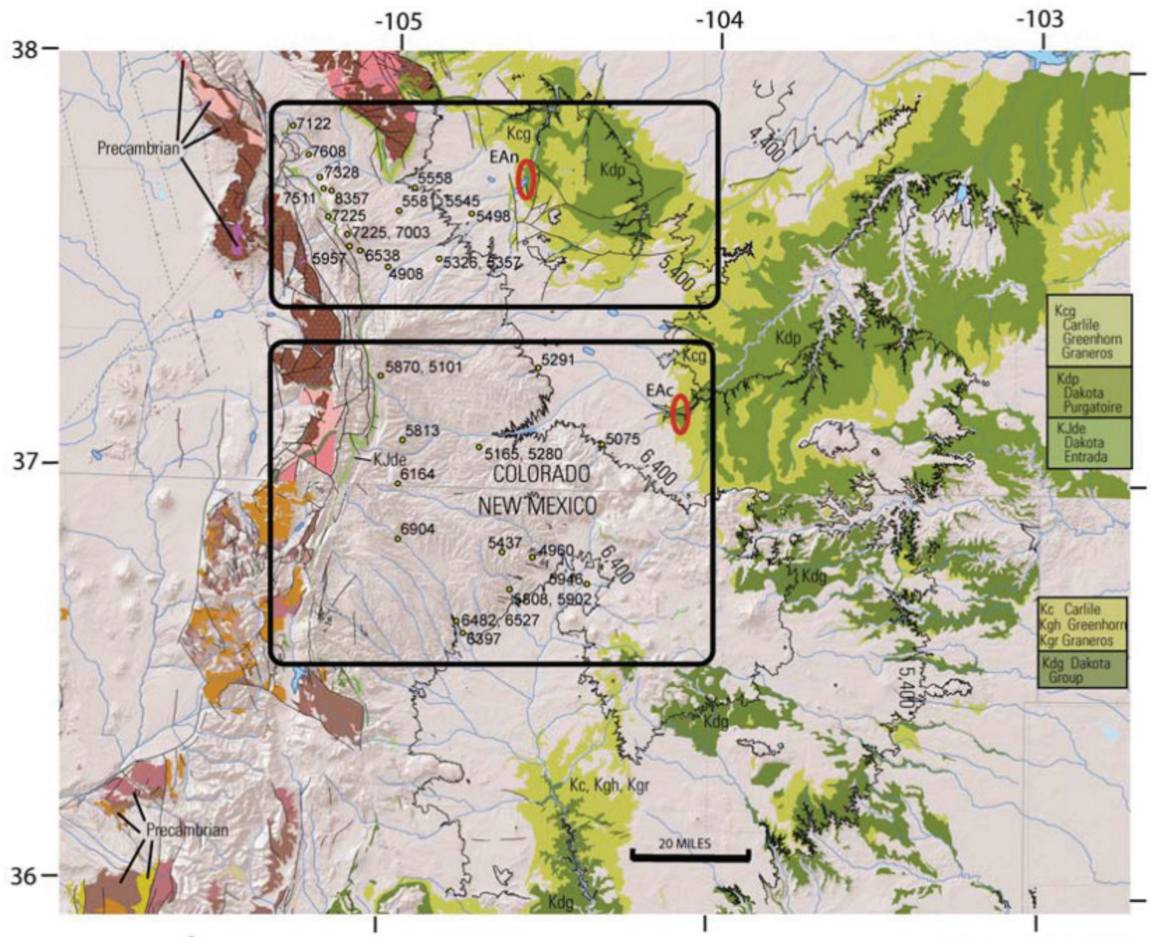

Figure 20. Hydraulic head in ft at the Dakota Formation [*Nelson et al.,* 2013]

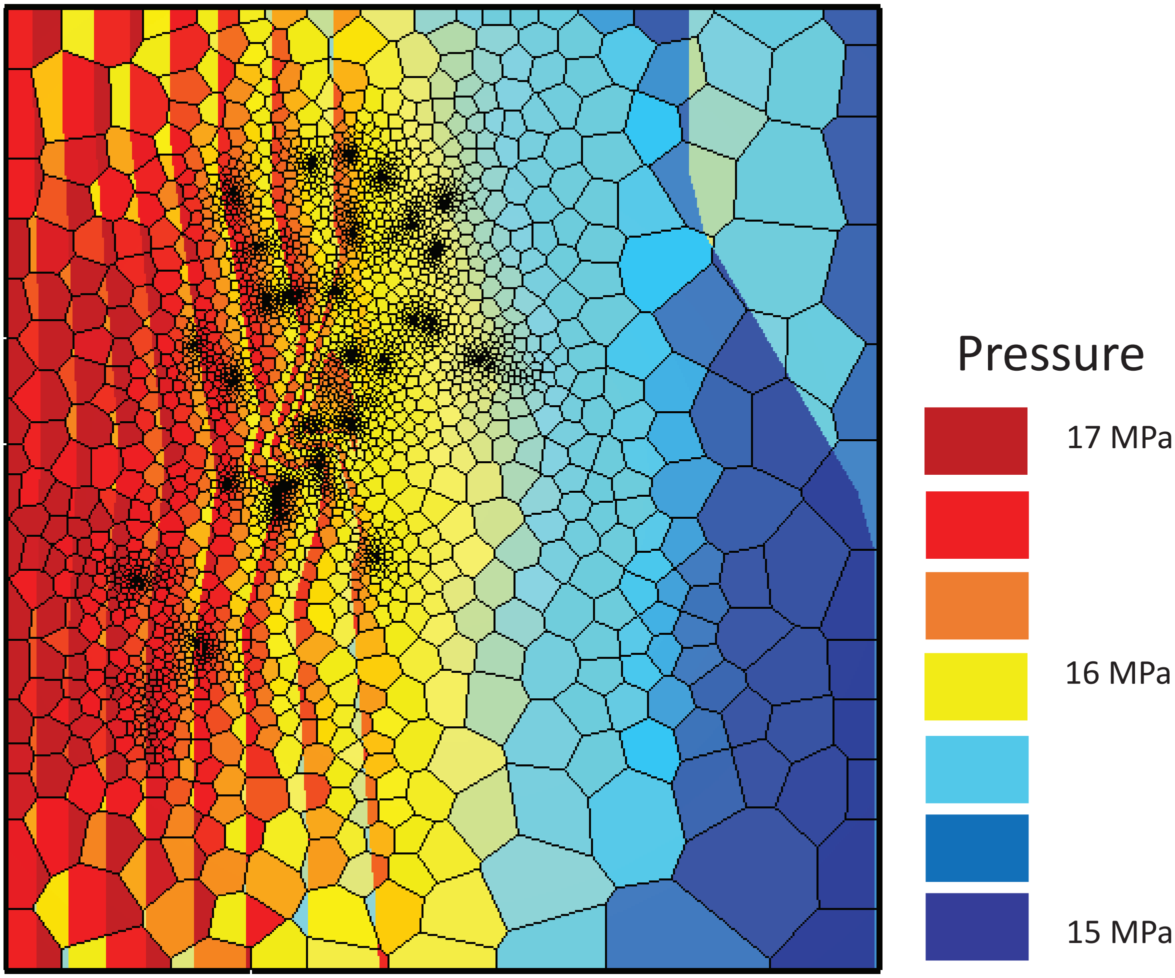

Figure 21. Initial pressure at the top of the Dakota Formation. Groundwater flows from high pressure on the west side to low on the east.

The initial temperature regime was calculated from the interpolation of BHT data (Figure 22). 1,627 points were input representing the temperature at the top of each hydrologic unit. The interpolation used in the model is a linear triangulation algorithm.

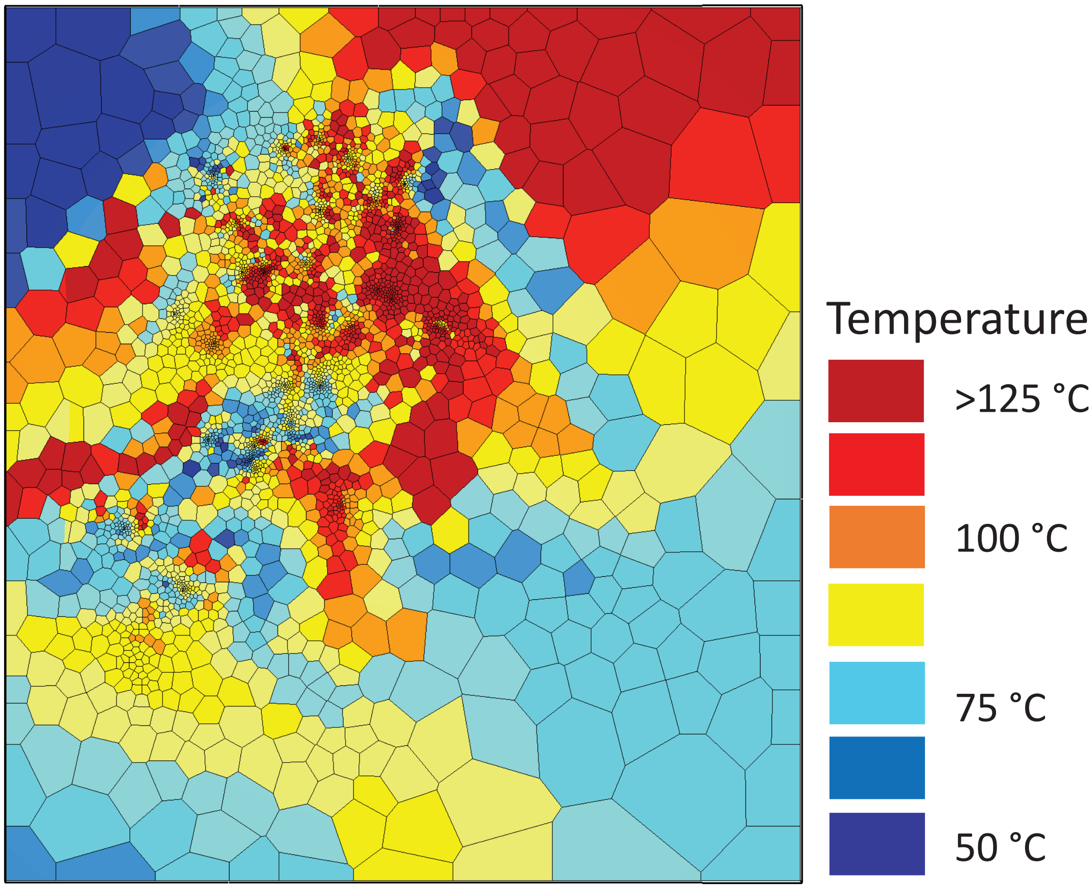

Figure 22. Initial Temperature at the top of the Dakota Formation.

4.3.3 Faults

There are a number of faults in the crystalline basement, with some cutting into the permeable sedimentary layers that lie above it [*Meremonte et al.,* 2002, *Barnhart et al.,* 2014, *Nakai et al*., 2017] These crystalline basement faults are critical for earthquake occurrence because of thermal contraction due to temperature differences between the cooler wastewater and hot subsurface moving through the faults. This could allow a pathway for stress differences due to thermo-elasticity effects. Faults were added into the model to facilitate a conduit for temperature and pore pressure changes to reach the crystalline basement, which is the depth at which a majority of the earthquakes occur. Faults are important in facilitating seismicity. Fluid pressure increase transmitted to a fault lowers the stress holding the fault closed (normal stress) and then results in a lower effective stress. Faults are more prone to failure or slip because the lower effective normal stress lowers the frictional resistance to slip [*Rubinstein et al.*, 2015]. Because PetraSim does not allow faults to be put into the model, two parallel vertical planes (i.e. layers) created an internal boundary that cut through the crystalline basement layer of the model (Appendix – Figure 42). Parameters for the rock between the two areas, mainly permeability, were changed to simulate a fault area. The permeability within the faults was set to 10^{-14} m^2. Sensitivity analysis was also performed with multiple permeability values ranging from 10^{-16} m^2 to 10^{-14} m^2 . Previous studies have shown that this fault can provide a conduit to flow, which allows for pore pressure to increase within the range to induce seismicity [*Barnhart et al.,* 2014, *Nakai et al.,* 2017]. These modeled normal faults begin at 3 km bgs, or slightly into the Sangre de Cristo sandstone, and extends through the crystalline basement to the base of the model at 5 km.

An internal boundary was placed where known faults and earthquakes have occurred [*Barnhart et al.,* 2014; *Nakai et al*., 2017]. This fault represents a normal fault starting at a depth of 3.3 km, or the top of the crystalline basement. The fault strikes 35 NE and dips 65 SE through the central part of Raton Basin (Figure 23, *Barnhart et al.,* 2014). The Wild Boar well, which is located 1 km away from the fault location is in a high geothermal gradient area (Figure 23).

A second fault zone, the Tercio, was modeled on the western edge of the Basin [*Nakai et al.,* 2017; Figure 23]. The Tercio fault has 129 earthquakes associated with it. Lineation of seismicity and mapped surface faults 10 – 15 km of Tercio have been used as evidence for the presence of this fault. The Mw 5.3 occurred 4 km east of the Tercio fault with a moment tensor indicating an east- west normal fault. In addition, a moment tensor for a Mw 3.53 earthquake that occurred on September 29, 2009 at the northeast terminus of the Tercio fault indicates a northeast-southwest normal fault [Nakai et al., 2017].

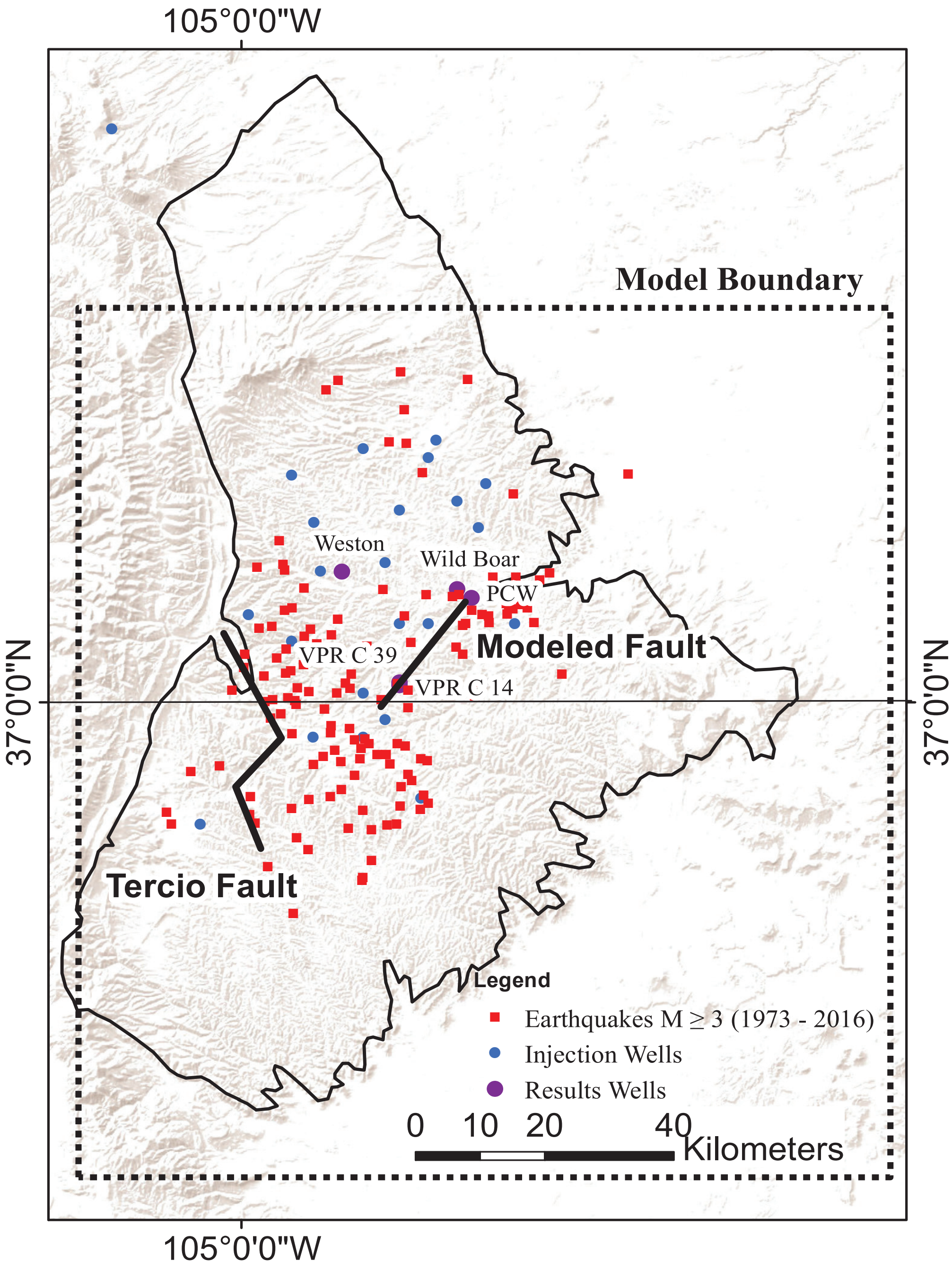

Figure 23. Fault locations that were added into the model. The Tercio fault has been named while the earthquake labeled as “modeled fault” does not have a specific name in literature. Red squares represent earthquakes M ≥ 3 while injection wells are in blue. The five wells that will be analyzed in the results section are shown as purple dots and labeled with their names.

4.4 Model Sources and Input Parameters

Input data sources for the model include the 28 injection wells that were active from January 1999 to December 2016. Model inputs include well locations and monthly injection rates. Hydrologic and geologic parameters were collected from literature. The average temperature of wastewater injection at the time of injection is 20°C (Figure 16).

4.5 Model Results

Pore pressure and temperature change from injection were modeled using TOUGH2 [*Pruess et al.,* 2012] (Figures 24 – 35). Modeling shows that pore pressure increased up to 0.2 MPa, at a depth of 3.3 km bgs (Figure 35). These model results support previous studies that point to pore pressure increase as the main cause for induced seismicity. These studies have shown pore pressure increase between 0.5 and 1 MPa in the basement, where the earthquake nucleation has occurred [*Weingarten*, 2015; *Nakai et al.,* 2017; *Rubinstein et al.*, 2014]. In addition, pore pressure increases up to 0.8 MPa within 100 m of the injection well at the injection well depth (Figure 26). This is showing that pore pressure is highest at the injection depth and diffuses towards the basement. However, temperature does not seem to show any change at crystalline basement depths and therefore, there is no temperature contrast created from the wastewater injection and the rock in the subsurface at the depths at which earthquakes are occurring. Five of the twenty-eight injection wells modeled had a temperature decrease 100 m away in the injection interval depth. However, results show that the temperature remains unchanged directly below all injection wells at the top of the crystalline basement (3.3 km bgs).

Faults were included in the model as a conduit to see if the temperature difference between the wastewater injection and rock would be able to reach the basement depth (Figure 23). With the addition of fault – induced permeability, pore pressures increased approximately

0.1 MPa at the crystalline basement, but temperature remained constant in all scenarios (Figures 30, 32 - 35). Weston Injection well had a pore pressure increase of 0.075 MPa at the crystalline basement (3.3 km bgs) with a constant temperature of approximately 160°C (Figure 30).

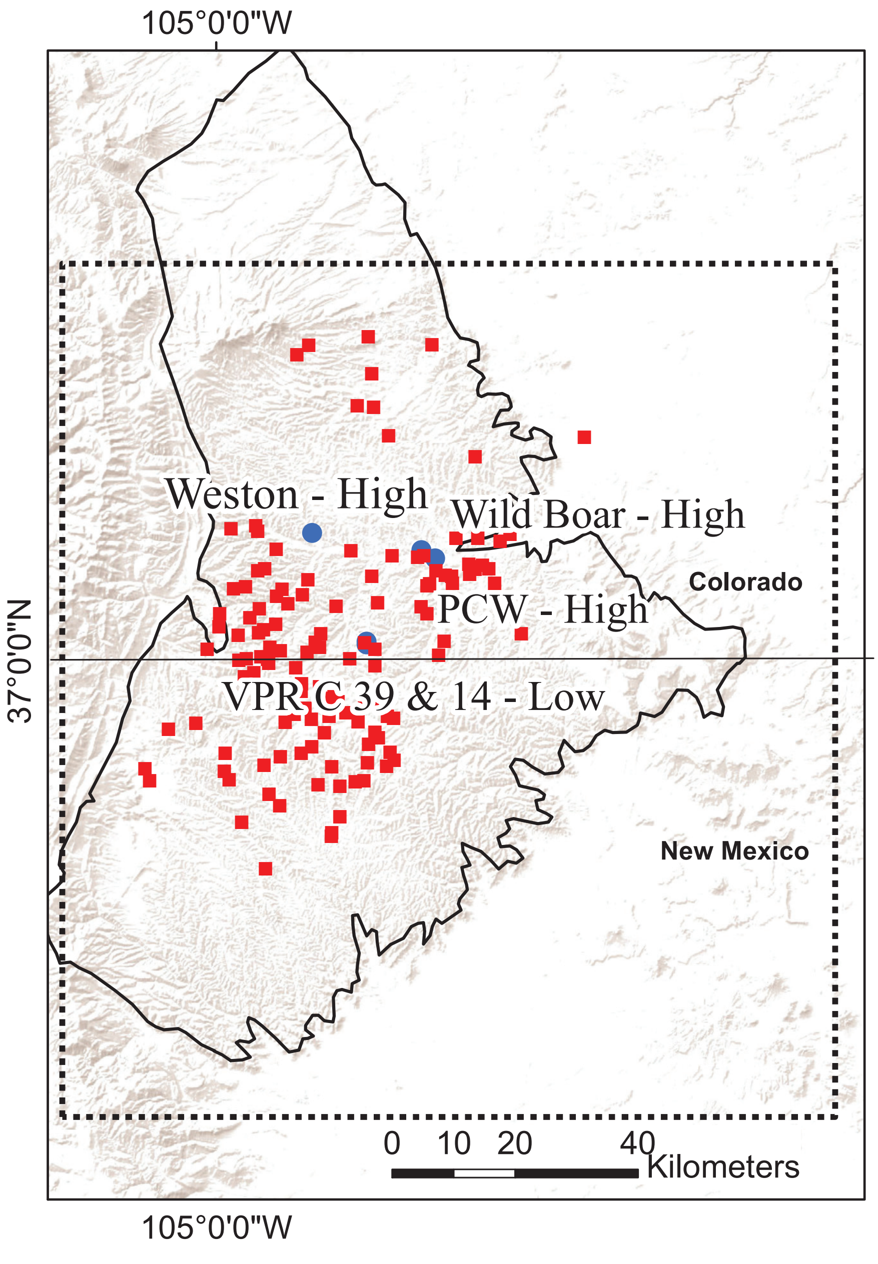

Figure 24. Location of wells analyzed for results. It is annotated if they are in low or high geothermal gradient areas.

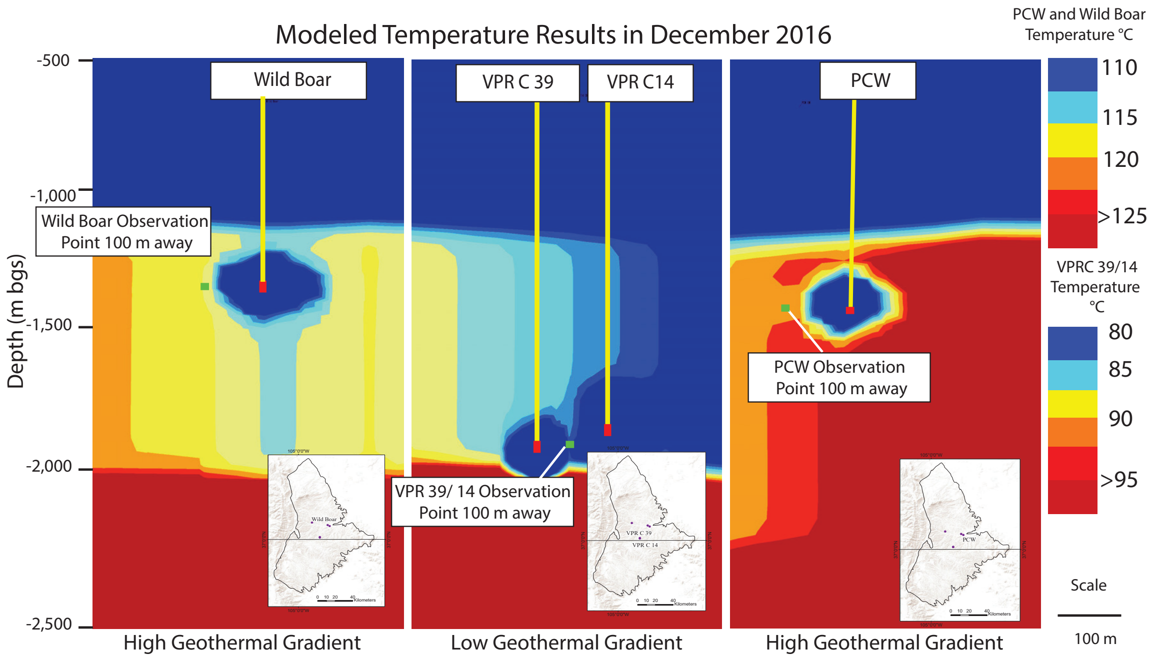

Figure 25. Modeled Temperature surrounding four injection wells (Wild Boar, VPR 39/14, and PCW).

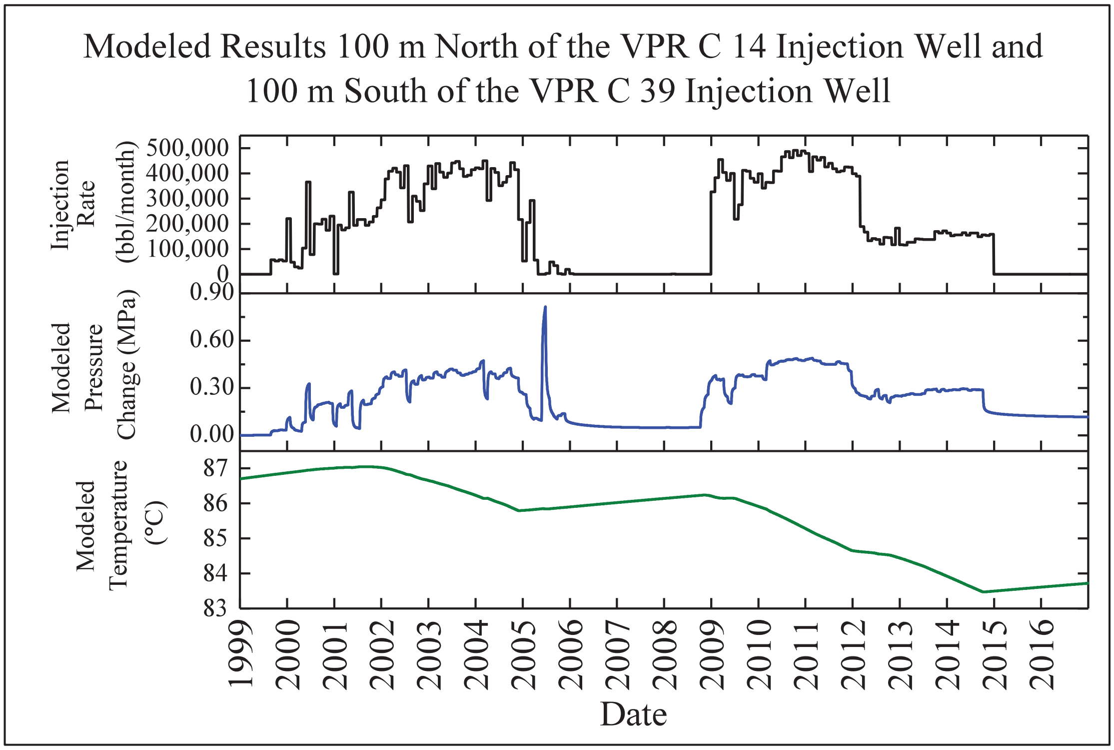

Figure 26. Modeled pressure and temperature for VPR C 14 and VPR C 39 injection wells at an observation point 100 m away from both wells in Raton Basin from 1999 – 2016. As shown in Figures 8 and 24, they are in a low geothermal gradient area. There is a break in injection due to the status of the wells being either closed or shut in for a few years.

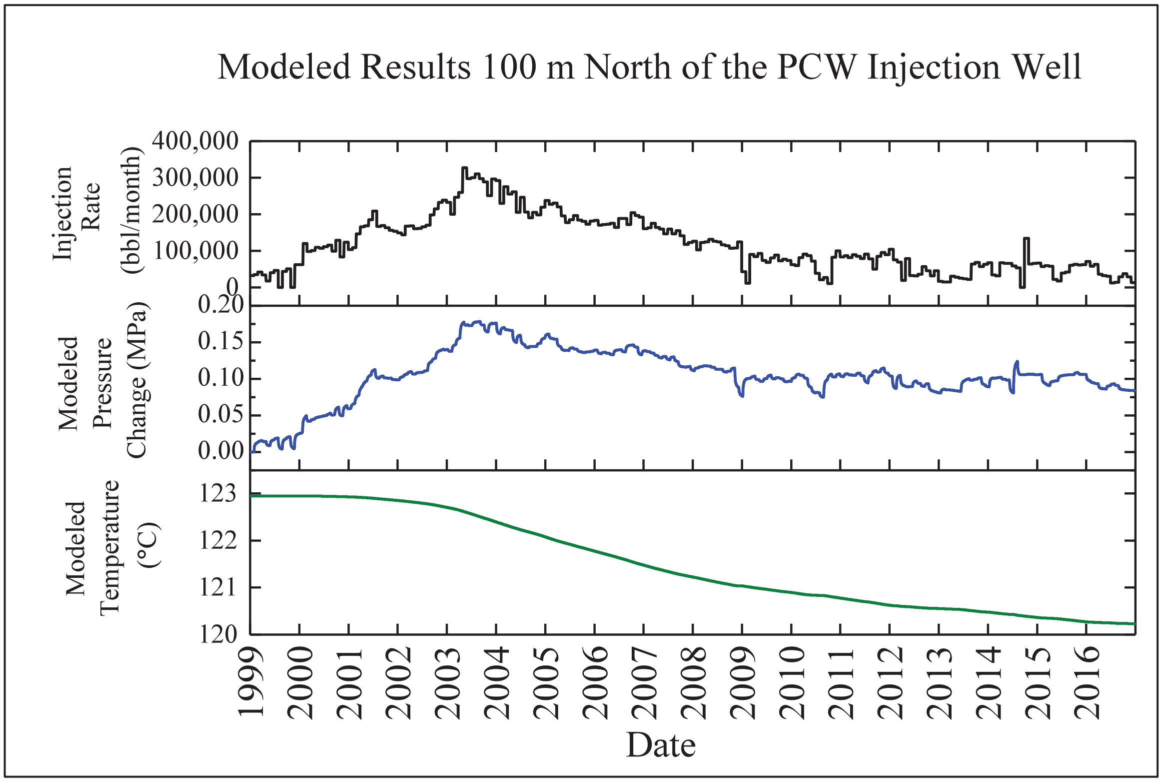

Figure 27. Modeled pressure and temperature at an observation point 100 m north of the PCW injection well in Raton Basin from 1999 – 2016. As shown in Figures 8 and 24, PCW is in a high geothermal gradient area.

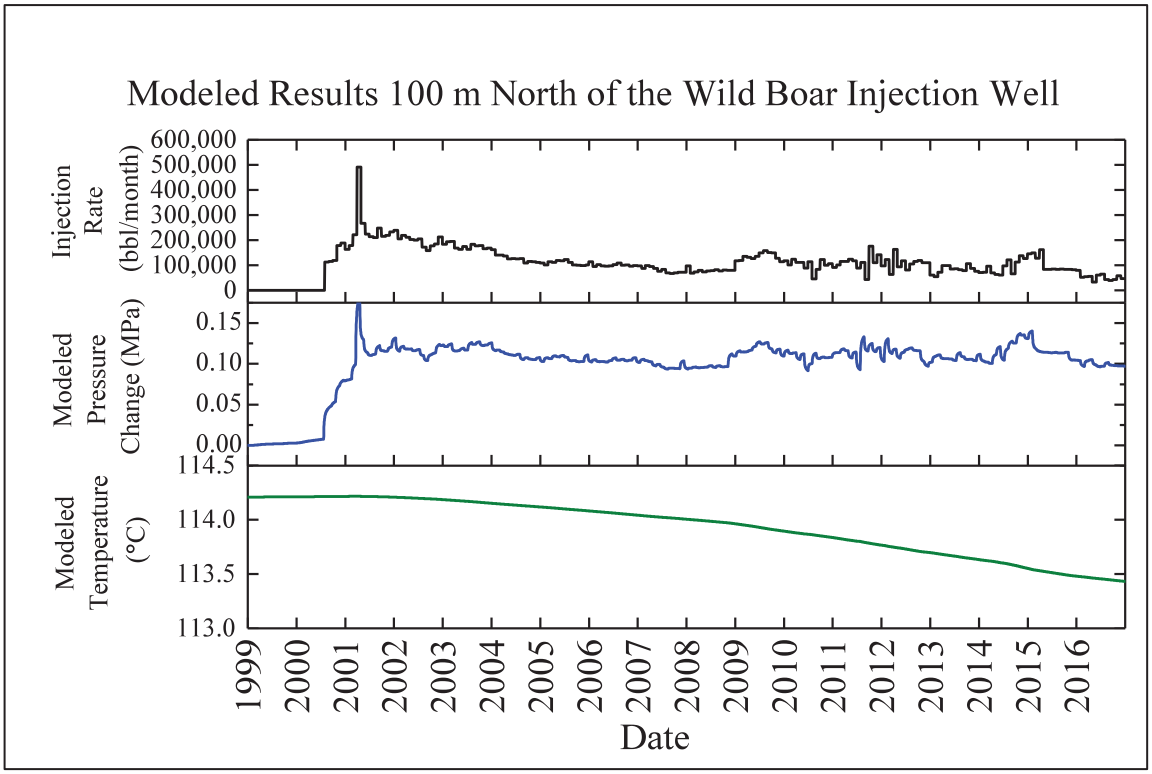

Figure 28. Modeled pressure and temperature 100 m north of the Wild Boar injection well in Raton Basin from 1999 – 2016. As shown in Figures 8 and 24, Wild Boar is in a high geothermal gradient area.

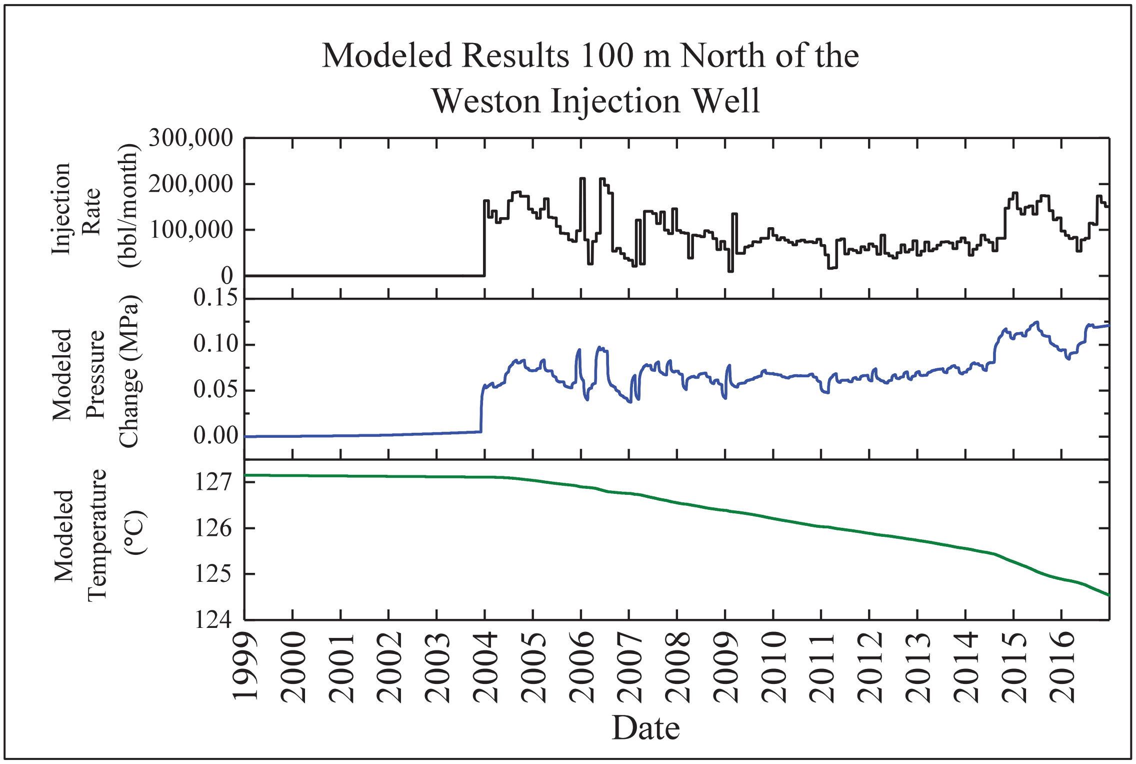

Figure 29. Modeled pressure and temperature 100 m north of the Weston injection well in Raton Basin from 1999 – 2016. As shown in Figure 8 and 24, Weston is in a high geothermal gradient area.

4.5.1 High Geothermal Gradient Wells

Disposal at the Weston well began in January 2004, and continues as of December 2016. The average disposal rate is 93,723 bbls/month (~3,000 bbl/day) and a maximum injection rate of 203,122 bbl/month (~7,000 bbl/day). The depth of the disposal is from 1,879 and 2,077 m bgs, primarily into the Purgatoire Formation (Appendix). Modeling indicated pore pressure increased up to 0.1 MPa at 100 m from the injection interval depth and 0.075 MPa at a depth of 3.3 km bgs directly below the well at the top of crystalline basement (Figures 29 and 30). Temperature decreased by approximately 3°C in the injection interval, but did not change at the basement depth (Figure 30).

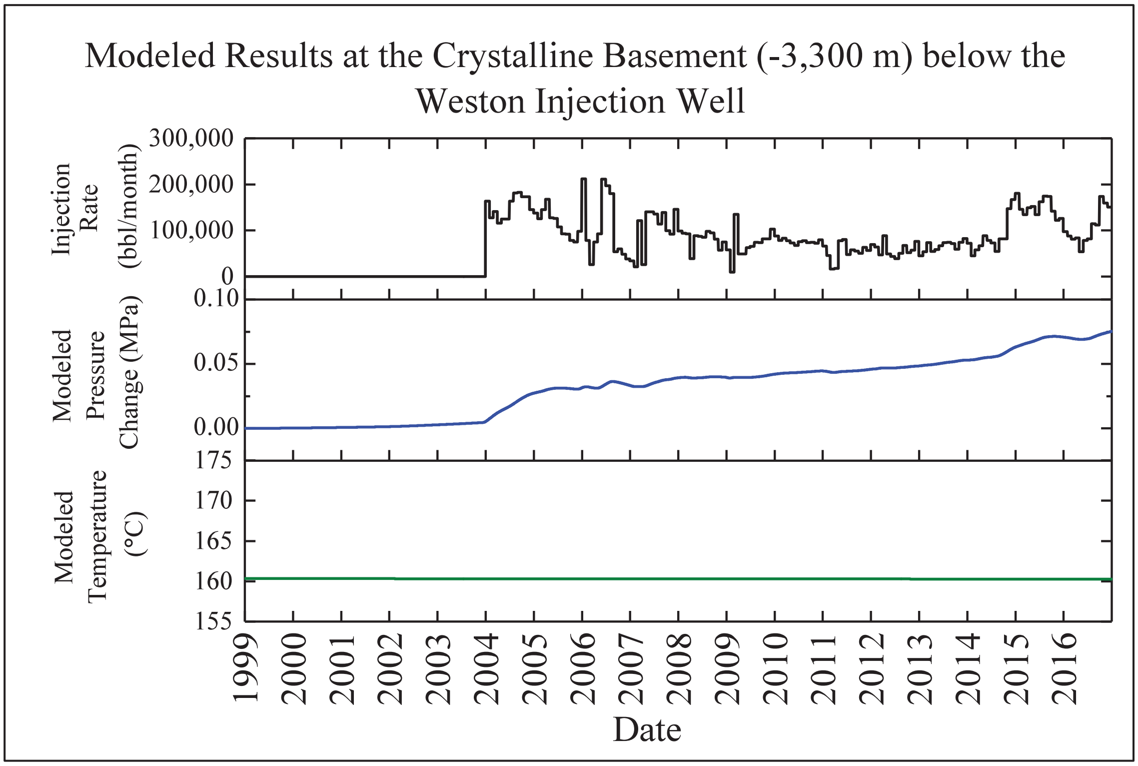

Figure 30. Modeled results at the crystalline basement below the Weston Injection well.

The PCW injection well is in the area of higher geothermal gradient within Raton Basin. PCW has been actively disposing since 1999. Its average injection rate is slightly higher than the Weston Well with a rate of 115,832 bbls/month (~3,900 bbl/day). Its injection interval is from a depth of 1,208 and 1,225 m bgs, into the Dakota Formation. Per the modeling results, pore pressure increased up to 0.15 MPa during its peak injection period in the injection interval (Figure 27). Temperature decreased up to 2°C at the injection interval depth and did not change at the basement depth.

A "worst case" scenario was run with this well injecting wastewater at 500,000 bbl/month at 11°C, instead of 20°C. The minimum temperature that wastewater is injected as recorded at disposal tanks is 11°C [Macartney, personal comm.]. This resulted in a modeled pressure change of 0.3 MPa and a temperature decrease of 20°C, 100 m from the injection well within the injection interval (Figure 31). However, the temperature remained constant below the

PCW injection well at the crystalline basement depth (Figure 32).

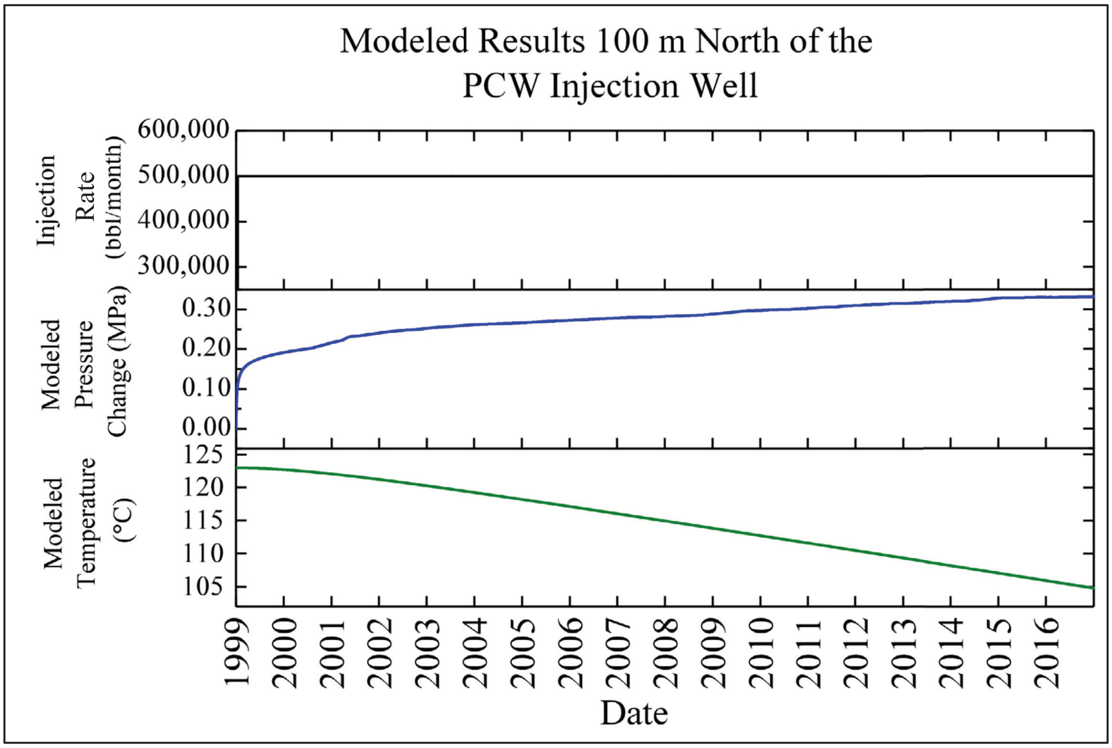

Figure 31. “Worst Case Scenario” for the PCW Injection Well. Injection was set to 500,000 bbl/month with an injection temperature of 11°C.

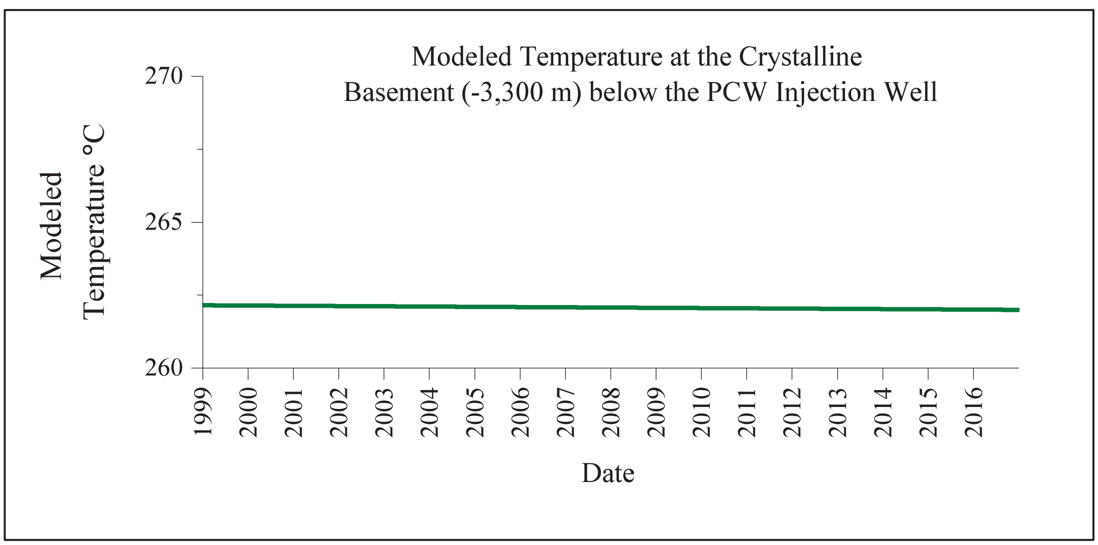

Figure 32. Modeled temperature at the basement for the PCW Injection Well.

The Wild Boar well, which began disposing in August 2000 has an average injection rate of 118,928 bbls/month (~3,900 bbl/day), with a maximum of 491,058 bbls/month (16,368 bbl/day). The cumulative volume is 23,428,799 barrels. Its injection interval ranges from 1,257 and 1,292 m bgs into the Dakota Formation. Modeling results indicate pore pressure increased by 0.15 MPa in the injection interval depth while temperature decreased by less than 1°C (Figure 16). Pore pressure increased approximately to 0.075 MPa in 17 years and temperature remained constant in the crystalline basement (Figure 33). The Wild Boar well is located 1 km from the normal fault that was added to the model (Figure 23). Modeling results showed similar ranges of pressure change below the injection well in the crystalline basement relative to the results from model simulations without the fault. Temperature did not change (Figure 34).

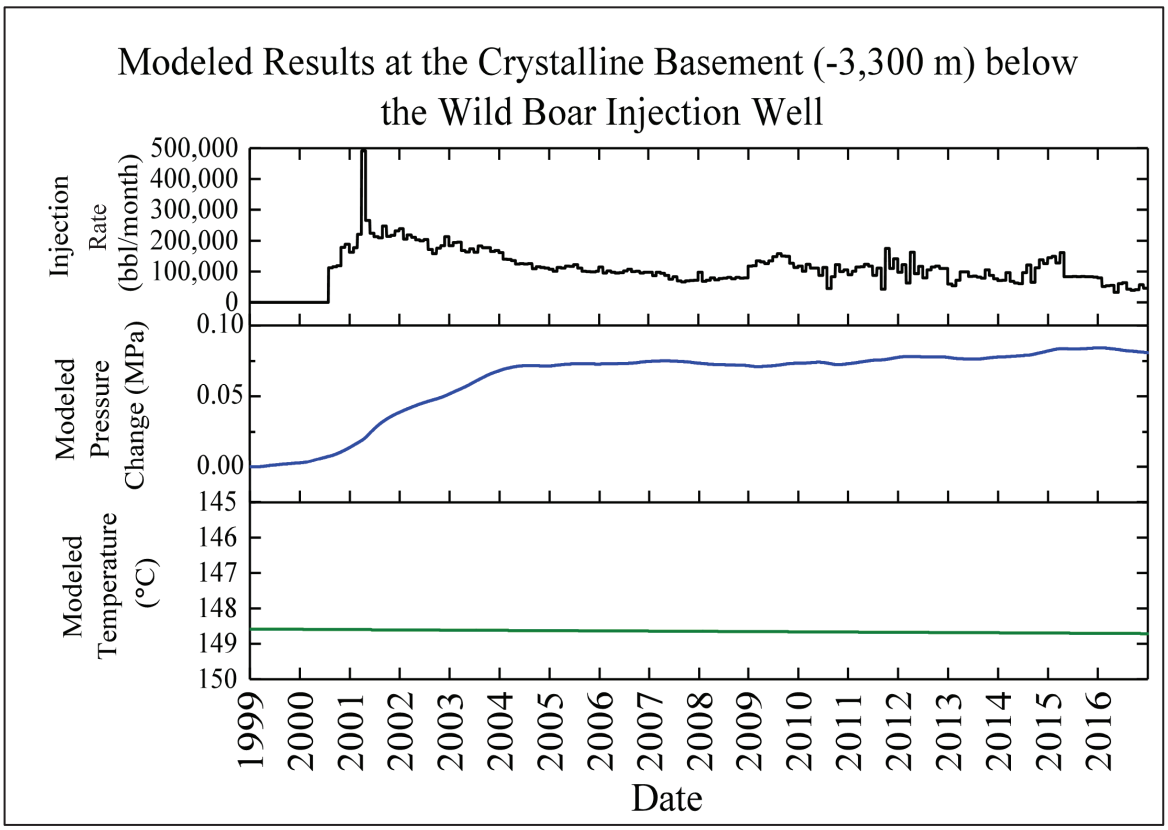

Figure 33. Modeled Results at the crystalline basement for the Wild Boar Injection Well.

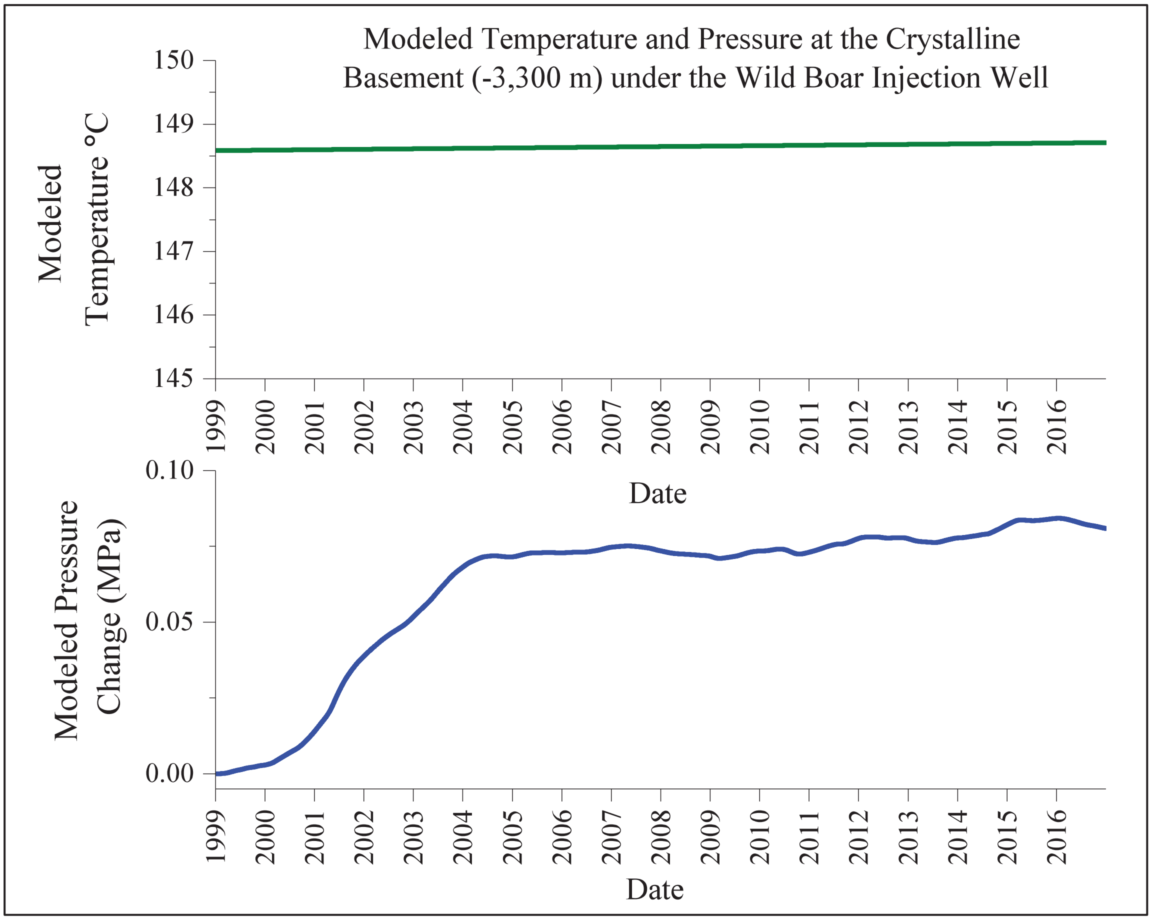

Figure 34. Modeled pressure and temperature at the crystalline basement under the Wild Boar Injection Well after the normal fault was added. See Figure 23 for the location of Wild Boar in relation to the fault. It is 1 km away from the fault.

4.5.2 Low Geothermal Gradient Wells

The VPR C 39 and VPR C 14 disposal wells are both located close to the Colorado-New Mexico border and are wells in a low geothermal gradient area (Figure 24). The injection intervals are at depths of 1,973 and 2,007 m (VPR C 39) and 1,682 and 2,020 m (VPR C 14) in the Entrada and Glorieta formations. VPR 39 started injecting in May 2000 and was shut-in in 2015. Its average injection rate is 115,757 bbls/month with a maximum rate of 356,826 bbls/month. VPR C 14 was an active injection well from September 1999 to 2002 and was closed in 2002. The average injection rate was 84,416 bbls/month and had a maximum injection of 378,554 bbls/month. Cumulative injection for these wells was 32,432,569 barrels. Modeling results indicate that pore pressure increased up to 0.6 MPa with a temperature decrease of 3°C (Figure 14). Pore pressure at the top of the crystalline basement (-3,300 m bgs) increased approximately 0.2 MPa and did not show any temperature difference between steady state temperature when cooler wastewater was injected (Figure 35).

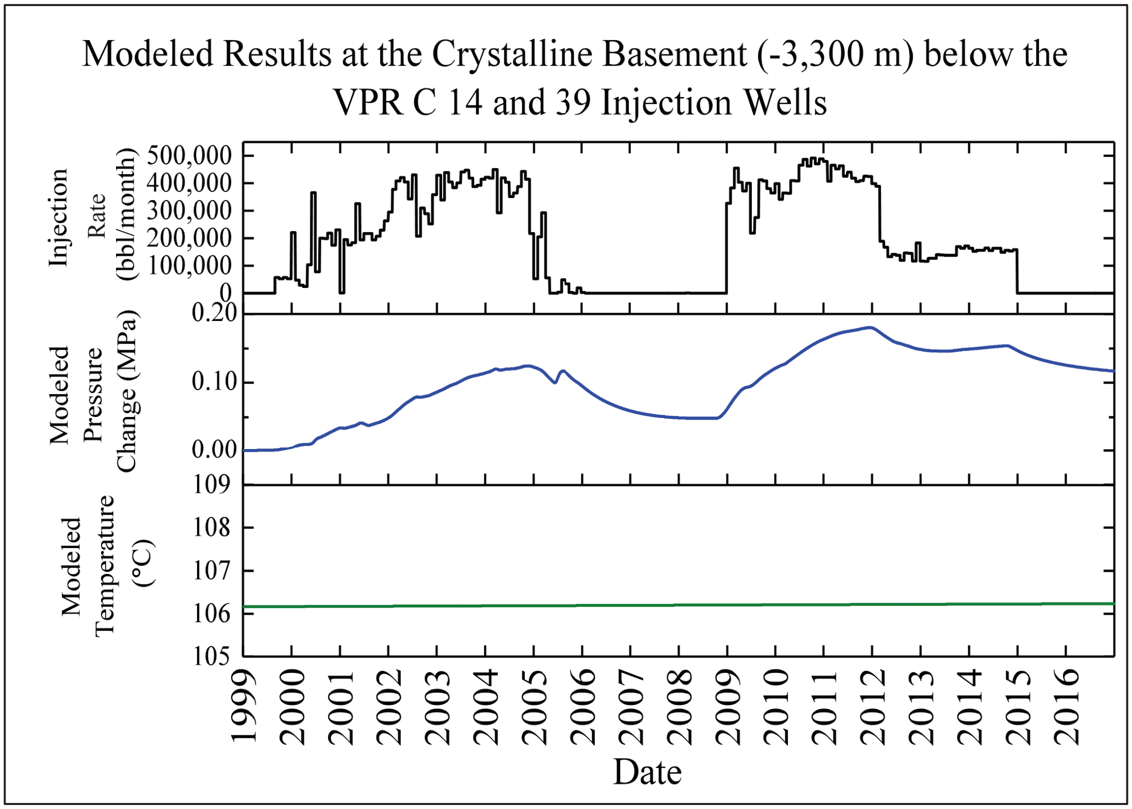

Figure 35. Modeled results at the basement below the VPR C 14 and 39 Injection Wells.

4.6 Sensitivity Analysis

Varying wastewater temperatures were used to determine if cooler wastewater would reach the basement. These temperature values were chosen from the varying temperatures that Pioneer Natural Resources had sampled over a 14 - year period. Since the wastewater is stored at above ground storage tanks, they are subject to the ambient air temperature. Therefore, the temperature of the water that is injected varies seasonally. Sensitivity tests were run using an injection temperature of 11°C and 28 °C before converging on an overall average of 20 °C (Figure 36). The injection temperature did not show any significant change to the overall temperature distribution at the injection well or the surrounding area [Figure 42-44 – Appendix].

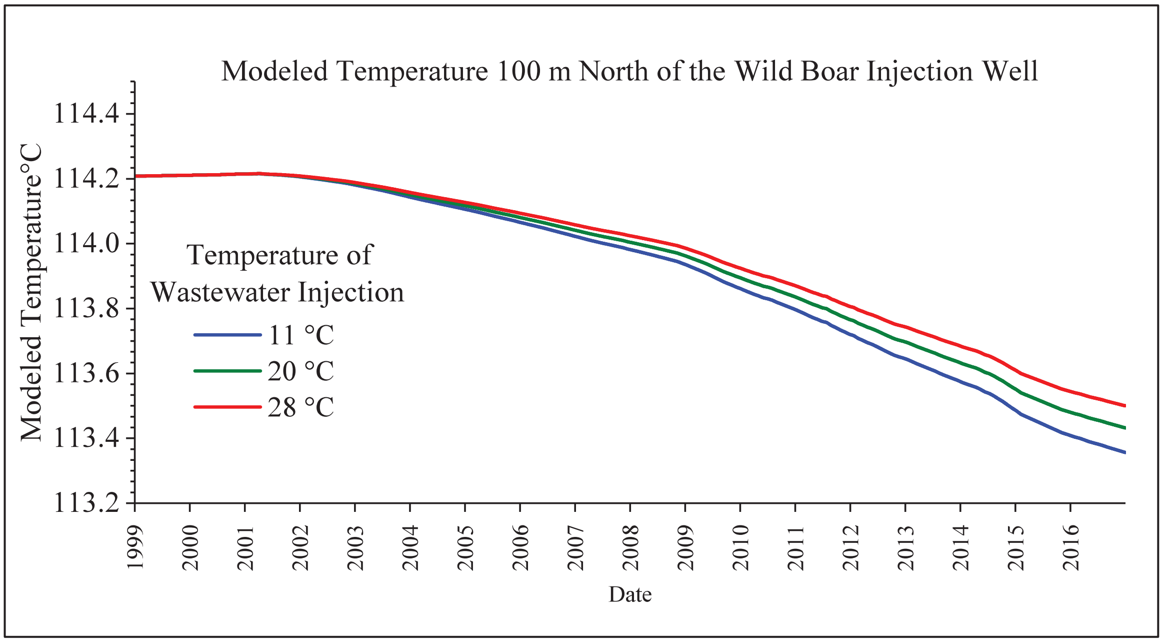

Figure 36. Sensitivity for Wastewater Injection Temperature on the Wild Boar Injection Well.

In addition to injection temperature, the permeability was varied for the Dakota Formation, as well as the Sangre de Cristo Formation. This was to see if water could migrate farther by increasing permeability in the formations. Similarly to the injection temperature, the change in permeability of the formations did not provide any significant difference for the temperature contrast and its inability to reach crystalline basement. The permeability of the fault was also changed to see if that would facilitate temperature changes or higher pore pressure diffusion, as shown by previous studies. However, modeling showed that there was not a notable difference (Figure 37).

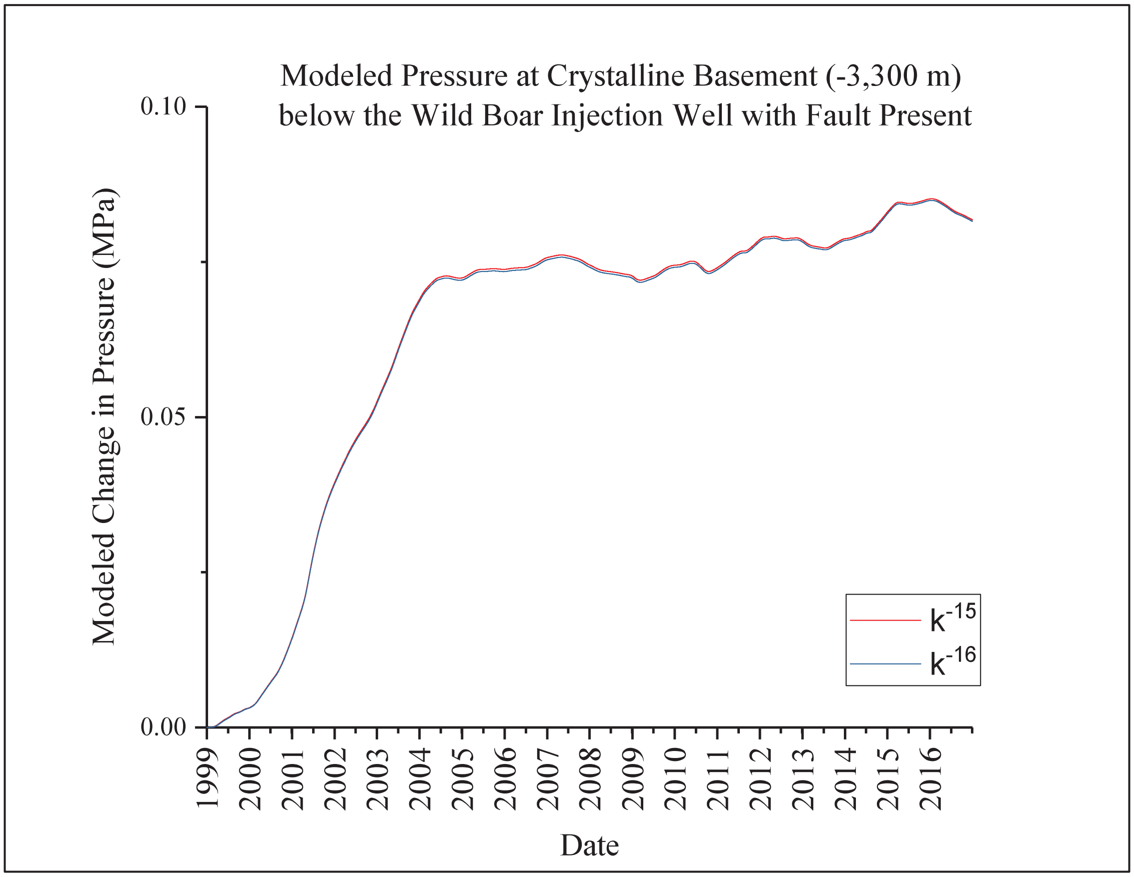

Figure 37. Modeled pressure at the crystalline basement below the Wild Boar Injection Well. Hydraulic conductivity by adding a fault was changed to see if it caused pore pressure change in the basement.

5. DISCUSSION

Diffusivity is the measurement of the area of influence (m^2) per unit of time (s). By comparing hydraulic diffusivity and thermal diffusivity in rock over the 17-year time span that the model was run, it becomes evident why the pore pressure was able to reach the depth of the crystalline basement, but any temperature change was not. Hydraulic Diffusivity (Dh) is calculated from hydraulic conductivity (K) over specific storage (Ss) (Dh = K/Ss). K is 10^{-7} m/s in the Dakota Sandstone, while specific storage is 10^{-6} m^{-1}, which gives a D of 10^{-1} (m^2/s). Diffusivity (D) is ~ L^2 (m) / T (s) where L^2 is the area of influence and T is the time that the model ran (10^8 s or 17 years). Therefore $L^2 = 10^7$ m^2 which translates to an affected area for hydraulic diffusivity on the scale of a few kilometers. Therefore, pore pressure has the ability to reach the crystalline basement, or depths that earthquakes are occurring.

Thermal diffusivity is calculated in a similar way. Thermal diffusivity of sandstones (D_T) is approximately 10^{-6} m^2/s [*Robertson*, 1988]. $D_T \sim L^2$ (m) / T (s) where T is 10^8 s (17 years that the model ran). This results in an area of influence L^2 of only tens of meters. This accounts for the inability for any temperature difference to travel the ~1.5 km to the crystalline basement from where the cooler water is being injected.

Thermal stress is calculated as $\sigma = E\ \alpha\ (\Delta T)$ where σ is the thermal stress (Pa), E is Young's modulus (Pa), α is coefficient of thermal expansion (1/°C), and ΔT is the change in temperature in °C. The total thermal stress 100 m away from the well is 0.09 MPa, which is enough to induce seismicity. α is 3×10^{-5} 1/°C and E ranges from 1 – 20 GPa (1,000 – 20,000 MPa) for sandstones [*Robertson*, 1988, UT JSG, 2018]. ΔT is 3°C at its maximum at an observation point 100 m away, resulting in a stress change between 0.09 – 1.8 MPa 100 m away from the disposal well.

Advection of heat with groundwater flow is critical to get the temperature decrease away from the disposal well. Velocity of the groundwater V = K (dh/dl) / n. K is the Hydraulic Conductivity (m/s) and is 10^{-7} m/s in the Dakota Sandstone. The Hydraulic Gradient (dh/dl) is 2×10^{-3} , which is calculated from the pressure gradient as discovered from Nelson et al., [2013]. The western edge of the model is 17 MPa and the eastern edge is 15 MPa. Therefore, the gradient of 1733.96 – 1529.96 m/ 100,000 m of the length of the basin is 2×10^{-3}. By dividing this by the effective porosity, of 0.14 for the Dakota Sandstone, the velocity of the groundwater in our model is calculated to be 1.43×10^{-9} m/s. Therefore, the area of influence with heat that will move with groundwater over the 17 years that the model is ran (10^8 s) is approximately 0.14 m.

Our hypothesis that wells in high geothermal gradient areas have higher correlation with earthquake occurrence due to thermal contrast from relatively cold wastewater injection into warmer formation rock was not validated by the TOUGH2 modeling that was performed. Although three of the wells that show a temperature decrease were located in high geothermal gradient areas, the injected water did not result in a temperature decrease close to the depth where earthquakes are occurring.

5.1 Limitations and Future Work

A number of limitations were encountered during this study. Regarding the modeling, limitations include the number of cells that the graphical interface, PetraSim, allows. The number of cells corresponds to the model grid. A finer grid (smaller area per individual cell) allows for a more accurate depiction of changes in temperature and pressure in a given area. Therefore, ideally more refined grids in the area of the disposal well sites may show the most change. The maximum number of cells that can be used in PetraSim is 200,000. Therefore, grid refinement had to be manipulated to show finer resolution at well sites without losing accuracy or exceeding the 200,000 cell limit. There is an upgraded version of PetraSim that allows for millions of cells, but was not feasible for this study due to the cost of the upgrade.

In addition to model limitations, there are also data limitations. For example, disposal well information prior to 2006 was not available for the New Mexico side of Raton Basin [NMOCD, 2016]. In addition, not all wastewater produced from CBM production is disposed of in the sub-surface. Therefore, it is not an accurate assumption that all produced water in Raton Basin is being disposed of in these disposal wells. Along with injection well data limitations, fault locations are another major gap in data collection. Seismic data would have been very helpful to accurately determine the total number and the location of faults in the subsurface. There was not any publically available seismic data.

Another limitation is uncertainty in the earthquakes' horizontal and depth locations. The USGS ANSS catalog was used in this study because it included a wide variety of earthquakes M ≥ 3 that occurred during the time frame investigated for this study (1999 – 2016). The USGS has depth error up to 8 km (Figure 2). Horizontal error is also a limitation and corresponds to as much as 5.7 km of potential error. [Table 6 - Appendix] There are other catalogs that have focused on specific sequences of earthquakes. These catalogs include *Meremonte et al.* [2002], *Rubinstein et al.,* [2014], *Barnhart et al*., [2014], and *Nakai et al.,* [2017].

Meremonte et al. [2002] investigated aftershocks and earthquakes associated with the August 2001 swarms in Raton Basin. Meremonte deployed 12 seismographs on September 6th and recorded events from September 7th – October 15th in the Fall of 2001. A total of 39 earthquakes were located and Meremonte was able to identify a 6 km long north-east trending normal fault with a dip of 70 – 80 ° to the southeast [Table 10 – Appendix]. This fault extends from 3 – 6 km bgs. Most earthquakes in this 2001 catalog occur at these depths and their depth errors are +/- 1.5 km (Figure 38). This catalog supports the hypothesis that earthquakes are occurring along faults at crystalline basement depths.

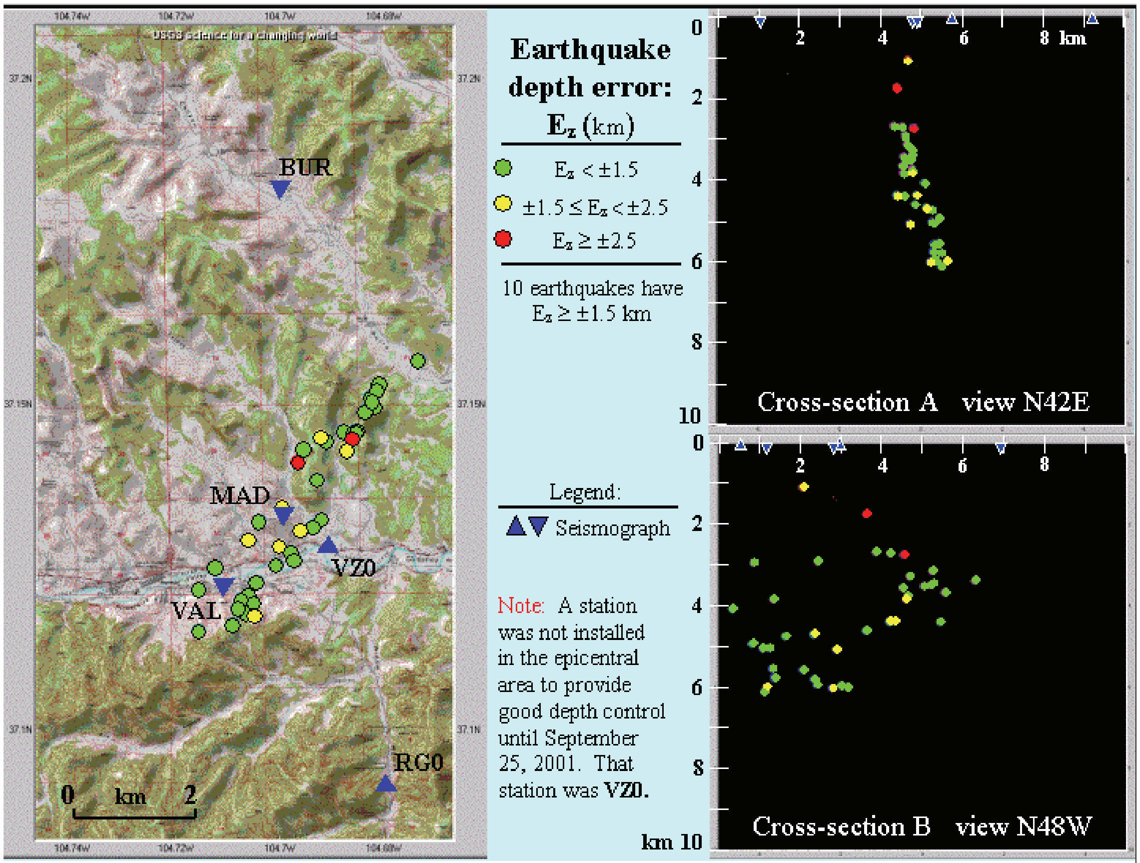

Figure 38. Depth errors in Meremonte catalog from aftershocks to the August 2001 earthquakes [*Meremonte et al*., 2002].

Barnhart et al., [2014] looked at earthquakes associated with the 2011 Mw 5.3 event. Following this event, four more seismometers were deployed in the region to record aftershocks. The USGS National Earthquake Information Center (NEIC) located 584 aftershocks from August 23, 2011 to December 15, 2011. These were traced to the crystalline basement along an 8 – 10 km normal fault. Depths range from 1.5 to 6 km. *Rubinstein et al.,* [2014] analyzed M ≥ 3.8 earthquakes from August 2001 – 2013 in Raton Basin. 16 events were observed and have epicenter uncertainties of +/- 15 km. Although the earthquakes were located without the use of high density array, the uncertainties for the 2001 and 2011 sequences have lower uncertainties of 2 km. Epicenters for these events are within 2 km of high, volume, high injection rate wells.

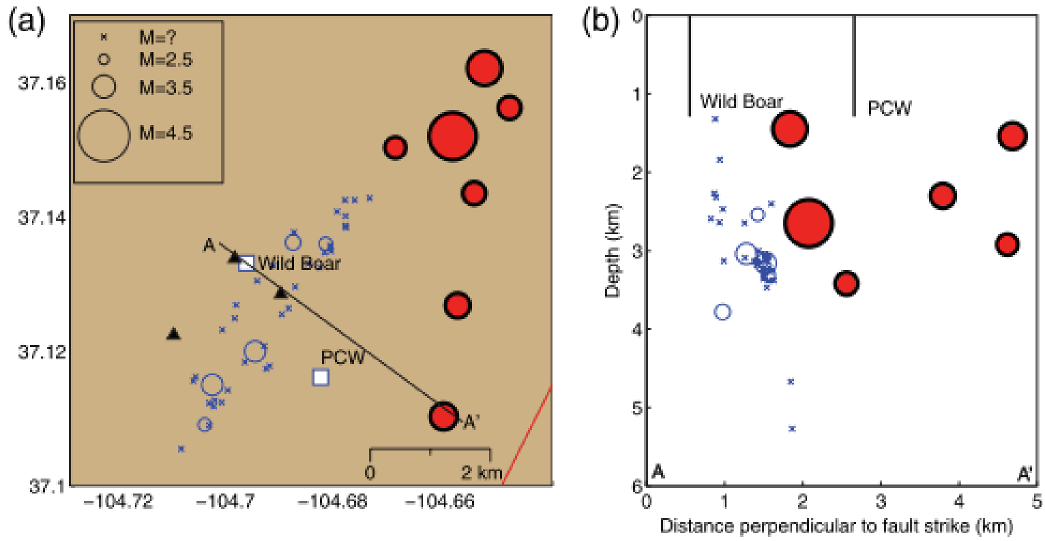

Figure 39. Earthquake epicenters near the Wild Boar and PCW disposal wells. A) Plan view of the earthquakes. B) Cross section view with the two disposal wells. The lineation of earthquakes corresponds to the modeled fault that was added into the model (Figure 23) [*Rubinstein et al.* 2014]

Nakai provided the last catalog that was used to determine epicenter depth. The EarthScope Transportable Array (TA) provided additional seismic coverage that allowed for improved earthquake epicenter locations. Nakai et al., [2017] manually located 1,881 earthquakes with P and S waves from 2008 - 2010. A majority of the earthquakes were located between 4 – 6 km, at basement depths, but had depths extending from 1 – 20 km depending on the velocity model that was used. The epicentral errors for Nakai et al., 2017 catalogs are +/- 2 km for the catalog. The depths Nakai determined are similar to *Rubinstein et al.,* [2014] and *Barnhart et al*. [2014].

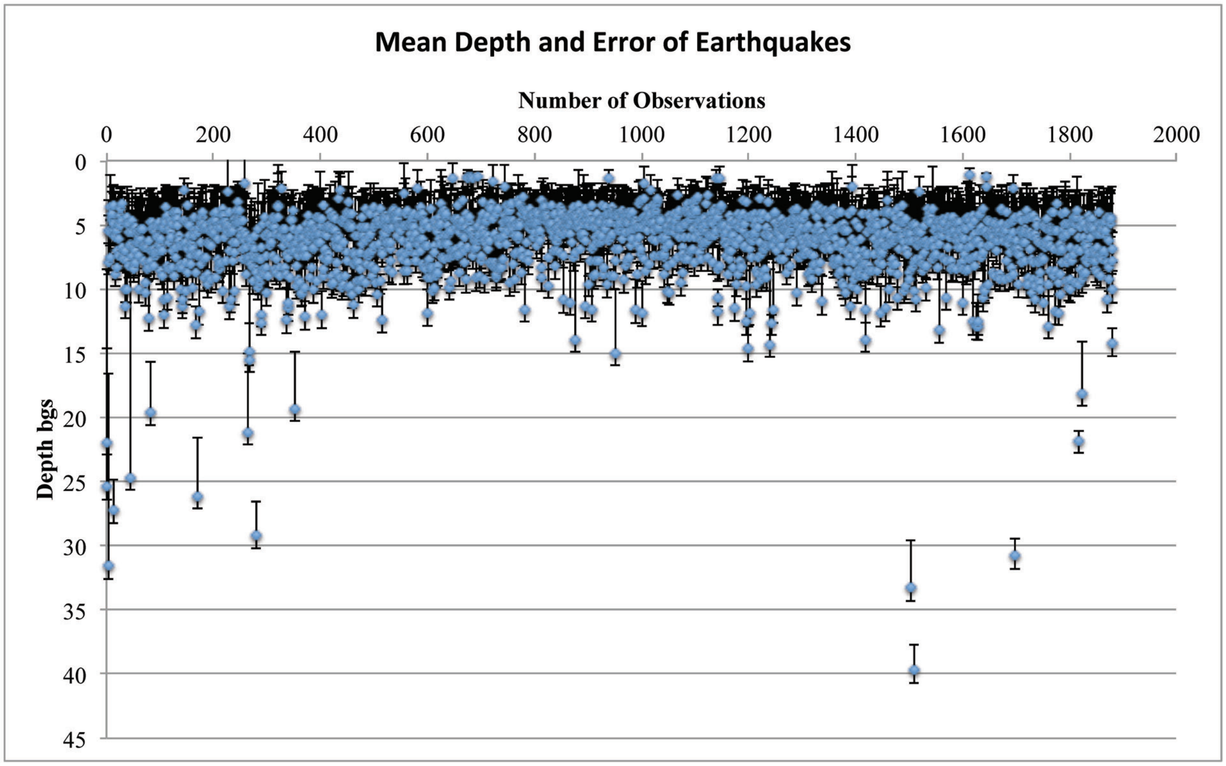

Figure 40. Mean depth with vertical depth error for earthquakes from Nakai's Catalog [Nakai et al., 2017]

6. CONCLUSION

Model results show that temperature can decrease up to 3°C at 100 m from injection wells over a period of 17 years in the injection interval of Raton's wastewater disposal wells. This cooling does not appear to cause significant thermal contraction and therefore rock failure because it is not reaching the depths at which earthquakes are occurring. Results from the crystalline basement directly below the injection wells show that temperature remains unchanged throughout the 17 years. (Figures 18 – 23). Thus the geothermal gradient does not seem to play any significant role with respect to induced seismicity as shown by hydrogeologic and thermal modeling. Modeling shows that there is only a limited spatial relationship between the geothermal gradient, injection wells, and earthquakes. Our modeling further solidified the theory that pore pressure increase in the basement, as a result of wastewater injection, is a major mechanism for induced seismicity in Raton Basin as it is within the range to create earthquakes (>0.01 MPa) [*King et al.,* 1994].

References

Abbott, P. O., A. L. Geldon, D. Cain, A. P. Hall, and P. Edelmann (1983), Hydrology of Area 61, Northern Great Plains and Rocky Mountain Coal Provinces, Colorado and New Mexico, *U.S. Geologic Survey. Water Resources Investigations Open File Report 83-132*, 1-99.

ANSS, (2016) Advanced National Seismic System Catalog by the United States Geological Survey. Search - USGS. Accessed October 2016. https://earthquake.usgs.gov/monitoring/anss/

AAPG Wiki, (2016) Province, basin, system, play, and prospect. Accessed October 2018. http://wiki.aapg.org/Province,_basin,_system,_play,_and_prospect

Baltz, E. H. (1965), Stratigraphy and History of Raton basin and Notes on San Luis Basin, Colorado – New Mexico, *Bulletin of the American Association of Petroleum Geologists*, *49*(11), 2041–2075.

Barnhart, W. D., H. M. Benz, G. P. Hayes, J. L. Rubinstein, E. Bergman, H. M. Benz, G. P. Hayes, J. L. Rubinstein, and E. Bergman (2014), Seismological and geodetic constrains on the 2011 Mw 5.3 Trinidad, Colorado earthquake and induced deformation in the Raton Basin, *Journal of Geophysical Research : Solid Earth*, 7923- 7933, doi:10.1002/2014JB011227.Received.

Belitz, K., and J. D. Bredehoeft (1988), Hydrodynamics of Denver basin: explanation of subnormal fluid pressures, The *American Association of Petroleum Geology Bulletin, 72*(11), 1334–1359, doi:10.1306/703C999C-1707-11D7-8645000102C1865D.

Billingsley, Lee (1977), Stratigraphy of the Trinidad Sandstone and Associated Formations Walsenburg Area, Colorado, Exploration Frontiers of the Central and Southern Rockies, Rocky Mountain Association of Geologists – 1977 Symposium, 235 – 246.

Blackwell, D. (2011), SMU Geothermal Laboratory Heat Flow Map of the Conterminous United States, 2011, Available at http://www.smu.edu/geothermal

Bohlen, K., (2012), Preliminary Geothermal Resource Assessment for the Raton Basin, Colorado, Geothermal Resources Council (GRC Transactions), *36*, 1327 – 1334. http://pubs.geothermal-library.org/lib/grc/1030403.pdf

Bohlen, K. (2013), Pre-Exploration Geothermal Resource Assessment for the Raton Basin, Colorado — The Rest of the Story, Geothermal Resources Council (GRC Transactions), *37*, 933 – 940. http://pubs.geothermal-library.org/lib/grc/1030683.pdf

Brodsky, E. E., and L. J. Lajoie (2013), Anthropogenic Seismicity Rates and Operational Parameters at the Salton Sea Geothermal Field, *Science*, 341, 543 – 546(August).

Brown, M.R.M. and S. Ge, 2018, Distinguishing Fluid Flow Path from Pore Pressure Diffusion for Induced Seismicity, Bulletin of the Seismological Society of America, doi: 10.1785/0120180149

Carlton, D. R. (2006), Discovery and Development of a Giant Coalbed Methane Resource, Raton Basin, Las Animas County, Southeast Colorado, *The Mountain Geologist*, *43*(3), 231–236.

COGCC (2016), Colorado Oil and Gas Conservation Commission, Available from: http://cogcc.state.co.us/#/home (Accessed October 2016).

Comsol, 2017, Poroelasticity, Multiphysics Cyclopedia Accessed September 2018. https://www.comsol.com/multiphysics/poroelasticity

De Simone, S., V. Vilarrasa, J. Carrera, A. Alcolea, and P. Meier (2013), Thermal coupling may control mechanical stability of geothermal reservoirs during cold water injection, *Physics and Chemistry of the Earth, 64*, 117–126, doi:10.1016/j.pce.2013.01.001.

Dolly, E. D., and F. F. Meissner (1977), Geology and gas exploration potential, Upper Cretaceous and lower Tertiary strata, northern Raton Basin, *Explor. Front. Cent. South. Rockies*, 247–270.

Ellsworth, W.L (2013) Injection – Induced Earthquakes, *Science,* 341 (6142), 1225942-1 - 1225942-8, doi: 10.1126/science.1225942

Environmental Protection Agency (EPA, 2018). General Information About Injection Wells – Underground Injection Control. Accessed July 2018 https://www.epa.gov/uic/general-information-about-injection-wells

Evans, D. M. (1966), The Denver Area Earthquakes and the Rocky Mountain Arsenal Disposal Well, *The Mountain Geologist*, *3*(1), 23–36.

Folger, P., and M. Tiemann (2015), Human-Induced Earthquakes from Deep-Well Injection: A Brief Overview, Congressional Research Service, 1–26.

Foulger, G. Miles ,P. Wilson, J. G. Gluyas, B. R. Julian, R. Davies (2017), Global review of human-induced earthquakes, *Earth- Science Reviews*, 179, 438 – 514.

Gabelman (2005), Geology of the Sangre De Cristo Mountains of Colorado and New Mexico, OCGS Guidebook – Panhandle of Oklahoma, Northeastern New Mexico, South- Central Colorado; 35th Anniversary Field Conference, 1956, 173 – 189

Gaucher, E., M. Schoenball, O. Heidbach, A. Zang, P. Fokker, J.-D. van Wees, and T. Kohl (2015), Induced Seismicity in Geothermal Reservoirs: Physical Processes and Key Parameters, *Proceeding World Geothermal Congress 2015*, Melbourne, Australia, April, 2015, 1– 14.

Geldon, A. L. (1989), Ground-Water Hydrology of the Central Raton Basin, Colorado and New Mexico, *U.S. Geologic Survey Water-Supply Paper 2288*, 1 – 90.

Higley, Debra (2005) National Assessment of Oil and Gas Project – Raton Basin – Seirra Grande Uplift Province (041) Boundary, *USGS,* USGS Digital Data Series DDS – 69- N.

Hubbert, M. K. and W. Rubey (1959), Role of Fluid Pressure in Mechanics of Overthrust Faulting, *Bulletin of the Geological Society of America,* 70, 115-166.

Kelley, S. A. (2015), Geothermal potential of the Raton Basin, New Mexico, *New Mexico Geological Society*, Guidebook 66 - Geology of the Las Vegas Area, New Mexico Geological Society 66th Annual Fall Field Conference Guidebook, 261 – 275.

Kelley, S. (2011), New Mexico Borehole Temperature, Available from: http://search.geothermaldata.org/dataset/new-mexico-borehole-temperatures (Accessed 22 January 2018)

King, G. C. P., R. S. Stein, and J. Lin. (1994), Static stress changes and the triggering of earthquakes, *Bulletin of the Seismological Society of America*, 84, 935-953.

Macartney, H., and P. Morgan (2011), The Potential for Geothermal Energy Recovery from Enhanced Geothermal Systems in the Raton Basin of Southern Colorado, USA, *Enhanced Geothermal Systems, AAPG/SPE/SEG Hedberg Conference*, (March 14 – 18, 2011), 1.

Majer, E. L., R. Baria, M. Stark, S. Oates, J. Bommer, B. Smith, and H. Asanuma (2007), Induced seismicity associated with Enhanced Geothermal Systems, *Geothermics*, *36*(3), 185–222, doi:10.1016/j.geothermics.2007.03.003.

Meremonte, M., J. C. Lahr, A. D. Frankel, J. W. Dewey, A. J. Crone, D. E. Overturf, D. L. Carver, and W. T. Bice (2002), An Investigation of an earthquake swarm near Trinidad, Colorado, August- October 2001, *U.S. Geologic Survey Bulletin Series 02 - 0073*

Morgan, P. (2009), A Preliminary Analysis of Geothermal Resources in the Central Raton Basin, Colorado, from Bottom-Hole Temperature Data, *GRC Transactions.*, *33*, 509–514.

Morgan, P., and J. C. Witcher (2011), Geothermal Resources Along the Southern Rocky Mountains and the Rio Grande Rift, *The Mountain Geologist*, *48*(4), 81 – 93.

Morgan, Personal communication. (2017).

National Geothermal Data System, 2017, New Mexico Borehole Temperatures. http://search.geothermaldata.org/dataset/new-mexico-borehole-temperatures

Nakai, J. S., Weingarten, M., Sheehan, A. F., Bilek, S. L., & Ge, S. (2017). A possible causative mechanism of Raton Basin, New Mexico and Colorado earthquakes using recent seismicity patterns and pore pressure modeling. Journal of Geophysical Research: Solid Earth, 122, 8051 - 8065. https://doi.org/10.1002/2017JB014415

Nathenson, M., and M. Guffanti (1988), Geothermal gradients in the conterminous United States, *Journal of Geophysical Research, 93*(6), 6437– 6450.

Nelson, P. H., N. J. Gianoutsos, and L. O. Anna (2013), Outcrop Control of Basin-Scale Underpressure in the Raton Basin, Colorado and New Mexico, *The Mountain Geologist.*, *50*(2), 37–63.

NMOCD (2016), New Mexico Oil Conservation Division - OCD Permitting- Well Search, Available from: https://wwwapps.emnrd.state.nm.us/ocd/ocdpermitting/Data/Wells.aspx

Osterhourt, S. L., B. W. Rothkopf, and H. Soetrisno (2014), Raton Basin: Raton Basin Coal Bed Methane Gas Field, Colorado and New Mexico, The Rocky Mountain Association of Geologist, 267–292.

Pruess, Karsten, Oldensurg, Curt and Moridis, George (2012), TOUGH2 User Guide, Version 2.1, Berkley, CA, USA: Earth Science Division, Lawrence Berkeley National Laboratory, November 1999.

Sares, M., P. Morgan, and V. J. Grauch (2009), Geothermal Resources of Colorado and the Potential for Electrical Power Generation, *Search and Discovery. Artic. #80069*.

Stevens, S. H., T.E. Lombardi, B.S. Kelso, and J.M. Coates (1992), A geologic assessment of natural gas from coal seams in the Raton and Vermejo Formations, Raton Basin, *Gas Research Inst. Top. Rep*., 92/0345, 1 – 84.

Thunderhead Engineering, (2016), PetraSim User Manual

Topper, R. K. Scott. N. Watterson (2011), Geologic Model of the Purgatoire River Watershed in the Raton Basin, Colorado, Colorado Geological Survey, 1 – 53.

Robertson, E.C. (1988) Thermal properties of rocks, *USGS,* 88-441

Rubinstein, J. L., and A. B. Mahani (2015), Myths and Facts on Wastewater Injection, Hydraulic Fracturing, Enhanced Oil Recovery, and Induced Seismicity, *Seismological Research Letters, 86*(4), 1060–1067, doi:10.1785/0220150067.

Rubinstein, J. L., W. L. Ellsworth, A. McGarr, and H. M. Benz (2014), The 2001 to present induced earthquake sequence in the Raton Basin of northern New Mexico and southern Colorado, *Bulletin of the Seismological Society of America, 104*(5), 2162–2181, doi:10.1785/0120140009.

U.S. DOE (2006), U.S. Department of Energy – Geothermal Technologies Office, Available from: http://energy.gov/sites/prod/files/2014/02/f7/egs_factsheet.pdf (Accessed 23 March 2017)

University of Texas – Austin Jackson School of Geoscience, (2018), Some Useful Numbers on the Engineering Properties of Materials (Geologic and Otherwise) GEOL 615, Accessed October 2018, https://www.jsg.utexas.edu/tyzhu/files/Some-Useful-Numbers.pdf

Viegas, G., K. Buckingham, A. Baig, and T. I. Urbancic (2012), Large Scale Seismicity Related to Wastewater Injection near, AAPG Search and Discovery Article # 90174, *GeoConvention May 14 – 18 2012*, 1–7.

Weingarten, M., S. Ge, J. W. Godt, B. A. Bekins, and J. L. Rubinstein (2015), High-rate injection is associated with the increase in U.S. Mid-Continent Seismicity, *Science, 348*(6241).

Weingarten, M. B. (2015), On the Interaction Between Fluids and Earthquakes in Both Natural and Induced Seismicity, Chapter 5 – Fluid- Pressure modeling of Injection in Raton Basin, Colorado – New Mexico : A Case Study of Induced Seismicity, University of Colorado, Boulder, CO.

Zang, A., V. Oye, P. Jousset, N. Deichmann, R. Gritto, A. Mcgarr, E. Majer, and D. Bruhn (2014), Analysis of induced seismicity in geothermal reservoirs – An overview, *Geothermics*, *52*, 6–21.

Appendix

Table 3. Disposal Well Locations

Name	Latitude	Longitude	Top Injection Depth(m)	Bottom Injection depth (m)
Jarosa 32-33 WD	37.09	-104.78	1667	1710
SouthPaw	37.3	-104.729	1711	1710
Cottontail Pass Disposal 32-33	37.22	-104.78	1899	1986
Cimarron 32-18 WD	37.26	-104.93	2116	2149
Ferminia	37.29	-104.83	1834	1899
Sawtooth	37.2	-104.67	1344	1383
La Garita	37.16	-104.8	1624	1632
San Pablo 11-4 WD	37.206	-104.899	1879	2077
Weston 24-23 A WD	37.15	-104.86	1680	1710
Long Canyon 43-12 WD	37.09	-104.62	1128	1172
Apache Canyon 19-10	37.07	-104.93	1879	1938
Apache Canyon 10-3	37.1	-104.99	2147	2179
VPR C 204 WDW	37.01	-104.83	1648	1929
PCW	37.12	-104.68	1208	1225
Wild Boar	37.13	-104.7	1257	1292
Hill Ranch Deep	37.09	-104.74	1454	1489
Beardon	37.25	-104.66	1459	1489
Polly	37.23	-104.7	1431	1612
Del Agua	37.28	-104.74	1733	1737
Lopez Canyon SWD	37.15	-104.89	1837	1985
VPR A 007	36.955	-105.4	1951	2001
VPR C 39	37.023	-104.78	1973	2007
VPR C 14	37.02	-104.78	1682	2020
VPR A 182	36.98	-104.8	1842	2148
VPR A 500	36.89	-104.75	2078	2171
VPR B 027	36.8	-104.94	1950	2240
VPR D 025	36.86	-105.057	1935	2240
VPR A 042	36.96	-104.83	2063	2273
VPR E 099	36.96	-104.9	2163	2301

Table 4. Disposal Operator and target formation for disposal [COGCC, 2016; NMOCD, 2016].

Name	Operator	Years Active	Formation of Injection
Jarosa 32-33 WD	Pioneer Natural Resources	2007-2016	Dakota, Purgatoire
SouthPaw	Pioneer Natural Resources	2009-2016	Dakota
Cottontail Pass Disposal 32-33	Pioneer Natural Resources	1999-2016	Dakota, Purgatoire
Cimarron 32-18 WD	Pioneer Natural Resources	2005-2016	Dakota, Purgatoire
Ferminia	Pioneer Natural Resources	2007-2016	Dakota
Sawtooth	Pioneer Natural Resources	2000-2016	Dakota, Purgatoire
La Garita	Pioneer Natural Resources	2001-2016	Dakota
San Pablo 11-4 WD	Pioneer Natural Resources	2014-2016	Dakota,Entrada, Morrison, Purgatoire
Weston 24-23 A WD	Pioneer Natural Resources	2004-2016	Dakota (primary Purgatoire)
Long Canyon 43-12 WD	Pioneer Natural Resources	2004-2016	Dakota, Purgatoire
Apache Canyon 19-10	XTO Energy	1999-2016	Dockum
Apache Canyon 10-3	XTO Energy	1999-2016	Dakota, Entrada
VPR C 204 WDW	ARP Production Company	2012-2016	Dakota, Entrada, Glorieta
PCW	Pioneer Natural Resources	1999-2017	Dakota
Wild Boar	Pioneer Natural Resources	1999-2018	Dakota, Purgatoire
Hill Ranch Deep	Pioneer Natural Resources	2005-2016	Dakota
Beardon	Pioneer Natural Resources	2001-2016	Dakota, Purgatoire
Polly	Pioneer Natural Resources	2009-2015	Dakota, Entrada
Del Agua	Pioneer Natural	2005-2013	Dakota

	Resources		
Lopez Canyon SWD	XTO Energy	2010-2016	Dakota, Entrada, Purgatoire
VPR A 007	ARP Production Company	2006-2016	Dakota
VPR C 39	ARP Production Company	2000-2016	Entrada, Glorieta
VPR C 14	SONAT Raton LLC	1999-2002	
VPR A 182	ARP Production Company	2006-2016	Entrada and Glorieta
VPR A 500	ARP Production Company	2006-2017	Glorieta, Dakota
VPR B 027	ARP Production Company	2006-2018	Entrada and Glorieta
VPR D 025	ARP Production Company	2006-2019	Dakota, Entrada
VPR A 042	ARP Production Company	2006-2020	Dakota, Entrada
VPR E 099	ARP Production Company	2006-2021	Entrada and Glorieta

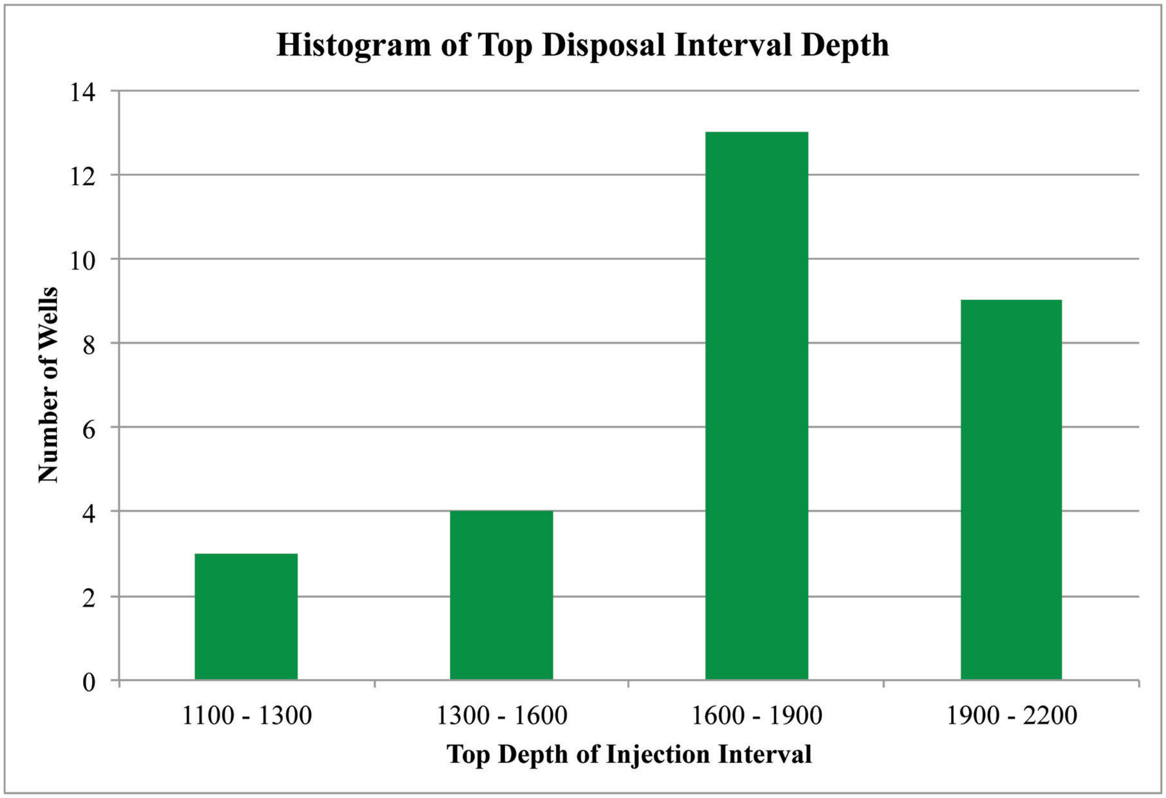

Figure 41. Histogram of injection well depths [COGCC, 2016; NMOCD, 2016].

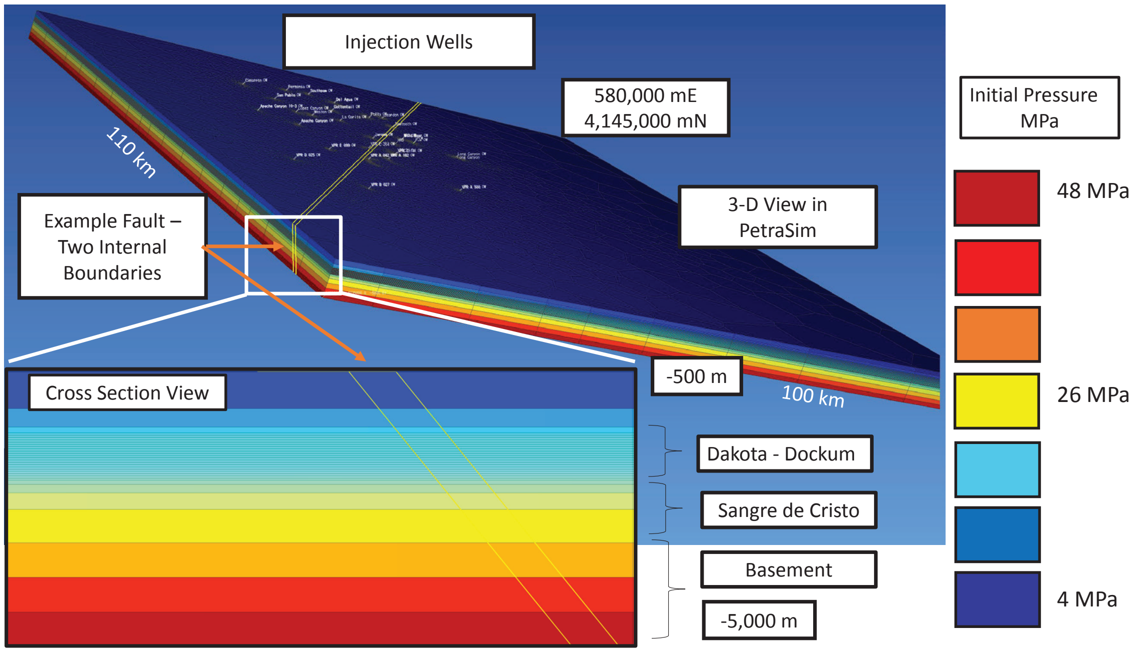

Figure 42. Model in 3-D with Initial Pressure shown in MPa. Cross Section view shows the grid refinement in the disposal interval.

Table 5. Earthquake Locations from USGS Catalog [ANSS, 2018]

Date	Time	Lat	Long	Depth	Magnitude	Measurement Type
9/23/73	58:54.9	37.148	-104.571	5	4.2	Mb
4/15/92	46:05.1	37.335	-104.773	5	3.3	Unknown
5/2/92	19:29.8	37.378	-104.778	5	3.1	Unknown
8/28/01	16:09.5	37.088	-104.692	5	3.4	ML
8/28/01	22:00.3	37.091	-104.655	5	3.5	ML
9/4/01	22:45.0	37.107	-104.622	5	3.4	ML
9/4/01	45:53.2	37.143	-104.65	5	4	ML
9/5/01	52:07.9	37.143	-104.618	5	4.5	ML
9/5/01	48:58.3	37.112	-104.611	5	3.7	ML
9/6/01	41:43.6	37.11	-104.628	5	3.6	ML
9/6/01	28:26.5	37.14	-104.585	5	3.5	ML
9/10/01	56:00.4	37.108	-104.602	5	3.4	ML
9/13/01	39:05.4	37.091	-104.593	5	3	ML
9/21/01	10:59.7	37.121	-104.706	5.4	3.4	ML
12/15/01	58:31.4	36.859	-104.797	5	3.3	ML
1/26/02	06:03.9	36.86	-104.784	5	3.4	ML

6/18/02	12:36.7	36.881	-104.779	5	3.5	ML
11/14/02	56:52.3	36.917	-104.768	5	3.2	ML
4/28/03	32:26.0	36.844	-104.923	5	3.6	ML
6/3/03	09:27.8	36.994	-104.768	5	3.3	ML
6/15/03	22:18.0	36.91	-104.763	5	3.6	ML
8/14/03	11:09.0	36.945	-104.87	5	3.3	ML
9/8/03	02:49.3	37.369	-104.685	5	3	ML
9/13/03	22:41.0	36.831	-104.907	5	3.8	ML
11/24/03	05:57.7	36.958	-104.828	5	3.1	ML
2/3/04	34:22.6	36.932	-104.861	5	3.4	ML
3/22/04	09:56.5	36.855	-104.851	5	4.4	Mb
3/30/04	02:55.4	36.892	-104.876	5	3	ML
3/30/04	23:37.9	36.876	-104.831	5	3.1	ML
3/30/04	41:04.1	37.036	-104.931	5	3.5	ML
5/31/04	27:43.8	36.935	-104.835	5	3.3	ML
8/1/04	50:47.6	36.874	-105.104	5	4.3	Mw
1/10/05	14:59.1	37.007	-104.675	5	3.4	ML
4/24/05	02:35.9	36.92	-105.07	5	3.4	ML
7/4/05	45:24.5	36.86	-105.097	5	3	ML
7/8/05	24:01.1	36.938	-104.886	5	3	ML
8/10/05	08:17.0	36.952	-104.822	5	4.1	Mb
8/10/05	08:22.6	36.947	-104.833	5	5	Mw
8/10/05	24:33.9	36.982	-104.959	5	3	ML
10/20/05	15:36.6	36.97	-104.849	5	3	ML
1/27/06	48:49.2	37.03	-104.968	5	3.3	ML
5/6/06	07:01.3	37.014	-104.768	5	3.1	ML
5/26/06	14:25.1	36.795	-104.832	5	3.1	ML
7/11/06	53:37.8	36.964	-104.929	5	3.2	ML
8/24/06	04:25.9	37.014	-105.013	5	3.1	ML
9/9/06	54:06.6	37.296	-104.77	5	3.2	ML
9/9/06	53:14.2	37.368	-104.865	5	3	ML
9/9/06	14:35.5	37.298	-104.794	5	3.6	ML
9/14/06	03:24.3	37.01	-104.867	5	3	ML
10/30/06	35:13.5	36.811	-104.963	5	3.5	ML
11/24/06	22:24.1	37.04	-104.996	5	3.1	ML
12/24/06	50:21.5	36.935	-104.75	5	3.6	ML
1/3/07	34:38.5	37.067	-104.895	5	4.4	Mw
1/14/07	17:36.7	36.878	-104.93	5	3.2	ML
2/25/07	24:19.1	37.099	-104.773	5	3.1	ML
3/12/07	32:14.6	37.061	-104.937	5	3.4	ML

6/9/07	45:44.7	36.929	-104.793	1	3.3	Mw
1/29/08	30:24.3	36.871	-104.988	5	3.1	ML
4/21/08	36:29.9	37.158	-104.942	5	3.2	ML
4/24/08	21:51.4	37.032	-104.847	5	3.1	ML
8/24/08	48:31.5	37.095	-104.866	5	3.4	ML
9/25/08	55:35.3	37.357	-104.882	5	3.2	ML
10/4/08	41:20.9	37.263	-104.748	5	3.4	ML
2/3/09	27:10.3	36.992	-104.884	5	3	ML
3/22/09	14:40.1	37.261	-104.462	5	3	ML
5/1/09	34:03.9	36.818	-104.819	5	3.2	Mw
6/27/09	44:39.9	36.888	-104.906	5	3	ML
7/29/09	00:36.7	36.799	-104.831	5	4.1	Mw
9/29/09	20:27.8	37.055	-104.995	5	3.1	ML
9/29/09	54:07.5	37.003	-104.805	5	3.5	Mw
10/3/09	45:31.9	37.022	-104.855	5	3.6	ML
11/20/09	54:30.1	36.892	-104.987	5	3.7	ML
12/11/09	32:27.2	36.927	-105.03	5	3.2	ML
1/18/10	41:07.4	36.854	-104.819	5	3.8	Mw
4/8/10	36:57.4	36.916	-104.842	5	3.5	ML
5/27/10	43:11.1	37.012	-104.906	5	3.6	ML
2/13/11	44:52.6	37.005	-104.935	5	3.6	ML
3/12/11	16:05.6	36.861	-104.981	5	3.2	ML
5/9/11	28:52.8	37.021	-104.783	5	3.7	Mw
5/11/11	06:15.3	37.1	-104.665	5	3.8	Mw
8/22/11	30:19.9	37.032	-104.554	5	4.7	Mw
8/23/11	48:51.0	37.023	-104.667	5	3	ML
8/23/11	46:18.2	37.063	-104.701	4	5.4	Mw
8/23/11	56:58.5	37.113	-104.631	5	3.5	ML
8/23/11	01:34.1	37.105	-104.679	5	3.2	ML
8/23/11	17:58.3	37.101	-104.63	5	3.5	Mw
8/23/11	37:56.8	37.068	-104.764	5	3.2	ML
8/23/11	11:12.8	37.055	-104.692	5	4	Mw
8/24/11	15:57.3	37.129	-104.803	5	3	ML
8/25/11	44:38.4	37.123	-104.697	5	3.2	ML
9/13/11	37:18.5	36.94	-104.798	5	3.5	ML
9/13/11	24:39.6	36.933	-104.741	5	4	ML
9/16/11	51:51.3	36.884	-104.74	5	3.9	Mw
10/10/11	26:29.2	37.09	-104.688	5	3.2	ML
11/22/11	20:02.9	37.003	-104.956	5	3.4	ML
12/9/11	54:15.8	37.099	-104.656	5	3.4	ML

12/17/11	16:49.3	37.043	-104.913	5	3	ML
3/6/12	10:21.7	37.002	-104.925	5	3.3	ML
5/24/12	44:37.6	37.123	-104.743	5	3.2	ML
9/16/12	15:31.7	37.064	-104.825	5	3	ML
12/4/12	15:26.8	37.033	-104.938	5	3.5	Mw
12/13/12	05:52.2	36.952	-104.783	8.3	3.3	ML
4/20/13	47:15.9	36.973	-104.875	5	3	ML
9/8/13	15:31.1	36.9651	-104.8757	5	3.6	Mw
1/22/14	45:03.5	37.2381	-104.6215	1.26	3.6	ML
4/11/14	47:46.2	37.1848	-104.9467	7.44	3.2	ML
7/10/14	22:47.6	37.0008	-104.9669	3.91	3.1	ML
10/10/14	57:21.9	37.0836	-104.9037	1.36	3.3	Mb
10/17/14	01:05.4	37.0163	-104.9216	4.6	3.8	ML
10/24/14	50:47.8	36.9972	-104.9233	5	3.3	ML
11/2/14	16:18.7	37.0753	-104.9121	6.07	3	ML
12/2/14	57:20.3	37.1054	-104.9393	2.99	3	ML
12/23/14	33:36.4	36.9501	-104.7718	8.59	3.4	ML
12/27/14	23:24.8	37.0159	-104.8487	3.51	3	ML
1/7/15	40:26.6	36.8765	-104.751	4.33	3.7	ML
2/2/15	10:13.0	37.0845	-104.975	5	3.1	ML
2/22/15	31:48.2	37.1545	-104.978	5	3.4	ML
2/22/15	20:34.7	37.0503	-104.9507	5	3.6	ML
3/5/15	49:01.0	36.9283	-104.8993	1.81	3.4	Mb
3/7/15	59:35.5	37.0771	-104.8742	5.74	3.5	ML
3/14/15	17:30.6	36.9028	-104.7774	1.64	3.6	ML
3/20/15	19:18.9	36.8932	-104.7459	5	3.8	ML
8/20/15	14:09.5	37.1078	-104.9291	1.08	3.9	Mw
12/29/15	25:32.5	37.1308	-104.9126	5	3.2	ML
2/3/16	59:19.0	37.1511	-104.9396	1.42	3.5	ML
2/6/16	09:11.0	37.0868	-104.957	1.57	4	Mb
5/21/16	51:16.8	36.9398	-104.8106	2.3	3.2	ML
8/23/16	56:11.5	36.9863	-104.9449	3.6	3.9	Mw
11/6/16	48:36.4	36.8997	-104.8605	5	3.2	ML
12/23/16	31:13.0	36.7571	-104.9277	3.55	4.2	Mw
1/21/17	57:54.3	36.9566	-104.8425	6.27	3.1	ML

Table 6. Earthquake Depth and Horizontal Errors from USGS Catalog [ANSS, 2018].

Date	Lat	Long	Depth	Magnitude	Horizontal Error (km)	Depth Error (km)
9/8/13 9:04	36.9372	-104.9105	7.46	2.6	4.7	7.1
8/31/14 10:20	37.0434	-104.9181	7.2	2.7	4.3	8.1
9/30/14 9:55	37.0584	-104.9273	6.67	2.9	3.7	3.1
10/6/14 8:10	37.0937	-104.8877	4.44	2.9	4	7.5
10/8/14 0:16	37.1423	-104.9102	2.32	2.6	2	8
10/10/14 22:57	37.0836	-104.9037	1.36	3.3	5.7	7.2
10/17/14 17:01	37.0163	-104.9216	4.6	3.8	4.3	6.9
10/20/14 4:01	37.172	-104.9084	5	2.5	1.8	2
10/21/14 4:33	37.0675	-104.9663	5	2.6	2.2	1.9
10/24/14 12:50	36.9972	-104.9233	5	3.3	3.3	1.8
10/26/14 20:11	37.0106	-104.9475	5	2.5	2.3	2
10/28/14 6:26	37.0768	-104.9233	5	2.7	3.4	2
11/2/14 13:16	37.0753	-104.9121	6.07	3	4.7	7
11/4/14 16:59	36.9459	-104.8544	2.23	2.7	3.3	8
11/8/14 1:31	37.0645	-104.9411	5.02	2.8	4.9	8
12/2/14 21:57	37.1054	-104.9393	2.99	3	3.1	7
12/23/14 12:33	36.9501	-104.7718	8.59	3.4	5.3	7.5
12/27/14 8:23	37.0159	-104.8487	3.51	3	4.2	6.7
1/7/15 0:40	36.8765	-104.751	4.33	3.7	5	6.6
1/10/15 19:04	37.1436	-104.8777	1.34	2.5	1.9	8
1/20/15 13:53	36.8765	-105.0072	0	3.3	5.5	2
1/31/15 10:48	36.9807	-104.8584	5	2.6	4.6	2
2/2/15 14:10	37.0845	-104.975	5	3.1	3	2
2/22/15 7:31	37.0797	-105.0638	1.31	2.6	4.1	7.9
2/22/15 7:31	37.1555	-104.9824	5	3.6	4.6	2
2/22/15 7:36	37.1008	-105.0038	5	2.7	4.1	2
2/22/15 8:20	37.0503	-104.9507	5	3.6	2.5	1.8
3/5/15 14:49	36.9461	-104.8989	2.52	3.4	4.4	7.5
3/7/15 8:59	37.0719	-104.9376	1.17	3.5	2.9	7.2
3/9/15 18:14	37.0553	-104.9871	5	2.7	2.2	2
3/14/15 20:17	36.9028	-104.7774	1.64	3.6	5.3	7.5
3/19/15 11:48	36.8128	-104.6004	5	2.6	3.5	2
3/20/15 5:19	36.8932	-104.7459	5	3.8	5	0.7
4/22/15 18:28	37.091	-104.9699	5	2.5	3.5	2
4/27/15 4:49	37.0527	-104.985	5	2.9	3.3	2

8/18/15 2:37	36.9044	-104.8848	3.49	2.7	3.1	2.1
8/20/15 5:14	37.1001	-104.921	1.08	3.9	4.9	7.6
8/25/15 23:08	37.162	-104.9149	5	2.8	3	2
10/14/15 8:23	37.0651	-104.8339	5	2.8	3.1	2
10/18/15 1:47	37.0899	-104.8818	6.54	2.9	1.9	8
12/29/15 12:25	37.1308	-104.9126	5	3	4.1	2
1/6/16 12:45	36.9218	-104.8414	5	2.6	2.7	2
1/13/16 18:58	36.9677	-104.8247	6.74	2.6	4.3	5.6
1/15/16 1:54	36.928	-104.7711	7.59	3	5.3	8
2/3/16 14:59	37.1533	-104.9544	3.13	3.3	3.2	6.9
2/6/16 23:09	37.0868	-104.957	1.57	4	2.4	8.3
3/5/16 3:13	37.2732	-104.9779	5	2.9	1.9	2
3/13/16 22:17	37.054	-104.9731	5	2.8	2	1.9
5/21/16 20:51	36.9398	-104.8106	2.3	3.2	4.4	7.9
6/19/16 5:46	36.9366	-104.8569	1.83	2.9	3.4	8
8/7/16 9:28	36.8459	-105.1098	1.33	2.6	3.6	8.1
8/23/16 16:56	36.9863	-104.9449	3.6	3.9	3.2	1.6
11/6/16 4:48	36.9233	-104.889	1.49	3.2	5.4	2.9
12/6/16 16:41	36.9968	-105.0412	5	2.7	1.2	2
1/21/17 3:57	36.9566	-104.8425	6.27	3.1	3.3	6.5
6/11/17 8:58	37.0704	-104.9702	5	2.8	2.8	2
6/17/17 6:42	37.0352	-104.8986	1.93	3.5	4.9	11.1

Table 7. Nakai Catalog with depth errors. Depth_sd represents km vertical error. ml is magnitude (-999 is a magnitude that was not determined) [Nakai, personal comm.]

year	mo	day	lat_mean	lon_mean	depth_mean	depth_sd	ml
2009	6	5	36.8283	-104.1325	25.4103	10.8221	1.07
2009	7	29	36.8537	-104.1017	21.9162	13.5052	1.01
2009	11	2	36.9621	-104.5801	31.5914	15.0534	-999
2009	12	13	37.3051	-104.9362	5.4287	2.3968	-999
2009	12	15	37.3051	-104.9335	7.8719	3.6	0.76
2009	12	16	36.8482	-104.861	5.602	2.5561	1.48
2009	12	17	36.8726	-104.8715	7.5483	2.8499	1.52
2009	12	17	36.8221	-104.8482	3.6076	2.4683	1.51
2009	12	17	36.8681	-104.8711	4.6788	2.2779	1.39
2009	12	17	36.8691	-104.871	4.4205	2.0136	1.36
2009	12	19	37.0487	-104.9785	4.1866	2.1012	1.41

2009	12	19	36.9342	-104.877	27.2308	2.3455	1.16
2009	12	20	37.1109	-104.717	3.4321	1.4809	1.33
2009	12	22	37.0435	-104.9665	5.466	2.9329	1.61
2009	12	23	37.3078	-104.9333	4.9545	2.3525	1.84
2009	12	24	36.8553	-104.8695	5.84	2.6247	1.37
2009	12	24	36.885	-104.868	5.9135	3.3133	1.52
2009	12	24	36.8568	-104.8723	8.8322	1.8332	1.58
2009	12	25	36.8548	-104.87	8.2911	1.0354	1.85
2009	12	25	36.8961	-104.8756	5.3818	2.3879	1.35
2009	12	25	36.8958	-104.8716	7.0438	3.3564	-999
2009	12	26	37.3066	-104.9353	4.891	2.332	1.64
2009	12	27	36.8541	-104.8721	6.0371	2.9781	0.99
2009	12	28	37.1942	-104.7527	7.3589	4.091	-999
2009	12	28	37.2317	-104.6277	5.0993	1.9785	2.54
2009	12	28	37.2322	-104.6265	4.1972	1.7365	2.08
2009	12	28	37.2315	-104.6248	3.7986	1.69	1.76
2009	12	28	37.2337	-104.6286	3.3575	1.3736	1.66
2009	12	28	37.2311	-104.6283	4.6358	1.8596	2.3
2009	12	29	37.3401	-104.2853	6.7859	3.0473	0.95
2009	12	30	37.3079	-104.9362	7.5057	3.7569	1.26
2009	12	30	37.3047	-104.9352	7.3993	3.8666	-999
2009	12	31	37.3069	-104.937	7.6131	1.1569	1.92
2010	1	1	37.3079	-104.9294	6.9553	2.3081	1.69
2010	1	1	36.8083	-104.8635	10.0324	4.2971	-999
2010	1	1	37.3276	-104.9158	11.3146	5.4677	1.32
2010	1	1	36.8789	-104.8432	4.9214	2.3034	-999
2010	1	2	37.3355	-104.9035	10.0614	4.8016	1.14
2010	1	2	36.8469	-104.8552	4.437	2.3736	1.34
2010	1	2	37.31	-104.9356	7.7846	2.9593	1.4
2010	1	3	36.8787	-104.8402	4.9789	2.4557	1.72
2010	1	3	36.8718	-104.8313	8.1538	3.9888	-999
2010	1	3	36.8983	-104.8723	5.598	2.6631	1.37
2010	1	6	37.0908	-105.0036	24.6865	17.6643	0.99
2010	1	6	36.8483	-104.8671	6.5554	2.6802	1.77
2010	1	6	37.3117	-104.9328	6.6124	2.5758	-999
2010	1	7	36.8707	-104.8494	5.5895	2.3835	1.37
2010	1	7	36.8697	-104.8676	7.4283	3.9903	-999
2010	1	7	36.8727	-104.8519	4.6987	2.4014	1.29
2010	1	8	37.3123	-104.936	8.1758	1.1975	2.46
2010	1	9	36.8843	-104.8542	6.7835	2.8071	1.62

2010	1	9	36.9029	-104.8613	8.4442	4.4905	-999
2010	1	10	37.0246	-104.9735	5.2045	2.6132	1.63
2010	1	10	37.3143	-104.9362	6.9901	1.4545	2.14
2010	1	11	36.9143	-104.8482	7.9475	3.5323	1.64
2010	1	12	36.8885	-104.8732	5.549	2.5596	2.46
2010	1	12	36.8912	-104.8728	6.3723	3.1633	1.33
2010	1	12	36.8907	-104.8725	6.3065	3.5374	1.08
2010	1	12	36.8798	-104.8456	6.0214	2.6267	1.85
2010	1	12	36.8708	-104.8299	10.0587	4.4109	-999
2010	1	12	36.893	-104.8735	7.405	2.5762	1.61
2010	1	12	36.8915	-104.8734	6.3142	2.6534	2.17
2010	1	12	37.3044	-104.9416	6.0944	2.797	1.23
2010	1	13	36.8988	-104.8782	5.3853	2.2395	1.51
2010	1	13	36.8967	-104.9046	5.4969	3.2713	-999
2010	1	13	36.8969	-104.8747	5.3224	2.7474	1.17
2010	1	14	36.8946	-104.875	5.338	2.2408	1.49
2010	1	14	36.8075	-104.8601	5.3312	2.7929	1.5
2010	1	14	36.8946	-104.874	6.8103	2.8101	-999
2010	1	15	36.8826	-104.8377	7.8304	1.4056	2.48
2010	1	15	36.8811	-104.8367	6.6137	2.0286	1.92
2010	1	15	36.884	-104.8393	6.8003	3.3256	-999
2010	1	15	36.8888	-104.8376	9.4541	2.6024	1.43
2010	1	16	37.3388	-104.9037	10.2949	4.5435	-999
2010	1	16	37.3137	-104.9368	8.0004	1.2466	2.19
2010	1	16	36.8093	-104.8657	8.4417	4.1575	-999
2010	1	17	36.8052	-104.861	6.7424	3.809	-999
2010	1	17	36.8095	-104.8664	12.2534	2.854	0.84
2010	1	17	37.3081	-104.928	6.2933	3.8422	-999
2010	1	17	36.8073	-104.8618	8.2918	3.7206	1.39
2010	1	17	36.7955	-104.8538	7.0348	4.6932	1.22
2010	1	17	36.8081	-104.865	7.826	2.1071	1.92
2010	1	17	36.893	-104.8713	4.8197	2.174	-999
2010	1	17	36.9146	-104.8007	19.5946	3.9812	1.32
2010	1	18	36.8511	-104.8681	5.3719	1.4839	4.27
2010	1	18	36.8497	-104.8706	4.7713	2.574	-999
2010	1	18	36.8571	-104.873	6.9852	3.733	1.17
2010	1	18	36.8526	-104.8723	8.2024	4.3162	1.31
2010	1	18	36.9134	-104.8473	6.8351	3.6485	1.11
2010	1	18	36.8514	-104.8684	5.1612	2.3621	1.14
2010	1	18	36.8513	-104.8697	5.5197	2.358	1.51

2010	1	18	36.8511	-104.8699	7.4214	2.8955	1.42
2010	1	18	36.8555	-104.8683	7.1511	3.9811	1.12
2010	1	18	36.867	-104.8707	5.8949	2.2351	1.57
2010	1	18	36.8492	-104.8703	4.9923	2.4403	-999
2010	1	18	36.8555	-104.8711	5.9072	2.5317	-999
2010	1	18	36.8501	-104.8709	4.8017	1.7594	1.8
2010	1	18	36.8508	-104.8669	6.5224	3.6002	-999
2010	1	18	36.8632	-104.8609	6.9504	3.7853	-999
2010	1	18	36.8702	-104.871	6.5707	3.1035	1.19
2010	1	18	36.8546	-104.8699	8.6215	1.9123	1.64
2010	1	18	36.8514	-104.8727	6.1159	2.5827	1.74
2010	1	18	36.8669	-104.87	7.0782	2.9531	-999
2010	1	18	36.8528	-104.8704	5.2295	2.8275	-999
2010	1	18	36.8545	-104.8699	9.0337	0.8144	2.26
2010	1	18	36.8535	-104.8575	10.7543	6.0061	-999
2010	1	18	36.7943	-104.857	12.0322	3.9624	1.56
2010	1	18	36.8843	-104.8758	5.2932	2.0716	1.81
2010	1	18	36.8858	-104.8746	5.1493	2.6218	1.5
2010	1	18	36.8518	-104.8682	3.6689	1.709	2.1
2010	1	19	36.8533	-104.8692	4.503	2.3192	1.02
2010	1	19	36.854	-104.8702	4.8103	2.4961	1.32
2010	1	19	36.8083	-104.8646	4.3076	2.2227	1.98
2010	1	19	36.865	-104.8653	10.6591	4.6497	-999
2010	1	19	36.8795	-104.8445	8.2085	2.7247	1.69
2010	1	20	36.8104	-104.8627	8.4387	3.2865	1.09
2010	1	20	36.8978	-104.8771	6.3861	3.197	1.28
2010	1	20	36.8935	-104.8752	5.2868	2.8765	1.59
2010	1	20	36.8925	-104.8745	4.6903	2.3267	1.5
2010	1	20	36.894	-104.8769	5.5795	2.5045	1.69
2010	1	20	36.8925	-104.8754	5.9141	2.5671	1.77
2010	1	20	36.8933	-104.8803	4.913	2.7262	0.89
2010	1	20	36.9973	-104.9753	8.3889	4.1238	1.27
2010	1	20	36.8922	-104.8764	6.9728	3.5552	1.52
2010	1	21	36.8931	-104.8765	4.047	1.8212	1.8
2010	1	21	36.8786	-104.8717	9.034	1.2981	3.28
2010	1	21	36.8781	-104.8716	4.0175	1.9835	2.55
2010	1	21	36.8749	-104.8677	4.1366	2.0609	1.19
2010	1	21	36.8774	-104.8709	4.5776	2.2695	1.49
2010	1	21	36.8746	-104.8738	7.5894	2.4187	2.38
2010	1	21	36.8759	-104.8712	6.7006	2.1485	2.02

2010	1	21	36.8796	-104.8699	4.0396	1.9849	1.42
2010	1	21	36.8812	-104.8714	4.5845	2.4526	1.72
2010	1	21	36.8795	-104.8741	5.1002	2.3481	1.83
2010	1	21	36.8496	-104.8694	5.8418	2.823	1.21
2010	1	22	36.877	-104.8702	6.2714	2.7829	1.73
2010	1	22	36.8787	-104.8739	8.349	3.118	1.57
2010	1	22	36.8085	-104.8564	10.0143	4.2564	1.55
2010	1	22	36.8457	-104.8569	6.5863	3.2232	1.46
2010	1	22	36.808	-104.858	8.0928	3.2293	1.3
2010	1	22	36.9656	-104.8666	11.2924	3.8649	1.54
2010	1	23	36.8076	-104.8575	10.8681	2.101	1.65
2010	1	23	36.8137	-104.8633	8.3797	3.2854	1.59
2010	1	23	36.8131	-104.8601	6.4763	3.1945	1.56
2010	1	23	36.8966	-104.8758	4.665	2.5612	-999
2010	1	23	37.1153	-104.5273	2.265	0.8995	1.72
2010	1	24	37.3117	-104.9344	6.4221	3.4369	1.59
2010	1	24	36.8115	-104.8571	7.8802	2.5616	1.32
2010	1	26	36.8084	-104.8616	10.2176	2.9086	1.32
2010	1	26	36.8885	-104.8728	8.7519	5.0266	-999
2010	1	26	36.8138	-104.8618	4.8267	2.6653	1.54
2010	1	27	37.1777	-104.6542	3.4629	1.6325	0.74
2010	1	27	36.8839	-104.8806	6.8562	3.1956	1.26
2010	1	27	36.8061	-104.8632	5.8998	2.9965	1.67
2010	1	27	36.8094	-104.8593	4.9219	2.5455	1.6
2010	1	30	36.8781	-104.871	5.0159	2.4862	1.08
2010	1	31	36.8537	-104.8702	6.5258	3.023	1.31
2010	1	31	36.8544	-104.8684	7.4741	4.1414	1.35
2010	1	31	37.3138	-104.9341	8.0737	2.9928	1.46
2010	1	31	36.8893	-104.8743	6.6104	3.2351	1.09
2010	1	31	36.8478	-104.875	6.8875	2.5523	1.73
2010	1	31	36.8478	-104.874	9.8355	2.8403	1.56
2010	2	1	36.8814	-104.868	4.3806	2.2162	1.31
2010	2	1	36.8745	-104.8676	5.3891	2.5296	-999
2010	2	1	36.8844	-104.875	5.8881	2.9875	1.29
2010	2	2	36.8775	-104.8727	7.3157	3.4276	1.26
2010	2	2	36.8549	-104.8703	8.6861	3.1696	1.12
2010	2	4	37.3056	-104.7771	12.8478	1.5107	-999
2010	2	7	36.8758	-104.8711	5.552	2.5587	1.76
2010	2	7	36.8938	-104.7594	26.1416	4.5641	1.26
2010	2	7	36.8773	-104.8702	7.4286	3.8314	-999

2010	2	7	36.7362	-104.9626	11.7775	3.3333	1.66
2010	2	8	36.8955	-104.8757	5.1691	2.6475	1.54
2010	2	9	37.313	-104.7897	7.2307	2.7452	1.87
2010	2	13	36.8832	-104.8754	4.7695	2.568	-999
2010	2	15	36.865	-104.8631	6.3019	3.7632	-999
2010	2	15	36.8657	-104.8658	4.431	2.2881	1.33
2010	2	15	36.8941	-104.8604	8.0059	4.5093	1.94
2010	2	15	36.8816	-104.8473	4.4055	2.0143	1.68
2010	2	15	36.8814	-104.8459	4.8794	1.8	1.88
2010	2	15	36.8772	-104.8728	4.0088	2.0921	-999
2010	2	16	36.8788	-104.8754	5.337	2.0488	1.64
2010	2	19	36.8667	-104.8618	7.7346	4.3912	-999
2010	2	21	36.968	-104.8663	9.1511	3.8258	1.28
2010	2	21	36.9594	-104.8718	5.1306	3.0643	1.32
2010	2	22	37.3763	-104.8181	5.1045	2.7028	1.2
2010	2	22	36.9753	-104.8827	7.4788	3.057	1.25
2010	2	23	36.7875	-105.0355	9.6637	1.0446	2.84
2010	2	23	36.8893	-104.8763	6.3646	3.0276	0.88
2010	2	23	36.7707	-104.9845	8.8914	4.8912	-999
2010	2	23	36.7838	-105.0406	6.5013	2.474	1.67
2010	2	23	36.8845	-104.8408	5.4545	2.1288	1.16
2010	2	24	36.8895	-104.8782	6.4535	2.2428	2.27
2010	2	24	36.8852	-104.8765	4.7644	2.2781	2.08
2010	2	24	36.8893	-104.8805	6.5895	1.9299	2.59
2010	2	24	36.8905	-104.8767	9.274	1.5658	2.91
2010	2	24	36.9017	-104.8881	5.6669	3.1854	-999
2010	2	24	36.8921	-104.8774	5.1618	2.7691	1.15
2010	2	24	36.8885	-104.8751	4.9817	2.597	1.36
2010	2	24	36.9851	-104.9744	5.3717	3.0548	1.25
2010	2	25	36.8913	-104.8695	5.6072	2.6535	1.37
2010	2	26	36.891	-104.8756	4.1334	2.1757	1.9
2010	2	26	36.8948	-104.8783	4.7144	2.352	1.82
2010	2	26	36.893	-104.8773	4.6922	2.4276	1.32
2010	2	26	36.7455	-105.0127	9.0559	6.3015	-999
2010	2	26	36.9957	-104.9757	4.0372	1.9642	1.58
2010	2	26	36.8988	-104.8783	5.1858	2.9102	-999
2010	2	26	36.9887	-104.9684	7.6799	4.831	-999
2010	2	27	36.8892	-104.8795	6.0985	3.1289	1.75
2010	2	27	36.7771	-104.9923	8.3914	3.1311	1.58
2010	2	27	36.761	-104.9812	8.4762	4.0648	1.23

2010	2	27	37.0025	-104.9721	8.1147	1.9938	2.11
2010	2	27	37.0019	-104.9721	7.9899	1.6034	2.52
2010	2	27	36.9916	-104.9708	4.9349	2.7714	1.44
2010	2	27	36.9932	-104.9693	5.1551	2.7859	1.39
2010	2	27	36.8816	-104.8446	3.772	1.6939	2.09
2010	2	27	36.8839	-104.8476	10.1111	2.963	-999
2010	2	28	37.0052	-104.9719	4.2324	2.0436	2.73
2010	2	28	37.0033	-104.975	6.0088	2.2321	1.64
2010	2	28	36.8782	-104.845	4.2955	1.9539	2.04
2008	8	12	36.8607	-104.8733	4.7933	2.4358	0.53
2008	8	12	36.8611	-104.8701	4.824	1.9225	1.33
2008	8	12	36.8874	-104.8669	5.3647	2.501	1.22
2008	8	12	36.9003	-104.8704	4.8168	2.2621	1.33
2008	8	12	36.9013	-104.8679	7.8191	3.4934	1.37
2008	8	13	36.9023	-104.8691	5.0813	2.4458	0.82
2008	8	13	36.9246	-104.8014	2.4524	2.856	1.94
2008	8	13	36.8927	-104.8626	5.5743	3.2338	1.01
2008	8	13	36.8997	-104.8677	4.0263	1.8893	1.54
2008	8	14	36.8643	-104.8473	7.0427	3.4365	1.13
2008	8	14	36.9588	-104.8591	11.348	3.1333	0.92
2008	8	14	36.9583	-104.8605	10.8164	2.166	1.36
2008	8	14	36.9255	-104.8003	5.524	2.6355	1.66
2008	8	2	36.7891	-105.0369	5.1686	2.8229	1.47
2008	8	15	37.0132	-104.9775	5.4695	2.8594	1.46
2008	8	15	36.8981	-104.8609	7.825	3.2859	1.33
2008	8	15	36.8714	-104.8691	6.3964	3.3177	1.22
2008	8	15	36.8729	-104.8687	4.4826	2.4665	1.07
2008	8	15	36.8739	-104.8697	7.1201	3.4915	1.17
2008	8	16	36.8734	-104.8631	10.2199	4.6835	0.9
2008	8	16	36.8725	-104.868	4.933	2.4714	-999
2008	8	16	36.8776	-104.8812	6.3676	3.2756	0.68
2008	8	16	36.8796	-104.8789	3.8138	1.8192	1.44
2008	8	17	36.8823	-104.8792	4.5562	2.0421	1.35
2008	8	17	36.8797	-104.8736	4.7319	2.5882	1.01
2008	8	17	36.8837	-104.8808	4.7952	2.3256	1
2008	8	17	36.8819	-104.8788	3.2541	1.5678	1.14
2008	8	17	36.8824	-104.8781	4.5175	2.2403	1.79
2008	8	17	36.8828	-104.8774	3.9279	2.0315	1.17
2008	8	17	36.8831	-104.8746	4.7668	2.3969	1.04
2008	8	17	36.8822	-104.8781	5.3988	2.8071	1.03

2008	8	17	36.8818	-104.8751	5.8116	3.2403	-999
2008	8	17	36.8848	-104.8813	5.7798	2.8174	1.07
2008	8	17	36.8784	-104.8683	6.9478	5.2987	1.11
2008	8	17	36.8852	-104.8794	4.7054	2.3402	0.94
2008	8	17	36.8369	-104.8515	7.6445	3.5464	1.28
2008	5	28	36.8639	-104.8746	6.1721	3.4841	1.52
2008	5	29	36.864	-104.8697	5.5582	3.0518	1.19
2008	8	17	37.0354	-104.97	1.8094	2.3041	2.33
2008	5	31	36.9138	-104.871	5.8875	3.3424	1.54
2008	5	31	37.2999	-104.7778	8.8208	2.5081	1.54
2008	5	31	37.2881	-104.7757	6.7777	3.2954	1.21
2008	5	31	37.2915	-104.7768	7.7759	2.6182	1.54
2008	6	1	37.2909	-104.7836	7.5927	2.3608	1.44
2008	6	1	37.319	-104.653	21.1465	6.1334	1.09
2008	6	1	37.5224	-104.6703	14.9478	2.2551	0.87
2008	6	1	37.2855	-104.7776	7.5407	2.7221	1.24
2008	6	1	37.3386	-104.7423	15.5093	9.1863	1.16
2008	6	1	37.2791	-104.7788	6.0702	2.6356	1.48
2008	6	1	37.291	-104.7788	6.5367	2.8224	1.1
2008	6	1	37.2893	-104.7784	8.1259	2.8651	1.26
2008	8	17	36.8845	-104.8836	6.1172	3.1039	1.22
2008	6	1	37.2847	-104.7793	7.2256	2.8147	1.41
2008	6	1	37.2924	-104.7784	8.3789	2.4296	1.21
2008	6	1	37.292	-104.7789	9.3809	2.2513	1.97
2008	6	1	37.3	-104.7834	6.9209	3.01	1.12
2008	6	1	37.3016	-104.782	7.5603	2.9276	0.98
2008	6	1	37.2898	-104.7858	5.8874	2.6888	1.65
2008	6	1	37.2967	-104.428	29.1904	2.5669	0.9
2008	6	1	37.2939	-104.7821	8.4047	2.7436	1.31
2008	6	1	37.29	-104.7825	8.7499	1.9884	2.42
2008	6	1	37.2902	-104.7786	9.8806	1.4682	2.37
2008	6	1	37.2931	-104.7801	7.5889	2.6823	1.39
2008	6	1	37.3042	-104.7793	5.2827	3.4625	1.1
2008	6	1	37.292	-104.7756	9.4533	2.3995	1.29
2008	6	1	36.942	-104.8677	9.1212	3.5343	1.16
2008	6	1	37.4197	-104.7688	7.6845	3.3338	0.65
2008	6	1	36.8426	-104.8515	11.9521	4.7934	1.18
2008	6	3	37.3359	-104.7469	12.6146	2.6211	1.14
2008	6	5	36.9566	-104.8646	7.6736	3.4337	1.27
2008	8	17	36.8795	-104.8645	6.7581	3.4133	1.34

2008	6	5	36.8745	-104.8709	8.481	2.1112	2.51
2008	6	6	36.9572	-104.8657	4.9629	2.4021	2.72
2008	6	7	36.9509	-104.8691	8.7652	3.7254	1.19
2008	6	7	37.3218	-104.7783	5.8568	2.7036	1.44
2008	8	17	36.877	-104.8673	4.3362	2.8701	1.1
2008	6	12	37.2945	-104.7844	8.8738	2.0493	1.45
2008	6	12	37.299	-104.7825	7.3973	3.0768	0.95
2008	6	12	37.2838	-104.7735	10.2985	5.2116	0.66
2008	6	13	36.884	-104.8684	8.3113	3.3651	1.38
2008	6	15	36.8648	-104.839	5.6339	2.626	1.8
2008	6	15	36.883	-104.8436	5.6969	3.1295	1.05
2008	8	17	37.2953	-104.7962	8.9396	2.641	1.13
2008	6	15	36.8896	-104.8614	6.5816	2.0813	2.06
2008	6	15	36.893	-104.8672	4.8809	2.5945	1.51
2008	6	15	36.8892	-104.8595	6.1256	2.9205	1.2
2008	6	16	36.8904	-104.8673	5.8117	3.4289	0.86
2008	6	16	36.8645	-104.8556	5.8182	2.999	1.81
2008	6	17	36.8732	-104.8672	6.3991	3.5216	0.63
2008	6	18	36.8992	-104.873	7.4686	3.9196	0.96
2008	6	19	36.8796	-104.8714	5.0734	2.7914	1.09
2008	6	19	37.3027	-104.5996	4.3669	2.2808	0.58
2008	6	20	36.8784	-104.8704	5.1647	2.7079	1.63
2008	6	21	36.9379	-104.8376	8.432	5.2756	1.17
2008	6	24	36.8862	-104.8614	5.1312	2.5231	1.06
2008	6	25	36.8836	-104.8708	4.5587	2.5252	0.67
2008	6	26	36.9279	-104.8663	5.7066	3.1207	1.21
2008	6	27	36.8526	-104.867	7.6876	4.1193	1.11
2008	6	28	36.8543	-104.8714	8.6903	2.195	2.24
2008	8	18	37.0337	-104.9682	3.4477	2.4739	2.45
2008	8	18	37.034	-104.9714	3.5731	3.2511	1.48
2008	8	18	37.0335	-104.9682	4.4181	2.7728	1.65
2008	8	20	36.8383	-104.8601	8.2806	3.1268	1.08
2008	8	20	36.9995	-104.9689	8.984	4.1241	1.33
2008	8	20	36.8374	-104.8605	5.8634	2.9382	1.23
2008	8	20	36.8717	-104.8617	5.8728	2.8963	1.54
2008	8	21	37.0008	-104.9677	5.7932	3.908	1.6
2008	8	4	37.1811	-104.531	2.212	1.395	1.34
2008	8	21	36.8694	-104.8618	5.4203	2.8902	1.08
2008	8	22	36.8367	-104.8624	5.3425	2.5686	1.31
2008	8	22	36.8397	-104.8631	6.5858	3.256	0.83

2008	8	4	36.9039	-104.8593	5.3461	2.8102	1.6
2008	8	22	36.8351	-104.8639	6.0598	2.7157	1.5
2008	7	3	36.95	-104.8672	8.3429	3.3109	1.43
2008	7	3	36.8826	-104.8644	8.8941	3.0478	1.18
2008	7	3	36.9469	-104.8633	6.265	2.7295	1.69
2008	7	3	36.9664	-104.8615	12.4452	5.2937	1.49
2008	7	3	36.9617	-104.8647	7.2343	4.3144	1.56
2008	7	4	36.9577	-104.8612	7.5515	3.3274	0.89
2008	7	4	36.8768	-104.8566	11.4813	3.6504	1.55
2008	7	5	36.9266	-104.862	11.0454	3.7608	1.35
2008	7	5	36.8689	-104.856	6.5476	3.3167	1.2
2008	7	5	36.8755	-104.8568	5.9707	3.1397	1.2
2008	7	6	36.9486	-104.8667	9.0954	4.4639	-999
2008	7	7	36.9512	-104.8635	4.537	2.2474	1.64
2008	7	7	36.9504	-104.8637	4.7111	2.0053	1.92
2008	7	7	36.9589	-104.8695	7.014	4.1108	1.12
2008	7	7	37.3281	-104.7765	5.3044	2.1392	2.48
2008	7	7	36.9502	-104.8659	3.8605	1.6272	1.93
2008	7	7	37.3243	-104.779	6.6601	1.4896	1.99
2008	7	7	36.9523	-104.865	6.6248	3.4404	1.68
2008	7	7	36.882	-104.8588	6.9792	3.2716	1.89
2008	7	8	37.3557	-104.6763	19.289	4.4058	0.85
2008	7	9	36.8805	-104.8604	6.3271	2.0735	2.28
2008	7	9	37.3296	-104.7669	8.144	2.9896	1.06
2008	7	9	37.3276	-104.7594	9.7539	3.2156	0.49
2008	7	9	36.9532	-104.8634	6.014	2.8492	1.35
2008	7	12	37.3279	-104.7583	9.2591	4.1713	0.86
2008	7	12	37.3247	-104.775	7.3862	1.2233	1.56
2008	7	12	37.224	-104.5378	5.5131	2.2364	1.41
2008	8	22	36.8813	-104.8745	5.3089	2.7011	1.26
2008	7	14	37.3268	-104.7727	6.82	2.9674	1.08
2008	7	15	36.9599	-104.8606	9.4995	3.7503	0.64
2008	7	15	36.9504	-104.865	10.3953	2.5728	1.85
2008	7	16	37.3259	-104.7422	10.2801	4.2316	1.18
2008	7	16	36.9541	-104.8639	6.887	2.9348	1.64
2008	7	17	36.8858	-104.8668	6.0146	2.8875	1.72
2008	7	17	36.8832	-104.8629	6.6774	3.7117	1.37
2008	7	17	37.0021	-104.9732	7.4083	3.0748	2.79
2008	7	17	36.8924	-104.8661	9.9601	4.3107	0.9
2008	7	17	36.8909	-104.8633	12.1658	5.7334	1.41

2008	7	17	36.8915	-104.8691	6.9388	3.6087	1.51
2008	7	18	36.8968	-104.8748	7.3605	2.0686	2.68
2008	7	18	36.8967	-104.8777	4.9423	2.5326	1.7
2008	7	18	36.8941	-104.8666	5.566	2.941	0.99
2008	7	18	36.8931	-104.8763	5.5738	2.7734	1.68
2008	7	18	36.9001	-104.8815	6.1906	3.2568	1.39
2008	7	18	36.9002	-104.8758	4.3241	2.4119	1.35
2008	7	18	36.8904	-104.8702	9.1106	1.6084	2.57
2008	7	19	36.8883	-104.8706	5.779	3.1591	1.49
2008	7	20	37.0013	-104.9769	5.3457	2.8257	2.47
2008	7	20	36.8902	-104.8687	4.9789	2.6298	1.25
2008	8	23	36.8368	-104.8612	8.3541	3.2764	1.61
2008	7	20	36.8923	-104.8761	5.7089	2.9667	1.84
2008	7	20	36.8927	-104.8754	4.9143	2.633	1.28
2008	7	22	36.9716	-104.8798	6.9091	3.9491	1.28
2008	7	24	36.9292	-104.8016	6.7708	4.7607	1.25
2008	7	26	36.8333	-105.0597	10.0886	3.9078	1.37
2008	7	27	36.8449	-104.851	5.9596	3.6781	1.76
2008	7	27	36.8672	-104.8517	5.2868	2.5272	1.7
2008	7	29	37.3313	-104.7615	5.7059	2.9569	1
2008	7	30	36.8853	-104.8588	9.3641	3.6936	0.97
2008	9	1	36.8777	-104.8435	5.5006	2.5491	1.02
2008	9	2	36.8907	-104.8802	4.3777	2.2687	0.98
2008	8	23	36.8471	-104.8591	6.4203	3.4599	0.91
2008	9	3	36.8747	-104.8723	4.3887	1.899	-999
2008	9	3	36.8741	-104.8717	5.6412	2.5844	-999
2008	9	3	36.8725	-104.8681	5.6721	2.4811	1.18
2008	9	4	36.8151	-105.0268	6.3143	2.7473	1.4
2008	9	4	36.8298	-104.8606	4.4729	3.6166	1.28
2008	8	24	36.8887	-104.8743	4.9881	2.3853	1.14
2008	9	5	36.8194	-105.0268	4.547	2.2232	1.48
2008	9	5	36.8201	-105.0255	12.0599	1.8603	1.06
2008	9	5	36.8191	-105.0296	8.9916	3.0496	0.78
2008	8	24	36.888	-104.8758	7.54	1.2091	1.83
2008	9	5	36.8196	-105.0292	8.472	3.1491	1.83
2008	9	6	36.8934	-104.8735	3.4861	1.3669	2.03
2008	9	6	36.8511	-104.8741	6.975	3.0542	1.1
2008	9	6	36.9586	-104.8646	6.844	1.7425	1.97
2008	9	6	36.8934	-104.8762	5.7056	1.8428	1.58
2008	9	6	36.8739	-104.8718	5.8321	2.3309	2.79

2008	9	6	36.895	-104.8744	5.1167	2.0015	1.04
2008	9	6	36.9563	-104.863	7.8194	1.9096	0.64
2008	9	7	36.8811	-104.8427	7.3054	2.9677	0.81
2008	9	8	36.8917	-104.8771	5.0064	2.107	1.63
2008	9	8	36.8681	-104.8579	7.6497	3.4853	0.79
2008	9	9	36.8746	-104.8712	3.9832	2.0544	0.94
2008	9	9	36.8975	-104.8659	5.2794	2.2457	1.36
2008	9	10	36.8947	-104.8748	5.1832	2.0396	0.82
2008	9	10	37.2953	-104.7722	9.0163	0.673	2.16
2008	9	10	36.8707	-104.8715	4.4126	1.8607	0.98
2008	9	10	36.8749	-104.8717	9.6813	3.5057	0.3
2008	8	24	36.8867	-104.8739	9.4463	0.7249	3.67
2008	9	11	36.8945	-104.8763	5.2942	2.4944	0.69
2008	9	11	36.8939	-104.8794	4.2292	1.5461	1.72
2008	8	24	36.8743	-104.869	4.5699	2.9354	-999
2008	9	11	36.872	-104.8731	5.4881	2.189	1.26
2008	8	24	36.8903	-104.8808	6.5453	3.5608	-999
2008	9	12	36.8688	-104.8697	6.0668	2.9024	0.98
2008	9	12	36.961	-104.8641	7.9937	2.371	0.53
2008	9	12	36.8465	-104.8625	8.7807	2.0568	1.28
2008	8	25	36.8846	-104.8683	6.7565	3.8445	1.13
2008	9	14	37.256	-104.5521	2.9164	2.081	0.78
2008	8	25	36.8842	-104.8716	5.8554	2.6101	1.12
2008	9	16	36.8577	-104.858	6.0742	2.2894	1.06
2008	9	16	37.0258	-104.9721	2.244	1.2201	1.68
2008	8	25	36.89	-104.869	6.7096	5.5165	-999
2008	9	17	37.3803	-104.8142	9.1445	0.5042	2.45
2008	9	17	37.3802	-104.8151	9.8412	0.8303	1.55
2008	9	18	37.3814	-104.6115	4.669	2.239	1.92
2008	8	25	36.8888	-104.8776	4.7423	2.4298	1.29
2008	9	18	36.8725	-104.8714	4.734	2.051	1.31
2008	8	25	36.9626	-104.862	9.5885	3.2641	1.45
2008	9	19	36.9558	-104.8745	6.3828	2.5805	0.68
2008	9	19	36.9595	-104.8639	4.6212	2.2346	1.75
2008	9	20	37.3797	-104.8145	8.9228	0.8778	1.74
2008	9	21	36.9208	-104.8778	4.3854	2.3878	1.39
2008	9	21	37.3051	-104.7784	7.2009	2.3133	1.12
2008	8	25	36.8873	-104.87	4.0455	2.0022	1.52
2008	9	21	37.3054	-104.7816	7.8177	2.7204	0.89
2008	9	21	37.3051	-104.777	9.8727	0.6438	1.05

2008	9	21	36.9162	-104.8801	5.2138	3.1383	1.14
2008	9	21	36.9218	-104.881	3.1793	2.3669	1.31
2008	9	21	36.8666	-104.8618	4.0668	1.9299	0.48
2008	9	21	37.3044	-104.7791	9.8299	0.7629	1.3
2008	9	21	36.921	-104.8769	4.9169	2.0709	1.77
2008	9	21	36.9205	-104.8786	5.0287	2.4243	1.33
2008	8	25	36.8854	-104.8712	5.1436	2.5325	1.26
2008	9	21	36.921	-104.8784	4.14	2.0463	1.42
2008	9	21	37.3022	-104.7773	10.4882	2.3113	1.25
2008	9	21	37.3009	-104.7776	11.2453	0.7115	0.53
2008	9	21	37.3018	-104.7759	7.0837	3.054	0.57
2008	9	22	36.824	-104.8513	8.0612	3.7797	1.03
2008	9	22	37.2945	-104.7699	7.4144	2.275	1.06
2008	9	22	37.3034	-104.7797	7.3069	2.589	0.92
2008	9	22	36.8246	-104.8482	5.8591	2.9799	1.42
2008	8	25	36.8486	-104.8695	7.8927	3.2249	-999
2008	9	22	37.3019	-104.7801	7.7864	1.9036	0.65
2008	9	22	37.3035	-104.7791	9.3568	1.7484	0.67
2008	9	22	36.8235	-104.8479	10.0492	4.2961	0.83
2008	9	22	37.3798	-104.6138	7.9275	0.8963	2.72
2008	8	25	36.8849	-104.8691	5.8052	2.959	0.75
2008	9	23	37.3802	-104.8112	9.4238	1.4323	1.69
2008	9	23	37.3795	-104.8127	8.4904	1.8875	1.31
2008	9	23	36.8895	-104.8754	5.2129	2.2487	1.68
2008	9	23	37.2986	-104.7693	7.1673	1.5997	1.34
2008	9	23	37.3803	-104.6106	4.3513	1.8755	1.22
2008	8	25	36.887	-104.8696	6.5159	3.3901	1.07
2008	9	23	36.822	-104.8618	9.1821	3.9894	1.4
2008	9	24	36.843	-104.8317	5.7711	2.9593	1.52
2008	9	24	36.9485	-104.8716	5.8075	1.8071	1.92
2008	9	25	36.8211	-104.8506	5.1571	2.8203	1.07
2008	9	25	37.3325	-104.6215	3.7122	1.488	1.03
2008	9	25	37.2952	-104.77	9.5179	0.5517	3.29
2008	9	26	37.2989	-104.7668	6.2571	2.781	1.19
2008	9	27	36.957	-104.8609	5.2035	2.5917	0.96
2008	9	28	36.8372	-104.8555	7.3771	4.2725	1.06
2008	9	28	37.3797	-104.8164	8.0401	1.3008	0.96
2008	8	25	36.8911	-104.8755	7.3714	3.5601	1.55
2008	9	28	36.8771	-104.8416	7.1435	2.8446	1.06
2008	9	29	37.3014	-104.6485	6.0013	2.8616	1.31

2008	8	25	36.886	-104.8842	4.005	2.2038	1.38
2008	9	29	36.877	-104.8692	4.1066	1.9496	0.99
2008	8	25	36.8857	-104.8701	5.6567	2.9361	1.55
2008	9	25	37.2962	-104.77	8.9633	0.5856	2.41
2008	8	26	36.8767	-104.8675	8.2871	0.9786	2.35
2008	8	26	36.8778	-104.8687	6.9522	3.7708	0.84
2008	8	26	36.8841	-104.8676	8.2526	3.6988	1.15
2008	8	26	36.879	-104.8664	6.6509	3.9519	0.85
2008	10	1	36.8909	-104.8766	5.2405	2.2764	0.8
2008	10	1	36.8767	-104.8665	3.6688	1.8356	0.66
2008	10	1	37.2959	-104.7687	9.5487	1.6652	0.97
2008	10	2	37.2959	-104.7708	8.516	1.1415	0.74
2008	10	3	36.892	-104.8771	4.9104	2.1108	1.07
2008	10	3	36.8929	-104.8778	4.6579	2.1823	1.06
2008	10	3	36.891	-104.8767	10.3977	4.641	-999
2008	10	3	36.8931	-104.8745	4.22	1.8051	1.37
2008	10	3	36.8946	-104.8792	4.6901	2.0757	1.64
2008	10	4	37.3831	-104.6079	4.6267	2.1217	0.79
2008	10	4	36.8618	-104.8552	6.5059	2.8563	1.26
2008	10	4	37.2971	-104.7715	9.3793	0.5314	3.57
2008	10	4	37.2998	-104.773	3.6848	1.5047	1.79
2008	10	4	37.3869	-104.6034	4.9565	1.846	1.87
2008	10	4	37.2979	-104.7783	6.9558	0.9418	2.03
2008	10	5	36.9725	-104.8424	12.3832	2.3362	0.88
2008	8	27	36.8503	-104.8704	7.2674	2.7267	0.47
2008	10	5	36.8764	-104.8445	5.9186	2.425	1.39
2008	10	6	36.8964	-104.8644	4.9038	2.1963	1.18
2008	10	7	36.8925	-104.8552	5.5645	2.4312	0.6
2008	10	7	36.8481	-104.8529	4.7502	1.9256	1.19
2008	8	27	36.8838	-104.8695	4.2253	2.1112	0.71
2008	10	7	36.9634	-104.8692	4.5131	1.759	1.42
2008	10	7	36.8844	-104.8841	5.6911	2.5612	0.67
2008	8	27	36.8921	-104.8742	6.5014	3.2811	1.05
2008	10	8	36.895	-104.855	6.4195	2.6623	0.86
2008	10	10	36.9696	-104.8425	5.1209	2.745	1.82
2008	10	10	36.9	-104.8824	5.3404	2.2764	1.82
2008	10	10	36.8913	-104.8594	4.4735	1.9455	1.35
2008	10	11	36.8666	-104.8734	8.4836	3.666	0.66
2008	10	11	36.9494	-104.8705	6.8528	2.0873	1.28
2008	10	11	36.9425	-104.8655	6.2978	3.1564	1.39

2008	10	12	37.2956	-104.7683	7.8207	3.4918	-999
2008	10	13	37.2962	-104.774	8.6718	3.4161	0.91
2008	10	13	36.8818	-104.8714	5.2423	2.2615	1.22
2008	10	14	37.0202	-104.9749	4.0257	0.7655	1.2
2008	10	15	36.8251	-104.862	4.4992	2.3268	1.5
2008	10	19	37.0207	-104.9774	3.7395	0.7017	1.34
2008	10	19	37.01	-104.9796	3.8065	0.8319	1.01
2008	10	20	37.0204	-104.9776	4.3524	0.912	1.46
2008	10	20	37.0183	-104.9767	4.4881	0.9297	2.05
2008	10	20	37.021	-104.9782	4.2007	0.857	1.78
2008	10	20	37.0234	-104.9794	4.1285	0.8414	1.05
2008	10	20	36.8906	-104.8774	4.8255	2.3356	1.14
2008	10	20	37.2981	-104.7744	5.8494	2.3841	1.44
2008	10	20	37.0179	-104.9762	4.4849	1.4581	1.48
2008	10	20	36.8856	-104.875	5.0424	2.7284	0.7
2008	10	20	37.0036	-104.9831	3.9846	1.2385	1.18
2008	10	21	36.863	-104.8656	5.1519	2.4886	1.02
2008	10	21	36.8572	-104.8469	5.2627	2.1501	1.09
2008	10	21	36.8579	-104.8471	7.2203	3.0364	0.6
2008	10	21	36.8582	-104.8434	5.4145	3.0202	0.91
2008	10	21	36.8553	-104.8472	7.178	1.2687	2.3
2008	10	21	36.8557	-104.8467	6.2814	2.6034	0.89
2008	10	21	37.2953	-104.7737	7.6089	0.7453	1.53
2008	10	22	36.9253	-104.802	2.5308	2.3933	1.26
2008	10	22	36.8569	-104.8469	8.6234	0.9504	2.53
2008	10	22	36.9254	-104.8014	4.9972	3.2781	1.58
2008	10	22	36.9263	-104.8026	4.0944	2.6789	1.82
2008	10	23	37.3789	-104.8179	7.2217	2.2365	1.05
2008	8	29	36.8779	-104.8444	5.0222	2.482	-999
2008	10	24	37.2961	-104.7757	7.9783	2.3053	0.81
2008	10	24	37.3775	-104.8143	8.6003	0.8355	1.47
2008	10	25	36.8902	-104.8567	3.8309	1.6455	1.02
2008	10	25	37.297	-104.7753	6.2637	3.2167	0.73
2008	10	25	36.8942	-104.8761	6.993	2.8767	1.16
2008	10	26	36.8959	-104.8577	5.0706	2.3066	0.97
2008	10	27	37.3816	-104.8156	6.6032	2.7756	1.16
2008	10	27	36.89	-104.8744	5.7433	2.4166	-999
2008	10	27	36.891	-104.8746	4.8924	1.9124	1.32
2008	10	27	36.8934	-104.8752	4.7709	1.9286	1.16
2008	10	27	36.8924	-104.8757	5.0415	2.0187	1.34

2008	10	27	36.8916	-104.8754	4.7093	1.9241	1.06
2008	10	27	36.8902	-104.873	4.3493	2.1243	0.3
2008	10	28	36.8643	-104.8667	6.0997	3.2177	-999
2008	10	28	36.8931	-104.8581	4.1323	1.691	1.91
2008	10	28	36.8969	-104.8576	5.2317	2.2864	0.94
2008	10	29	37.1476	-104.8965	5.641	2.716	0.27
2008	10	29	36.8786	-104.8407	7.2377	3.0874	-999
2008	10	29	36.8783	-104.8427	7.7666	3.3825	0.84
2008	10	29	36.8783	-104.8415	6.4977	2.4534	1.39
2008	8	30	37.0261	-104.9737	2.2119	1.4535	0.62
2008	10	29	36.896	-104.8758	6.5195	2.1433	1.89
2008	10	30	36.894	-104.8727	6.1815	1.9035	1.14
2008	10	31	36.8842	-104.8708	6.4721	3.3781	1.04
2008	10	31	36.8837	-104.8722	4.2978	1.8517	1.37
2008	10	31	36.882	-104.8722	3.5806	1.8859	1.51
2008	10	31	37.1574	-104.9006	6.1188	2.9072	0.51
2008	10	31	36.8919	-104.8725	7.0135	3.4866	-999
2008	10	31	36.8944	-104.8704	6.1442	3.7678	1.07
2008	10	31	36.8971	-104.8773	5.2607	2.6187	0.81
2008	10	31	36.8879	-104.8786	4.1159	1.8267	1.5
2008	8	30	36.8802	-104.8461	8.0761	3.5351	0.69
2008	8	30	36.879	-104.8435	4.6567	2.2626	1.14
2008	11	1	36.8937	-104.8734	4.9707	1.7915	0.76
2008	11	1	37.6722	-104.7136	8.3123	2.9612	0.57
2008	11	1	36.8908	-104.874	4.798	2.2884	0.64
2008	11	1	36.8792	-104.8467	8.4165	2.5072	0.86
2008	8	31	36.8777	-104.8457	6.5606	2.2005	1.12
2008	11	3	36.8786	-104.8655	6.5668	2.7171	1.37
2008	11	4	36.9461	-104.851	11.8655	5.2821	1.24
2008	11	5	37.153	-104.9017	9.0757	0.5693	1.11
2008	11	5	37.2958	-104.7738	8.0588	0.7975	2.28
2008	11	5	37.1574	-104.8984	7.6378	0.8644	1.63
2008	11	7	37.1561	-104.9016	5.1548	2.4686	0.56
2008	11	8	36.8914	-104.8577	3.789	2.228	0.76
2008	11	8	37.2961	-104.7689	9.1704	0.498	2.6
2008	11	8	37.2954	-104.7683	8.2831	3.1484	0.8
2008	11	8	37.3031	-104.7834	8.5455	2.802	1.36
2008	11	8	37.2983	-104.7819	10.1362	3.1038	0.69
2008	11	8	37.3013	-104.7841	8.3216	3.2139	0.7
2008	11	8	37.3026	-104.7815	6.6327	3.0499	1.29

2008	11	9	36.8687	-104.8567	4.6622	2.2293	0.69
2008	11	9	37.38	-104.8123	7.1776	2.6617	1.1
2008	11	10	37.38	-104.8143	9.8847	0.9073	1.62
2008	11	10	37.0089	-104.9624	4.8787	1.1503	1.29
2008	11	10	36.8716	-104.8713	8.9617	0.4849	2.17
2008	11	10	36.8722	-104.8716	5.3538	1.8334	1.27
2008	11	10	36.8727	-104.8737	8.1642	2.3645	-999
2008	11	10	36.8716	-104.8736	5.5822	2.5785	-999
2008	11	10	36.872	-104.8726	8.7569	3.1695	-999
2008	11	11	36.8954	-104.8723	5.0345	2.1005	0.93
2008	11	11	36.8935	-104.8729	4.412	2.0989	1.14
2008	11	11	36.8942	-104.8737	6.134	2.2234	0.7
2008	11	11	37.3806	-104.8121	6.4369	2.9316	0.6
2008	11	11	36.9191	-104.801	3.3528	2.5799	1.55
2008	11	11	36.9187	-104.8009	4.9597	3.2937	0.82
2008	11	11	36.9229	-104.801	3.9977	2.7435	1.2
2008	11	12	37.1525	-104.9013	7.4792	1.5786	0.27
2008	11	13	37.1539	-104.9015	7.5687	1.5916	0.73
2008	11	13	36.8842	-104.8732	3.8383	1.9839	1.12
2008	8	5	36.8796	-104.8553	5.7764	2.9694	1.21
2008	11	14	36.8735	-104.8576	7.6749	4.2317	1.04
2008	11	14	37.3812	-104.8121	4.3945	2.173	1.28
2008	11	15	36.8765	-104.8596	6.3063	2.5312	1.4
2008	11	15	36.8926	-104.8629	6.5296	2.5807	1.05
2008	11	15	36.8278	-104.8585	4.1547	1.8331	2.09
2008	11	16	36.8884	-104.8768	5.0627	2.3229	0.58
2008	11	16	36.8767	-104.8713	5.8408	2.7889	1.08
2008	11	16	37.1508	-104.8978	6.4376	2.2338	1.66
2008	11	16	37.1506	-104.8971	7.537	1.7702	0.97
2008	11	17	36.8839	-104.8682	5.6203	2.9424	0.86
2008	11	17	37.3807	-104.8127	9.8594	0.6644	2.01
2008	11	17	37.3776	-104.8149	9.3213	3.5129	0.8
2008	11	17	37.3813	-104.8133	6.9588	3.5113	-999
2008	11	17	37.3053	-104.7854	5.4205	3.6903	1.27
2008	11	17	37.3794	-104.8125	7.314	2.7756	1.67
2008	11	18	36.9195	-104.8002	1.3341	1.0772	2.52
2008	11	19	36.8922	-104.8744	7.4231	2.0395	1.37
2008	11	19	36.8902	-104.8736	4.4605	1.8671	1.56
2008	11	19	36.8924	-104.8743	7.1456	1.786	1.4
2008	11	19	37.1503	-104.8991	7.0724	1.8742	1.43

2008	11	19	36.8256	-104.8603	6.9176	3.0377	1.49
2008	11	19	36.8688	-104.8466	5.1801	2.1385	1.09
2008	11	20	36.8452	-104.8659	4.6618	1.9842	1.31
2008	11	20	36.8856	-104.8779	3.4654	1.3178	2.18
2008	11	20	36.8403	-104.8521	7.3598	3.7638	-999
2008	11	20	36.8829	-104.8683	4.512	1.9733	1.24
2008	11	20	36.8373	-104.8569	5.5267	1.6607	1.84
2008	11	20	36.8558	-104.8446	4.9649	2.0477	1.35
2008	11	21	37.1504	-104.8979	8.7721	1.0691	1.12
2008	11	22	37.1569	-104.8969	7.3254	2.3778	0.86
2008	11	22	36.8715	-104.8719	5.21	2.5163	-999
2008	11	22	36.8826	-104.8718	5.0248	2.5135	-999
2008	11	22	36.8275	-104.8578	6.5858	2.0757	2
2008	11	22	36.8795	-104.8655	5.0827	2.6019	1.27
2008	11	22	36.8779	-104.8703	3.1301	1.4779	2.17
2008	11	22	36.8778	-104.8658	4.7124	2.6014	1.13
2008	11	23	36.879	-104.8703	5.9632	2.8089	1.37
2008	11	23	37.1566	-104.9015	7.029	1.4523	1.67
2008	11	23	37.1548	-104.902	7.9257	1.3551	0.16
2008	11	23	37.1532	-104.9024	9.2926	1.0329	1.19
2008	11	23	36.9285	-104.872	5.1155	3.0803	-999
2008	11	23	37.1554	-104.9006	4.0994	2.042	1.21
2008	11	24	37.0153	-104.9748	1.2791	0.2539	1.88
2008	11	24	37.015	-104.9766	1.4135	0.7145	1.66
2008	11	24	37.1534	-104.9027	6.7249	2.0906	1.08
2008	11	24	36.8797	-104.8665	4.833	2.3213	1.23
2008	11	24	36.8482	-104.8691	5.6044	2.898	0.6
2008	11	24	36.8804	-104.8713	4.3264	1.7431	1.88
2008	11	24	36.9977	-104.9678	5.4201	1.2689	1.84
2008	11	24	37.1567	-104.9007	5.4641	1.6615	1.75
2008	11	25	36.8993	-104.8499	5.484	2.3872	1.01
2008	11	26	37.0143	-104.9757	1.2325	0.3246	1.4
2008	11	26	37.0133	-104.9755	1.4273	0.6281	1.84
2008	11	26	36.8502	-104.8707	7.4277	2.7995	0.84
2008	8	5	36.8854	-104.8754	5.7717	3.2856	-999
2008	11	27	36.8706	-104.8719	5.984	1.9511	1.18
2008	11	27	36.8478	-104.8689	6.2356	2.2796	1.43
2008	11	27	36.8508	-104.8688	6.8353	2.8229	1
2008	11	28	36.8939	-104.8676	9.173	2.5004	1.3
2008	11	28	36.8488	-104.8687	6.3506	2.5574	1.31

2008	11	28	37.1524	-104.9021	6.7375	2.0276	1.18
2008	11	28	37.1557	-104.9037	6.2345	1.9248	0.96
2008	11	29	36.8492	-104.8681	5.0388	2.1407	1.01
2008	11	29	37.0152	-104.9729	1.1898	0.3626	1.82
2008	12	1	36.8494	-104.8699	6.0027	2.7541	1.65
2008	12	1	36.8491	-104.8693	5.6566	2.3997	-999
2008	12	2	36.8489	-104.8677	8.9192	1.9799	0.99
2008	12	2	36.8486	-104.8654	7.7612	2.7213	1.47
2008	12	4	36.8487	-104.8694	7.3948	1.7923	1.48
2008	12	5	36.9478	-104.8718	4.6675	1.8813	-999
2008	12	5	36.9484	-104.8721	5.367	2.1679	0.77
2008	12	6	36.88	-104.8736	4.4349	1.7585	1.68
2008	12	6	36.8795	-104.8751	3.1587	1.7036	1.89
2008	12	6	36.8846	-104.8735	4.1801	2.1908	1.25
2008	12	7	37.2955	-104.7688	9.2792	0.5142	1.82
2008	12	7	36.8857	-104.877	5.6478	2.0331	1.72
2008	12	7	36.8836	-104.8754	6.1959	2.6156	0.04
2008	12	7	36.8846	-104.8765	4.7908	2.2747	2
2008	12	7	36.9626	-104.8682	6.4458	1.9097	0.71
2008	12	7	36.8861	-104.8738	4.637	2.3363	0.57
2008	12	8	37.1524	-104.9032	6.8603	1.5384	0.85
2008	12	8	36.8985	-104.8714	5.8267	2.159	1.36
2008	12	9	36.891	-104.8674	4.2071	1.8806	2
2008	12	9	36.937	-104.8769	6.231	2.4112	1.09
2008	12	11	36.8854	-104.8653	3.5824	1.757	-999
2008	12	12	37.3793	-104.8161	7.9564	2.9616	0.93
2008	12	12	36.8817	-104.874	3.3601	1.5697	1.25
2008	12	15	36.8222	-104.8512	7.9311	3.2763	0.83
2008	12	16	36.8713	-104.8644	3.7032	1.4769	1.32
2008	12	16	36.8726	-104.8656	4.5191	2.0177	1.33
2008	12	16	36.9231	-104.8	1.6803	1.4077	1.44
2008	12	17	36.9579	-104.8623	8.2232	3.7356	1.37
2008	12	18	36.8246	-104.8504	5.6747	3.094	1.45
2008	12	18	37.3795	-104.8153	8.3711	1.2842	1.47
2008	12	18	36.8708	-104.8207	7.8805	3.1636	0.86
2008	12	18	37.3797	-104.8155	4.1291	2.0082	1.08
2008	12	18	37.3786	-104.8148	9.1123	0.5437	1.46
2008	12	18	37.3797	-104.8152	8.2003	1.871	0.74
2008	12	18	36.8929	-104.8644	8.8821	2.8806	1.41
2008	12	21	36.8028	-105.0168	6.1303	3.2915	1.4

2008	12	21	37.3802	-104.8168	8.3862	2.0353	1.67
2008	12	21	36.9843	-104.9737	3.7029	1.759	1.4
2008	12	21	37.154	-104.8993	6.3857	2.0817	1.85
2008	12	21	37.1554	-104.9029	8.4627	1.4911	0.9
2008	12	21	37.1522	-104.8999	6.5209	2.1534	0.39
2008	12	22	37.1538	-104.9029	8.2219	1.4449	0.92
2008	12	22	37.1525	-104.9037	8.3448	1.4472	0.91
2008	12	22	37.1559	-104.9003	5.998	1.6571	1.74
2008	12	22	37.1497	-104.9014	7.6264	1.3972	1.42
2008	12	22	37.154	-104.8968	5.2634	1.8313	1.47
2008	12	22	36.8924	-104.8729	4.8206	2.0824	0.8
2008	12	22	36.8949	-104.8704	1.9753	1.6491	1.76
2008	12	22	36.8715	-104.8248	5.8119	2.4741	1.37
2008	12	22	36.8935	-104.8706	4.2965	2.1873	1.48
2008	12	22	37.1584	-104.9012	4.5954	2.1596	0.17
2008	12	22	36.8587	-104.8544	6.5127	1.6029	2.74
2008	12	22	36.8605	-104.8531	3.5158	1.4375	1.84
2008	12	22	36.8631	-104.8563	3.9743	1.7295	1.05
2008	12	22	36.8716	-104.8224	3.57	1.421	2.1
2008	12	22	36.8575	-104.8715	5.4075	2.2707	1.47
2008	12	23	36.8575	-104.8688	4.688	1.6887	1.8
2008	12	23	36.8573	-104.8704	4.711	2.0899	1.67
2008	12	23	36.8835	-104.8614	3.8403	1.965	1.13
2008	12	23	36.8584	-104.8694	9.5369	2.2272	1.23
2008	12	23	36.8571	-104.8705	3.361	1.5812	1.53
2008	12	24	36.8832	-104.8624	3.2949	1.5408	1.62
2008	12	24	36.8735	-104.8716	5.0522	2.335	0.59
2008	12	24	36.8726	-104.8722	4.7166	2.2384	-999
2008	12	24	36.8746	-104.8683	5.3158	2.2809	1.05
2008	12	24	37.1508	-104.9045	8.0691	1.2914	1.43
2008	12	24	37.1534	-104.9048	7.2506	0.7302	1.78
2008	12	25	36.8537	-104.8676	9.2369	2.1359	1.33
2008	12	25	37.1545	-104.9021	5.7719	2.3683	1.32
2008	12	25	36.8924	-104.8629	4.8778	2.1482	1.26
2008	12	26	37.1544	-104.904	7.1384	0.6936	2.15
2008	12	26	37.1565	-104.8984	4.992	2.684	1.34
2008	12	26	36.86	-104.8533	6.0577	1.6892	2.54
2008	12	27	37.1507	-104.8999	5.8269	2.5716	0.38
2008	12	28	36.9319	-104.8766	3.1239	2.0421	1.34
2008	12	29	36.9363	-104.8649	4.8241	2.3042	1.25

2008	12	29	36.8597	-104.8537	5.0594	2.0965	1.39
2008	12	30	37.0088	-104.9786	3.5311	0.925	1.23
2008	12	30	36.8837	-104.8766	3.2855	1.3678	1.75
2008	12	31	36.8832	-104.8764	4.1448	1.8411	1.81
2009	1	1	36.8889	-104.859	8.661	3.9486	1.18
2009	1	1	36.8574	-104.8503	6.9774	2.4279	1.53
2009	1	2	37.0419	-104.9743	2.8087	1.0578	1.1
2009	1	2	36.9589	-104.8661	7.5796	2.2561	-999
2009	1	2	36.8767	-104.8729	3.7809	1.5114	1.37
2009	1	2	37.2108	-104.6258	11.5598	5.2633	0.54
2009	1	2	37.2325	-104.6316	3.868	1.7692	1.06
2009	1	2	36.8702	-104.8711	3.8968	1.7047	1.63
2009	1	3	37.2319	-104.6285	4.426	1.7504	1.3
2009	1	3	36.8613	-104.8585	6.4116	2.8507	1.37
2009	1	3	37.2338	-104.6283	4.0506	1.8717	0.48
2009	1	3	37.2341	-104.627	5.1015	2.4323	0.98
2009	1	4	36.8479	-104.8661	7.3008	2.6787	1.66
2009	1	4	36.9601	-104.8684	7.8553	1.6615	1
2009	1	4	37.2292	-104.6259	5.3061	2.5679	0.78
2009	1	4	37.2305	-104.6244	4.9276	2.0724	1.14
2009	1	4	37.2311	-104.6284	3.6982	1.398	1.36
2009	1	4	37.2308	-104.6285	4.416	1.767	1.53
2009	1	5	37.2317	-104.629	4.8797	1.801	2.03
2009	1	5	37.2323	-104.6284	4.7215	1.8338	1.31
2009	1	5	37.2326	-104.6261	4.8998	1.9263	1.45
2009	1	5	37.2323	-104.6272	4.1617	1.8054	1.74
2009	1	5	37.2294	-104.623	5.9526	2.4636	1.22
2009	1	5	37.2315	-104.6276	4.2308	1.688	1.44
2009	1	5	37.2322	-104.6261	4.9241	2.1357	1.4
2009	1	5	37.2316	-104.6248	4.6549	2.3228	0.5
2009	1	5	37.2324	-104.6256	5.6247	2.045	1.97
2009	1	5	37.2324	-104.6282	4.919	1.9647	1.72
2009	1	5	37.2336	-104.6231	4.0508	1.7953	1.25
2009	1	5	37.2306	-104.6231	6.6071	2.9576	0.88
2009	1	5	37.2314	-104.6272	4.3569	1.8367	1.16
2009	1	5	37.232	-104.6271	4.6819	2.1241	1.89
2009	1	5	37.229	-104.631	4.1509	1.8279	1.51
2009	1	5	37.2309	-104.6284	5.8099	2.4064	1.37
2009	1	5	37.2317	-104.6278	5.4074	2.2261	1.31
2009	1	6	36.8822	-104.8416	6.2413	2.44	1.11

2009	1	7	37.3335	-104.6235	3.0994	1.4681	1.08
2009	1	7	36.8444	-104.8617	8.2678	2.8628	1.77
2009	1	7	36.8474	-104.8639	9.1759	1.3346	1.86
2009	1	10	36.8898	-104.8639	4.4665	1.8754	1.04
2009	1	10	36.8627	-104.8604	4.3208	1.6814	1.77
2009	1	10	37.2305	-104.5901	3.6853	2.312	0.59
2009	1	10	37.2311	-104.5909	3.98	2.1122	0.34
2009	1	10	37.2317	-104.5961	3.5358	1.5683	-999
2009	1	11	36.9906	-104.9758	3.6619	1.5197	1.42
2009	1	11	36.9893	-104.9796	4.2266	1.9631	1.26
2009	1	12	36.8918	-104.8771	4.7629	2.0026	1.45
2009	1	12	36.8897	-104.8767	4.1152	1.7756	2.11
2009	1	13	36.8901	-104.8771	4.2181	1.6122	1.97
2009	1	13	36.8943	-104.8773	7.51	2.2621	1.09
2009	1	13	36.8934	-104.8749	9.7396	3.3132	0.98
2009	1	13	36.8929	-104.8765	4.586	2.0024	1.13
2009	1	13	36.8932	-104.883	4.7528	2.4374	0.73
2009	1	13	36.8922	-104.8752	5.2386	2.4018	1.05
2009	1	13	36.8817	-104.8374	4.8832	2.2336	1.03
2009	1	14	36.8798	-104.8731	3.4177	1.7084	0.56
2009	1	14	36.8835	-104.8393	5.4286	2.2378	1.41
2009	1	15	36.8815	-104.8391	4.9782	2.1013	1.44
2009	1	15	36.8793	-104.8392	7.0145	1.0906	1.92
2009	1	15	36.848	-104.8573	5.9197	2.9636	1.22
2009	1	15	36.8339	-104.8561	5.5244	2.2738	1.65
2009	1	15	36.8943	-104.8763	4.1121	1.8616	1.03
2009	1	16	36.8944	-104.8804	4.13	1.5948	1.66
2009	1	16	36.8949	-104.8825	8.2247	2.5911	1.2
2009	1	16	36.8947	-104.8792	6.3626	3.0645	0.52
2009	1	16	36.8365	-104.8566	6.9506	1.5333	2.03
2009	1	16	36.8697	-104.8564	5.2739	2.7968	1.59
2009	1	16	36.868	-104.855	5.3517	2.4485	1.15
2009	1	16	36.8351	-104.8552	5.9643	3.3241	1.47
2009	1	16	36.8914	-104.8614	4.6879	2.0052	1.69
2009	1	16	36.8838	-104.8749	5.1458	2.3267	1.39
2009	1	16	36.8833	-104.8747	7.1446	1.6433	2.47
2009	1	16	36.885	-104.8746	3.5846	1.6338	1.54
2009	1	16	36.8932	-104.8733	5.632	3.1696	-999
2009	1	17	36.8857	-104.875	3.8798	1.9406	1.31
2009	1	17	36.8854	-104.8735	4.0767	1.8587	1.08

2009	1	17	36.8884	-104.8626	4.9123	1.972	1.94
2009	1	17	36.8887	-104.8624	7.3497	1.6126	2.14
2009	1	18	36.9561	-104.8665	5.7334	2.5612	2
2009	1	18	36.8364	-104.853	10.849	3.1184	-999
2009	1	18	36.9541	-104.8648	5.0604	2.7284	0.97
2009	1	18	36.8915	-104.8522	4.3539	2.1058	-999
2009	1	18	37.3926	-104.6023	5.128	2.3051	0.94
2009	1	19	36.8854	-104.8698	5.2563	1.9302	1.63
2009	1	21	36.8933	-104.8821	4.6086	2.147	1.62
2009	1	22	36.8859	-104.8716	5.5332	1.7757	2.44
2009	1	22	36.8884	-104.8753	5.0257	2.4843	0.54
2009	1	22	36.8891	-104.8734	4.4683	2.5617	0.4
2009	1	23	36.8816	-104.8774	4.4068	1.884	0.63
2009	1	23	36.8882	-104.8612	5.0584	2.1024	1.57
2009	1	23	36.8397	-104.859	11.019	3.0357	1.39
2009	1	23	36.8375	-104.8631	4.5738	2.4232	1.44
2009	1	25	36.8718	-104.8712	5.6824	2.1748	1.47
2009	1	26	36.8592	-104.8516	6.3177	2.092	1.68
2009	1	27	36.8674	-104.8737	4.0097	1.807	1.29
2009	1	27	36.8913	-104.8772	4.7819	2.4062	0.8
2009	1	28	36.8642	-104.8616	4.3916	1.8926	1.21
2009	1	28	36.8602	-104.8515	3.6603	1.661	1.51
2009	1	29	36.9587	-104.8705	7.5888	2.3072	0.64
2009	1	29	37.2319	-104.6232	7.1668	1.8897	1.2
2009	1	29	36.8582	-105.0079	4.3163	2.2081	0.95
2008	8	6	36.9698	-104.8596	13.9297	9.7019	1.42
2009	1	30	36.8908	-104.8798	4.544	2.0294	1.6
2009	1	30	36.944	-104.8733	5.2289	2.1992	1.06
2009	1	31	36.8916	-104.881	4.3508	2.0823	0.94
2009	1	31	36.9601	-104.866	3.5081	2.7957	1.99
2009	1	31	36.8633	-104.8575	4.9914	2.4339	0.94
2009	1	31	37.2541	-104.5629	4.8223	1.949	0.69
2009	1	31	36.889	-104.8758	3.9364	1.4986	1.38
2009	1	31	36.9596	-104.8719	6.8681	1.5118	1.87
2009	1	19	36.8907	-104.8768	5.2956	2.985	-999
2009	1	9	36.8491	-104.8687	5.9407	2.6315	1.11
2009	2	1	36.9605	-104.8707	4.5735	1.7403	1.58
2009	2	1	36.9611	-104.8736	5.7066	1.9528	1.52
2009	2	1	36.8792	-104.8421	5.7014	2.7317	0.64
2009	2	2	36.8832	-104.8399	4.3152	2.3625	1.57

2009	2	2	36.827	-104.8357	5.7266	2.3401	1.11
2009	2	2	36.8811	-104.873	4.9178	3.7468	1.03
2009	2	2	36.881	-104.8502	11.2829	3.6571	0.94
2009	2	2	36.9605	-104.8719	6.2858	1.9784	1.66
2009	2	2	36.8833	-104.8696	3.7608	1.7098	1.39
2009	2	3	36.8799	-104.8677	4.633	2.918	1.15
2009	2	3	36.8705	-104.8641	4.4351	1.9711	1.16
2009	2	3	36.8789	-104.8656	4.7032	2.3188	0.67
2009	2	3	36.8811	-104.8734	4.1047	1.8225	1.57
2009	2	3	36.9463	-104.8716	9.5793	0.6176	3.12
2009	2	4	36.8903	-104.8817	5.0226	1.8477	1.32
2009	2	4	36.8377	-104.8543	7.8088	0.7897	2.06
2009	2	4	36.8816	-104.8393	4.325	2.4287	1.04
2009	2	5	36.8269	-104.8374	4.6941	2.0834	1.4
2009	2	5	36.8311	-104.8645	11.5543	4.8733	0.79
2009	2	5	36.8911	-104.8748	3.4474	1.7067	1.1
2009	2	5	36.8253	-104.8347	6.8846	2.7493	1.28
2009	2	6	36.8682	-104.8603	4.6496	2.1128	1.41
2009	2	6	37.2826	-104.4725	6.6242	3.2457	0.63
2009	2	6	36.8621	-104.864	8.9823	2.2676	1.41
2009	2	7	36.8594	-104.8626	5.1279	2.8201	0.86
2009	2	7	36.8384	-104.8549	7.8544	2.083	1.3
2009	2	8	37.3072	-104.7855	8.8336	1.9691	0.96
2009	2	8	37.3057	-104.784	5.9114	2.801	0.87
2009	2	8	36.8891	-104.8764	4.1065	1.8524	1.13
2009	2	8	37.3045	-104.7834	6.3102	2.4474	0.87
2009	2	9	36.8263	-104.8357	5.1751	2.59	0.94
2009	2	9	36.9636	-104.8719	4.7968	2.1631	1
2009	2	9	36.8724	-104.8716	5.6616	2.5516	1.39
2009	2	10	36.8236	-104.8354	7.8513	3.7448	1.44
2009	2	10	36.9302	-104.8742	6.3961	2.3979	0.86
2009	2	11	36.89	-104.8764	4.6859	2.1961	-999
2009	2	12	36.8645	-104.8587	4.749	2.2	1
2009	2	13	36.8495	-104.8686	6.2636	2.6739	1.46
2009	2	13	36.8485	-104.8703	5.8436	2.6493	1.25
2009	2	13	36.8886	-104.8607	3.462	1.7062	1.12
2009	2	13	36.889	-104.8622	8.8178	0.478	2.91
2009	2	13	36.8893	-104.8615	8.3158	2.7396	1.42
2009	2	14	36.8486	-104.8704	4.452	2.3288	1.68
2009	2	14	36.8478	-104.8712	3.6565	1.6258	1.18

2009	2	14	36.8491	-104.867	5.0763	2.118	1.55
2009	2	14	36.8482	-104.8686	5.2704	2.3508	1.18
2009	2	15	36.891	-104.8648	4.4064	2.1109	1.36
2009	2	16	37.3811	-104.8157	9.6632	2.6289	1.15
2009	2	17	37.0248	-104.9781	4.7464	0.8232	1.14
2009	2	18	36.8772	-104.8601	4.0826	1.723	1.21
2009	2	19	37.1132	-104.504	6.2719	0.7529	1.23
2009	2	19	37.0351	-104.967	1.3196	0.57	2.21
2009	2	19	37.0377	-104.9738	4.081	0.7579	2.21
2009	2	19	37.1123	-104.507	5.917	0.7423	1.18
2009	2	21	37.4212	-104.8385	9.0162	0.5889	2.01
2009	2	21	36.8913	-104.8605	4.8	2.0661	1.36
2009	2	21	36.8819	-104.8796	3.5668	1.6718	1.43
2009	2	21	36.881	-104.8781	4.0127	1.9687	1.04
2009	2	22	36.8892	-104.8814	5.6892	2.6036	1.29
2009	2	22	36.8772	-104.8671	4.1677	2.1742	0.84
2009	2	24	36.8967	-104.8552	4.298	2.4409	-999
2009	2	24	37.42	-104.8381	8.9934	1.1794	1.77
2009	2	25	37.4273	-104.8109	14.9691	4.9522	0.88
2009	2	25	37.4228	-104.8378	7.8103	1.5364	1.69
2009	2	25	37.3095	-104.7883	6.9221	3.8836	0.6
2009	2	25	36.8905	-104.8862	4.1375	2.2933	0.3
2009	2	26	36.8652	-104.8514	4.2368	1.9189	1.66
2009	2	27	36.8839	-104.8549	5.0495	2.6802	1.44
2009	2	28	36.8935	-104.8748	5.4564	2.9827	1.24
2009	2	28	36.8963	-104.8785	4.0963	2.0784	1.38
2009	3	1	36.8575	-104.8778	6.9074	3.7741	-999
2009	3	1	36.8895	-104.8648	4.4407	2.2041	2.1
2009	3	1	36.9029	-104.869	5.4946	2.4949	1.34
2009	3	1	36.8866	-104.8771	5.0026	2.7374	-999
2009	3	1	36.8931	-104.8765	4.7552	2.2227	1.55
2009	3	1	36.8924	-104.8745	4.0987	1.7015	1.36
2009	3	2	37.3782	-104.6019	3.8428	1.8947	1.11
2009	3	2	36.9628	-104.8652	6.0509	2.6783	0.33
2009	3	2	36.8878	-104.8621	4.1396	1.8798	1.5
2009	3	3	36.7247	-104.956	9.3012	1.2546	2.26
2009	3	3	36.8767	-104.8697	4.4708	2.4254	2.16
2009	3	3	36.8807	-104.8691	5.5686	2.6283	1.35
2009	3	4	36.8777	-104.8691	4.2242	1.9286	1.21
2009	3	4	36.8743	-104.8714	8.1944	1.0065	2.39

2009	3	4	36.8752	-104.8717	4.2309	2.113	1.54
2009	3	4	36.8724	-104.8711	4.848	2.0048	0.99
2009	3	4	36.874	-104.8661	7.754	3.0778	1.19
2009	3	4	36.8768	-104.873	4.8535	1.763	1.99
2009	3	4	36.8928	-104.8724	4.0379	1.4682	1.63
2009	3	4	36.8766	-104.8719	7.5494	1.7555	1.57
2009	3	4	36.8754	-104.8708	4.2883	2.0205	1.3
2009	3	5	36.9015	-104.8761	5.7333	2.8472	1.29
2009	3	5	36.8978	-104.8637	6.6393	3.7637	1.4
2009	3	5	36.8722	-104.8714	5.4049	2.5766	1.27
2009	3	5	36.8893	-104.8752	6.0598	2.8758	1.91
2009	3	5	36.8919	-104.8757	4.0184	1.7454	1.51
2009	3	5	36.8942	-104.8719	6.1296	3.2494	1.34
2009	3	6	36.8502	-104.8584	4.9929	2.4896	1.5
2009	3	6	36.8876	-104.8777	4.8938	1.8106	2.81
2009	3	6	36.8907	-104.8788	5.3582	2.696	1.17
2009	3	6	36.8953	-104.8761	4.6755	2.1052	1.95
2009	3	6	36.8952	-104.874	4.8722	2.2637	1.5
2009	3	7	36.9282	-104.8611	11.6452	2.4193	1.28
2009	3	8	37.2409	-105.0409	6.5075	1.7587	1.08
2009	3	8	37.2381	-105.0417	8.8963	0.9828	1.31
2009	3	8	36.8825	-104.8414	5.1361	2.4494	1.55
2009	3	8	37.24	-105.0424	5.1645	2.4209	0.86
2009	3	8	36.8689	-104.8593	3.3288	1.6676	0.97
2009	3	8	37.2377	-105.0413	5.9762	2.047	1.76
2009	3	9	36.8891	-104.8752	7.224	2.5501	0.99
2009	3	10	36.869	-104.863	3.1196	1.6139	1.35
2009	3	10	36.823	-104.8578	6.8806	3.1038	1.33
2009	3	10	36.8195	-104.8609	11.8803	2.4709	1.07
2009	3	10	36.8623	-104.8472	4.5172	1.9754	1.66
2009	3	11	36.8721	-104.8636	5.1357	2.6105	-999
2009	3	11	36.8968	-104.8641	4.3457	2.1501	0.46
2009	3	11	37.0437	-105.0228	2.9591	0.4654	1.44
2009	3	11	36.8908	-104.8791	7.6104	2.7171	1.6
2009	3	12	36.9805	-104.9685	1.8173	1.3051	2
2009	3	12	37.1095	-104.9786	4.2838	0.7291	1.29
2009	3	13	37.2381	-105.0402	8.618	1.4484	1.18
2009	3	13	36.8772	-104.866	4.8735	2.4727	1.48
2009	3	13	37.2401	-105.0388	4.8362	2.5455	0.61
2009	3	14	36.8944	-104.8764	3.7842	1.5323	1.21

2009	3	14	36.8946	-104.8756	5.4859	2.1913	0.78
2009	3	14	36.8987	-104.8552	4.3875	1.6868	1.67
2009	3	14	37.1512	-104.9084	8.1296	1.8353	0.35
2009	3	14	36.8774	-104.8671	4.5656	2.3886	0.76
2009	3	14	37.0432	-104.968	2.2515	1.1064	1.62
2009	3	15	36.8648	-104.863	4.827	2.2059	0.89
2009	3	15	36.8959	-104.8781	4.1525	1.7741	1.32
2009	3	15	36.8924	-104.8778	4.8928	1.7373	2.87
2009	3	15	36.897	-104.8749	6.1115	2.2762	1.24
2009	3	15	36.8913	-104.8755	3.4354	1.3094	1.93
2009	3	15	36.8938	-104.8735	7.4278	2.8215	0.59
2009	3	15	36.8934	-104.875	5.4158	1.5732	1.91
2009	3	16	36.9695	-104.8725	4.7547	1.9478	0.83
2009	3	16	36.873	-104.8644	4.1852	1.9936	1.3
2009	3	16	36.8964	-104.8724	3.8382	1.7101	1.52
2009	3	16	36.967	-104.876	6.2427	2.1461	0.78
2009	3	16	36.8915	-104.8784	3.5205	1.2679	2.97
2009	3	17	36.8793	-104.8692	3.2125	1.72	1.07
2009	3	17	36.8775	-104.8642	2.9713	1.4371	1.51
2009	3	17	36.8779	-104.8647	5.2142	2.8099	1.21
2009	3	17	36.8788	-104.8633	5.2997	2.4601	1.35
2009	3	17	36.893	-104.8746	5.2048	2.3133	1.46
2009	3	17	36.9752	-104.8766	7.349	3.4378	0.95
2009	3	17	36.8549	-104.8736	4.6333	2.1052	1.2
2009	3	17	36.8938	-104.8777	4.4994	1.9299	1.09
2009	3	18	36.8722	-104.8662	4.6828	1.9316	1.2
2009	3	19	36.9685	-104.8747	6.046	2.3423	1.36
2009	3	19	36.8893	-104.8539	5.9952	2.7824	1
2009	3	19	37.3799	-104.8416	7.3186	2.7532	0.75
2009	3	19	37.3797	-104.841	7.5502	2.1425	1.94
2009	3	19	37.3821	-104.84	8.8665	1.2892	-999
2009	3	19	37.5938	-104.9273	7.2156	3.3018	0.76
2009	3	20	36.7252	-104.957	6.2283	2.35	1.35
2009	3	20	37.4215	-104.8363	6.7431	2.9138	0.68
2009	3	20	37.3158	-104.7883	5.9095	2.7241	0.83
2009	3	21	37.3166	-104.7866	5.4491	2.7787	1.07
2009	3	21	37.3144	-104.7885	10.1359	1.1637	1.05
2009	3	21	36.8958	-104.8811	5.0983	2.4425	0.44
2009	3	21	37.3148	-104.7893	8.1759	2.1487	1.23
2009	3	21	36.8946	-104.879	4.293	1.8266	1.22

2009	3	21	37.3132	-104.7875	6.444	2.7033	1.57
2009	3	22	37.3146	-104.7892	10.2615	0.5736	2.95
2009	3	22	36.8788	-104.8706	4.4775	2.2022	1.54
2009	3	22	36.8808	-104.8646	4.6481	2.2919	0.99
2009	3	22	36.8748	-104.8631	5.4225	2.5257	1.59
2009	3	22	36.8759	-104.861	5.1876	2.7277	1.21
2009	3	23	37.1718	-104.8115	7.9173	1.696	1.39
2009	3	23	37.3188	-104.7884	5.106	2.6005	1.05
2009	3	24	36.8879	-104.8704	4.1117	1.7006	1.73
2009	3	24	36.8889	-104.8702	5.0981	2.0528	1.5
2009	3	24	36.8906	-104.8686	5.5536	2.7476	1.69
2009	3	24	36.8877	-104.8694	5.0151	2.194	1.31
2009	3	24	36.8893	-104.8695	5.1408	2.5644	1.2
2009	3	24	36.8882	-104.8689	4.6932	2.1831	1.4
2009	3	24	36.888	-104.8722	2.681	1.3599	2.4
2009	3	24	37.3148	-104.7876	7.4973	2.5114	0.82
2009	3	24	36.8871	-104.8693	4.3141	2.0016	1.04
2009	3	24	36.8905	-104.868	3.9019	1.9596	1.16
2009	3	25	37.3129	-104.7886	5.2819	2.1804	1.39
2009	3	25	36.8885	-104.866	6.0219	2.3795	0.93
2009	3	25	36.8821	-104.8591	5.0389	2.7457	1.07
2009	3	25	36.9583	-104.8708	9.5183	0.944	1.54
2009	3	25	36.8925	-104.8747	5.3505	2.2733	1.7
2009	3	26	37.2404	-105.0399	5.2276	1.9824	2.27
2009	3	26	37.2405	-105.0385	6.8167	1.491	1.04
2009	3	26	37.2415	-105.0398	7.216	1.9199	1.6
2009	3	26	36.8977	-104.8454	8.7351	4.8541	1.06
2009	3	26	36.8844	-104.8709	6.0268	2.9094	1.14
2009	3	27	37.2417	-105.035	7.6551	1.2442	1.76
2009	3	28	36.8909	-104.8726	4.8666	2.2442	0.95
2009	3	28	36.8837	-104.8648	3.9444	1.9565	1.11
2009	3	28	36.8849	-104.8651	3.6875	1.6867	0.94
2009	3	29	36.8894	-104.8743	4.9798	2.0179	1.16
2009	3	29	37.0364	-104.9814	3.2811	0.4791	0.93
2009	3	31	36.8138	-104.8661	7.4201	4.02	1.42
2009	3	31	37.2404	-105.0412	7.6615	1.5035	1.38
2009	3	6	36.8989	-104.8743	4.605	2.5573	1.01
2009	4	1	36.8969	-104.881	5.9667	2.8237	1.02
2009	4	2	36.8965	-104.8627	3.9113	1.5686	1.46
2009	4	6	37.3141	-104.7877	6.9943	2.3777	1.4

2009	4	6	36.8674	-104.8532	4.4933	3.0487	0.77
2009	4	7	36.8745	-104.8493	4.102	2.1056	1.3
2009	4	7	36.9886	-104.9756	3.2746	1.3983	1.82
2009	4	7	37.0041	-104.9619	5.3101	1.7475	0.43
2009	4	7	36.865	-104.8721	6.8978	2.0411	1.75
2009	4	7	36.8657	-104.8728	4.0755	1.7852	1.03
2009	4	7	37.4864	-104.713	7.9943	3.0526	1.35
2009	4	7	37.1935	-104.7166	3.636	1.6556	0.7
2009	4	8	36.8953	-104.8738	6.0141	2.5548	0.14
2009	4	9	37.194	-104.7163	3.0455	1.3877	0.98
2009	4	9	36.8805	-104.8397	4.0641	1.8661	1.84
2009	4	9	36.8766	-104.8778	3.8627	1.741	1.11
2009	4	9	36.8798	-104.8779	2.8547	1.2205	1.04
2009	4	10	36.8791	-104.867	5.4648	2.5475	-999
2009	4	10	36.8773	-104.8793	4.8943	2.2884	0.44
2009	4	10	36.8406	-104.8564	5.6649	2.6765	0.72
2009	4	10	36.8391	-104.8556	4.6174	2.4494	0.79
2009	4	10	36.8389	-104.8577	7.1627	2.9104	0.88
2009	4	10	36.8399	-104.8582	4.7052	1.7309	1.91
2009	4	10	36.8404	-104.8567	7.6095	3.4724	1.3
2009	4	10	36.8402	-104.858	6.2492	2.6351	0.99
2009	4	10	36.836	-104.858	5.4791	2.7075	0.91
2009	4	10	36.8367	-104.8582	6.6433	2.9627	0.54
2009	4	10	36.8365	-104.8557	5.1378	3.0336	0.87
2009	4	11	36.8422	-104.8594	4.3721	1.8891	2.24
2009	4	11	36.8413	-104.8566	4.4609	2.1399	1.66
2009	4	13	36.8391	-104.8543	6.3414	2.1489	1.71
2009	4	13	36.8381	-104.8573	6.2982	2.9823	0.75
2009	4	14	36.8775	-104.8722	5.4251	2.4659	1.03
2009	4	15	37.0006	-104.9605	3.295	2.0051	1.57
2009	4	15	36.896	-104.8745	4.9408	2.451	1.21
2009	4	15	36.8766	-104.8706	7.6027	2.2402	2.26
2009	4	15	36.8735	-104.8694	6.2409	1.9924	3.59
2009	4	15	36.8782	-104.8728	2.7116	1.3333	1.64
2009	4	15	36.8701	-104.8706	5.7249	2.8324	1.59
2009	4	15	36.878	-104.8709	5.8028	2.8968	1.41
2009	4	15	36.8849	-104.8504	4.5917	2.0303	1.72
2009	4	15	36.8776	-104.8723	4.1037	2.1261	1.59
2009	4	16	36.8734	-104.8715	4.6431	2.3855	0.94
2009	4	16	36.9688	-104.8641	5.8133	2.8812	1.06

2009	4	16	36.8738	-104.8731	4.5114	2.5375	-999
2009	4	16	36.8818	-104.8837	4.9594	3.151	1.11
2009	4	16	36.8738	-104.8652	7.9048	3.4679	1.17
2009	4	17	36.8795	-104.8452	5.8176	2.7744	-999
2009	4	18	36.886	-104.8668	3.6984	1.6997	0.83
2009	4	18	36.8782	-104.8694	4.0498	2.2309	1.86
2009	4	18	36.8868	-104.8641	4.7037	2.4493	1.1
2009	4	18	37.2311	-104.7356	5.4068	2.1927	1.07
2009	4	18	37.0157	-104.978	1.3102	0.5335	1.63
2009	4	19	37.2331	-104.7288	8.4323	1.8079	0.65
2009	4	19	37.5912	-104.6205	10.6886	0.6932	1.58
2009	4	20	37.0284	-104.9854	4.418	1.1582	0.81
2009	4	20	37.5934	-104.6199	11.7901	0.4754	2.24
2009	4	20	36.9629	-104.8654	8.2303	3.5893	0.05
2009	4	20	36.8781	-104.8695	3.8382	1.7141	1.03
2009	4	21	36.9831	-104.9721	1.3417	0.8198	2.03
2009	4	21	36.9838	-104.9776	3.5847	1.7181	1.36
2009	4	21	36.8526	-104.8719	3.5128	1.752	0.86
2009	4	21	36.8853	-104.8486	5.1772	2.3877	0.7
2009	4	22	36.8849	-104.848	4.8979	2.4495	-999
2009	4	23	36.8687	-104.856	5.4182	2.8789	1.04
2009	4	23	36.8506	-104.8736	5.0063	2.0753	1.56
2009	4	23	36.8501	-104.8692	6.3655	2.6988	1.2
2009	4	23	36.8723	-104.875	5.8856	3.0657	-999
2009	4	24	37.2751	-104.735	5.0039	1.9415	1.21
2009	4	24	36.8728	-104.8724	6.0518	3.078	-999
2009	4	25	36.9612	-104.8756	5.5244	2.0548	1.25
2009	4	28	36.816	-104.8617	7.456	2.7937	1.21
2009	4	28	36.8184	-104.8545	6.6858	3.2454	1.16
2009	4	28	36.8804	-104.8444	6.6063	2.5897	1.1
2009	4	28	36.8801	-104.8445	8.7871	2.4236	1.39
2009	4	29	36.789	-105.0401	6.9899	3.3711	1.7
2009	4	29	36.8767	-104.835	7.6389	3.055	0.82
2009	4	29	36.8908	-104.8806	4.3137	1.8973	1.04
2009	4	30	36.8792	-104.8441	5.2402	2.2103	2.12
2009	4	30	36.7896	-105.0373	7.0509	3.0829	1.81
2009	5	1	36.8766	-104.8708	6.2385	2.9639	1
2009	5	1	36.8746	-104.8709	4.6167	1.9406	1.04
2009	5	1	36.849	-104.7852	8.3356	2.3199	3.34
2009	5	1	36.871	-104.8713	5.7172	2.5463	1.05

2009	5	1	36.8737	-104.872	5.8513	2.2264	1.3
2009	5	1	36.876	-104.8701	4.8531	2.086	0.96
2009	5	1	36.8799	-104.8422	11.4831	1.8582	2
2009	5	1	36.8778	-104.843	6.3514	1.764	1.62
2009	5	1	36.8743	-104.8709	4.7215	2.1358	0.81
2009	5	1	36.9016	-104.8634	6.4656	2.8866	1.2
2009	5	2	36.816	-104.8551	9.6059	3.7593	1
2009	5	2	36.8794	-104.8465	5.2086	2.2693	1.01
2009	5	3	36.8755	-104.8701	4.1926	1.7962	0.06
2009	5	3	36.9606	-104.867	8.8061	1.5268	1.37
2009	5	3	36.9596	-104.8648	6.1108	1.8814	1.33
2009	5	4	36.8793	-104.8446	5.2426	2.3435	1.33
2009	5	4	36.8811	-104.8453	7.791	2.7872	1.5
2009	5	4	36.8813	-104.847	8.1383	3.1053	0.9
2009	5	4	36.8797	-104.8451	4.8336	1.894	1.46
2009	5	4	36.8798	-104.8476	8.2827	3.05	1.21
2009	5	4	36.8986	-104.8768	4.3674	2.2553	1.09
2009	5	4	36.8839	-104.8756	3.0162	1.4563	1.72
2009	5	4	36.885	-104.8771	4.1929	1.984	0.69
2009	5	4	36.8809	-104.8531	5.4074	2.5392	1.21
2009	5	4	36.8817	-104.8497	4.8811	2.3331	1.05
2009	5	4	36.8812	-104.8464	6.7762	2.7642	1.3
2009	5	5	36.8251	-104.8638	6.5713	3.0447	0.92
2009	5	5	36.8233	-104.8617	9.7844	3.0804	0.57
2009	5	6	36.8823	-104.8492	3.2005	1.5649	1.66
2009	5	7	36.8881	-104.8655	12.5703	4.9121	0.5
2009	5	7	36.8799	-104.8502	5.8597	2.714	1.42
2009	5	8	36.8923	-104.8777	4.4417	2.3807	1.03
2009	5	9	36.8939	-104.864	14.6411	1.7103	1.09
2009	5	10	36.959	-104.8579	11.8272	3.6341	1.01
2009	5	10	36.89	-104.8775	5.8481	2.6812	0.76
2009	5	11	36.8752	-104.8697	6.8548	3.1764	0.93
2009	5	13	36.8522	-104.871	7.548	2.3262	1.14
2009	5	13	36.9097	-104.8695	4.2982	1.8449	1.36
2009	5	16	36.8525	-104.8721	6.1974	1.7882	1.68
2009	5	16	36.8706	-104.8654	4.4626	2.3423	1.02
2009	5	17	36.9599	-104.8654	6.1861	3.2589	0.84
2009	5	17	36.8937	-104.875	5.718	2.7905	0.95
2009	5	18	36.8798	-104.8723	4.1489	2.2419	1.2
2009	5	18	37.0046	-104.9696	5.8947	3.2317	1.46

2009	5	19	36.8785	-104.8702	5.0903	3.0568	0.82
2009	5	20	36.8503	-104.856	5.6154	2.7831	1.17
2009	5	20	36.8823	-104.8413	8.5261	4.7017	0.73
2009	5	20	36.8778	-104.8338	9.6235	2.8062	1.09
2009	5	22	36.8529	-104.8731	4.6615	2.0985	1.45
2009	5	22	36.8495	-105.0232	5.1144	2.8693	0.99
2009	5	23	36.8534	-104.8728	7.56	0.8278	1.83
2009	5	24	37.2964	-104.7701	8.8152	1.8888	1.17
2009	5	25	36.9477	-104.8728	6.3086	2.2612	1.31
2009	5	26	37.6891	-104.6493	2.9387	1.6691	0.96
2009	5	28	37.0184	-104.9822	4.1472	1.0145	1.8
2009	5	29	36.8451	-104.8513	7.3148	1.6954	2.75
2009	5	30	36.8869	-104.8724	9.2106	1.6916	1.59
2009	5	30	36.8926	-104.8584	4.5506	2.3381	0.89
2009	5	31	36.8612	-104.8419	6.8604	2.3754	1.35
2009	5	31	36.8717	-104.8701	4.191	2.0237	0.68
2009	5	31	36.8713	-104.8671	8.9004	3.6066	0.95
2009	6	3	36.8695	-104.8425	8.4162	2.5795	1.14
2009	6	3	36.884	-104.8718	6.9228	2.8192	1.05
2009	6	3	36.8966	-104.8542	5.6678	2.4868	1.32
2009	6	5	36.8523	-104.8758	5.138	2.4819	1.21
2009	6	5	36.8235	-104.8507	6.459	3.2005	1.39
2009	6	6	36.85	-104.8718	5.7999	2.8818	1.45
2009	6	6	36.8231	-104.8529	9.15	4.2598	1.19
2009	6	7	36.8978	-104.8535	4.3632	2.4145	1.33
2009	6	7	36.8815	-104.8398	6.6611	2.7028	1.24
2009	6	9	36.8876	-104.8652	3.2125	1.7443	1.28
2009	6	10	36.8188	-104.8631	5.6288	2.6347	1.24
2009	6	10	36.8958	-104.8577	5.853	2.4013	0.98
2009	6	11	37.01	-104.995	14.3355	5.8337	1.2
2009	6	13	36.8142	-104.8589	6.4265	3.2131	1.37
2009	6	14	37.4806	-104.632	12.6001	0.6578	1.3
2009	6	14	36.8879	-104.8599	5.9199	3.3764	1.07
2009	6	15	37.3164	-104.7915	6.4549	2.2711	1.74
2009	6	15	36.9725	-104.8703	11.6315	6.7838	1.39
2009	6	15	36.8161	-104.8563	6.5761	3.4137	1.18
2009	6	16	36.8975	-104.858	4.8036	2.3588	1.22
2009	6	17	36.8962	-104.8515	4.0722	1.5556	2.24
2009	6	18	36.8807	-104.8397	3.9351	1.8775	1.4
2009	6	20	36.8495	-104.8718	6.9894	2.7526	1.59

2009	6	20	36.8476	-104.8677	6.1513	2.7519	1.17
2009	6	20	36.8483	-104.8694	6.2481	2.6937	1.18
2009	6	20	36.8498	-104.8731	5.0201	2.6462	1.25
2009	6	20	36.8484	-104.8699	5.5491	2.5917	1.29
2009	6	21	36.8789	-104.8353	5.3646	2.7705	0.97
2009	6	24	36.8688	-104.8726	5.5557	2.4707	1.4
2009	6	24	36.8685	-104.8709	6.2415	2.5319	1.38
2009	6	24	36.8692	-104.8726	7.6937	2.9527	1.16
2009	6	25	36.8684	-104.8722	5.7566	2.522	1.48
2009	6	25	36.9283	-104.8685	6.6606	3.2178	0.87
2009	6	25	36.8997	-104.8597	5.9866	3.8534	0.99
2009	6	26	36.9074	-104.8691	4.5219	2.2772	1.39
2009	6	26	36.9062	-104.8704	5.2483	2.2875	1.72
2009	6	26	36.9065	-104.8645	7.6693	3.5719	1.19
2009	6	27	36.9065	-104.8717	5.0332	2.3028	1.54
2009	6	27	36.909	-104.8735	5.2758	2.7248	1.71
2009	6	27	36.9073	-104.873	4.937	2.2121	1.79
2009	6	27	36.9106	-104.8714	5.357	2.4028	0.87
2009	6	27	36.9066	-104.8737	8.6743	0.7823	3.39
2009	6	27	36.9063	-104.874	4.7737	2.2306	0.92
2009	6	27	36.9054	-104.8691	5.1361	2.6623	-999
2009	6	27	36.9085	-104.8679	5.1853	2.7102	1.23
2009	6	27	36.9131	-104.8634	5.6681	2.9852	1.11
2009	6	27	36.9068	-104.8748	7.0532	3.3133	0.95
2009	6	27	36.9056	-104.8741	8.1376	1.0939	2.9
2009	6	27	36.9033	-104.8723	5.3974	2.2034	1.57
2009	6	27	36.9054	-104.8761	6.5103	2.8996	1.17
2009	6	27	36.9087	-104.8834	5.1216	2.6121	1.28
2009	6	27	36.9004	-104.8771	4.7332	2.2557	1.54
2009	6	27	36.9033	-104.8727	4.7332	2.2494	0.88
2009	6	27	36.8961	-104.8715	4.4998	2.3498	1.3
2009	6	28	36.9095	-104.8692	6.1814	2.2319	1.87
2009	6	28	36.8987	-104.8758	3.9239	2.0077	1.17
2009	6	28	36.9049	-104.8707	6.5546	3.3015	0.95
2009	6	28	36.9033	-104.8729	4.3381	2.0034	0.97
2009	6	28	36.9015	-104.8714	4.0535	2.2547	1.4
2009	6	28	36.9042	-104.875	4.5275	2.4474	1.06
2009	6	28	36.9008	-104.8729	3.6911	1.4034	1.79
2009	6	28	36.8982	-104.8695	4.6283	2.2636	1.7
2009	6	28	36.8945	-104.869	10.2835	4.669	1.41

2009	6	28	36.9063	-104.8726	5.0257	2.4623	1.81
2009	6	29	36.9009	-104.8716	7.5198	3.0771	0.97
2009	6	30	36.8978	-104.8688	5.7577	2.8266	1.28
2009	6	1	36.8978	-104.8544	4.5216	2.1443	2.05
2009	6	3	36.8817	-104.8441	7.4796	3.0282	-999
2009	7	2	36.8816	-104.8456	5.378	2.5175	1.15
2009	7	2	36.8818	-104.8458	6.7036	2.5641	1.4
2009	7	3	36.8827	-104.8434	6.091	3.26	1.35
2009	7	3	36.8798	-104.8438	5.2212	2.3964	1.12
2009	7	3	36.8829	-104.8471	7.2206	2.6468	1.77
2009	7	3	36.8911	-104.8377	7.2158	3.622	0.57
2009	7	3	36.882	-104.8465	4.5082	2.0611	2.08
2009	7	3	36.881	-104.8445	6.4066	2.5628	1.04
2009	7	4	37.0041	-104.9697	6.6968	3.4397	1.01
2009	7	5	36.8729	-104.8765	4.19	2.2454	0.99
2009	7	5	36.8831	-104.8457	7.3367	2.6454	1.44
2009	7	6	36.8617	-104.8736	6.9712	3.3393	1.15
2009	7	7	36.8664	-104.8506	5.276	2.6409	1.27
2009	7	8	36.8379	-104.8603	5.9518	2.0415	1.46
2009	7	8	36.884	-104.8565	6.3592	2.0812	1.58
2009	7	8	36.8743	-104.853	8.7961	2.7436	1.21
2009	7	9	37.0236	-104.976	5.0337	2.4769	1.7
2009	7	9	36.8219	-104.8512	8.6979	2.8674	1.51
2009	7	10	36.8211	-104.848	6.1044	3.3315	1.11
2009	7	10	36.8231	-104.8514	7.279	3.0317	1.53
2009	7	10	36.9632	-104.8674	8.4697	2.2784	1.29
2009	7	10	36.82	-104.849	9.2392	1.4477	1.75
2009	7	10	36.8199	-104.8521	6.3226	3.1117	1.36
2009	7	10	36.8241	-104.8505	8.0203	3.9573	1.05
2009	7	10	36.8229	-104.8484	3.8837	1.873	1.58
2009	7	10	36.823	-104.8512	7.418	3.5286	0.83
2009	7	10	36.8249	-104.851	8.0212	3.6194	1.22
2009	7	10	36.8968	-104.8585	6.5301	3.1769	1.09
2009	7	10	36.8803	-104.8434	5.9546	2.7456	1.34
2009	7	10	36.881	-104.8458	5.3792	2.6168	1.05
2009	7	12	36.8818	-104.8471	4.4218	2.0607	2.03
2009	7	12	36.8828	-104.8468	6.0619	2.8941	1.44
2009	7	15	37.2027	-104.7466	3.4821	1.5144	1.15
2009	7	15	37.2061	-104.7386	5.4247	2.2732	1.21
2008	8	8	36.9592	-104.8628	8.5978	3.345	1.13

2009	7	18	37.3745	-104.7885	4.989	2.531	0.62
2009	7	18	37.2045	-104.7411	3.7845	1.8612	1.18
2009	7	20	37.0401	-105.018	5.8178	2.8148	1.24
2009	7	22	37.3746	-104.7926	7.8979	1.5674	1.32
2009	7	23	37.0245	-105.0127	5.6002	3.0471	1.69
2009	7	23	36.8684	-104.85	11.0001	2.0437	1.4
2009	7	24	36.8862	-104.8658	6.0921	2.701	0.87
2009	7	26	37.2771	-104.6333	5.915	1.7788	1.46
2009	7	26	37.2776	-104.6336	3.9632	1.8852	0.93
2009	7	26	37.2976	-104.5961	6.6882	3.1975	0.53
2009	7	26	37.277	-104.631	6.1886	2.6301	0.43
2009	7	26	37.2777	-104.6309	3.8221	2.0159	1.02
2009	7	26	37.3776	-104.7877	6.8672	2.7311	0.45
2009	7	26	36.8781	-104.8706	4.2169	1.6631	1.68
2009	7	27	37.2765	-104.6335	5.8468	2.3497	0.58
2009	7	27	36.8779	-104.8713	5.9634	2.6189	1.31
2009	7	27	37.2787	-104.6282	6.6055	2.6031	0.72
2009	7	27	37.2861	-104.6185	5.0467	2.4508	1.04
2009	7	27	37.2763	-104.6328	3.9856	2.0282	1.24
2009	7	27	37.2794	-104.6331	4.1069	1.8402	1.47
2009	7	28	36.8403	-104.8476	6.8486	1.6319	2.14
2009	7	28	37.278	-104.627	4.4839	2.1626	0.54
2009	7	28	37.2758	-104.6307	5.5371	2.5333	0.49
2009	7	28	36.8401	-104.8417	5.6661	2.6251	0.85
2009	7	28	36.8403	-104.8461	5.385	2.6918	1.02
2009	7	28	36.8421	-104.8388	3.8746	3.0807	1.49
2009	7	28	36.8432	-104.8472	7.6778	1.1713	2.6
2009	7	28	36.8445	-104.8475	8.1217	0.8598	2.34
2009	7	28	36.8372	-104.8507	3.7453	1.9136	1.98
2009	7	28	36.8389	-104.8491	7.8188	1.2414	2.83
2009	7	28	36.8404	-104.8497	5.2446	2.5324	2.06
2009	7	28	36.8362	-104.8582	6.0823	3.0348	1.27
2008	8	8	36.8441	-105.0431	8.0699	4.0472	1.19
2009	7	29	36.8376	-104.85	4.0837	2.6787	1.79
2009	7	29	36.8421	-104.8532	6.6057	2.0793	1.59
2009	7	29	36.8387	-104.8519	7.8767	4.1403	1.18
2009	7	29	36.8357	-104.8494	7.6355	1.7092	1.9
2009	7	29	36.8365	-104.853	8.8701	0.5741	1.96
2009	7	29	36.8398	-104.8513	8.5351	0.7328	4.26
2009	7	29	36.823	-104.8014	4.0114	1.0248	4.19

2009	7	29	36.8407	-104.8542	4.0132	1.7667	2.1
2009	7	29	36.8317	-104.8552	5.0682	2.2311	1.55
2009	7	29	36.8418	-104.8571	6.9169	3.1038	1.48
2009	7	29	36.8509	-104.8489	6.407	3.3689	0.98
2009	7	29	36.848	-104.8461	9.4942	4.2577	1.1
2009	7	29	36.8444	-104.8525	4.9505	2.6957	1.36
2009	7	29	36.8039	-104.8007	9.7725	4.3594	1.44
2009	7	29	36.851	-104.855	5.4553	2.7751	1.52
2009	7	29	36.8437	-104.8455	5.4404	2.3737	1.96
2009	7	29	36.8292	-104.8581	10.279	4.7374	1.8
2009	7	29	36.8388	-104.8526	5.3375	3.1644	1.52
2009	7	29	36.8413	-104.8462	7.844	2.1737	1.89
2009	7	29	36.8403	-104.8598	5.5036	2.9982	1.49
2009	7	29	36.8386	-104.848	7.2086	1.8134	1.68
2009	7	29	36.8424	-104.852	4.1386	2.3102	1.28
2009	7	29	36.8458	-104.8416	7.7975	3.2301	1.11
2009	7	29	36.8408	-104.8514	8.632	0.585	3.22
2009	7	29	36.8376	-104.8514	7.3757	1.4236	2.16
2009	7	29	36.8344	-104.8523	11.3415	2.3461	1.21
2009	7	29	36.8339	-104.8418	6.7296	3.2006	1.05
2009	7	29	36.8285	-104.8569	3.8362	2.6316	1.91
2009	7	29	36.8523	-104.841	6.1149	2.905	1.51
2009	7	29	36.8332	-104.841	9.718	2.8058	1.39
2009	7	29	36.8359	-104.8536	2.093	1.7362	2.03
2009	7	30	36.8248	-104.8592	9.2116	1.6132	1.86
2009	7	30	36.8467	-104.847	6.8762	2.6603	1.65
2009	7	30	36.8293	-104.857	7.8779	0.9573	2.64
2009	7	30	36.8911	-104.8718	6.3088	2.605	1.51
2009	7	30	36.8387	-104.8509	8.822	1.7436	1.85
2009	7	30	36.8323	-104.8556	4.8464	1.996	1.4
2009	7	30	36.8294	-104.8518	10.0916	2.8304	1.6
2009	7	30	36.8528	-104.8426	7.2239	3.4009	0.94
2009	7	30	36.8342	-104.8549	7.0362	3.1304	2.58
2009	7	30	36.8327	-104.8521	8.5029	2.2351	1.49
2009	7	31	36.8244	-104.8572	7.4903	3.6251	1.5
2009	7	31	36.8502	-104.8511	5.2155	2.1064	1.81
2009	7	31	36.8325	-104.8579	6.1068	3.4221	1.14
2009	7	31	36.8367	-104.8463	9.0026	4.769	0.74
2009	7	31	36.8441	-104.8427	8.7627	2.2257	1.43
2009	7	31	37.2796	-104.6258	4.1359	1.9481	1.31

2009	7	31	36.8337	-104.8294	7.96	4.2755	1.41
2009	8	6	36.838	-104.8521	8.3165	0.8648	3.47
2009	8	1	36.8444	-104.8421	6.9888	2.5149	1.58
2009	8	1	36.8729	-104.866	7.7833	1.274	1.82
2009	8	1	36.8263	-104.8578	8.0886	2.2375	2.36
2009	8	1	36.8256	-104.8522	13.9312	5.1556	1.45
2009	8	1	36.829	-104.8613	7.9988	3.1036	1.35
2009	8	1	36.8291	-104.8519	8.9895	4.8709	1.03
2009	8	1	36.8295	-104.8662	11.6162	2.5589	1.09
2009	8	1	36.8572	-104.8681	5.6362	2.7247	1.27
2009	8	1	36.8455	-104.8402	7.3069	3.7052	1.06
2009	8	1	36.8234	-104.869	7.2897	3.2207	1.59
2009	8	1	36.8333	-104.8554	4.1085	2.1653	1.74
2009	8	2	36.8352	-104.8558	8.235	2.442	1.5
2009	8	2	36.8912	-104.8716	8.5695	5.0452	1.01
2009	8	2	36.8917	-104.8746	5.2602	2.6642	1.28
2009	8	2	36.8938	-104.8724	4.9234	2.7061	1.24
2009	8	2	36.8921	-104.874	4.3315	2.2111	1.18
2009	8	2	36.8936	-104.8748	5.2592	1.9494	1.75
2009	8	2	36.8924	-104.8697	8.6388	4.1907	0.45
2009	8	2	36.8224	-104.8578	4.9778	2.4942	1.29
2009	8	2	36.8527	-104.8673	6.1059	2.7041	1.38
2009	8	2	36.885	-104.8407	7.2451	2.441	1.11
2009	8	2	36.8547	-104.8692	4.6075	2.4233	1.02
2009	8	2	36.8815	-104.8388	5.3241	2.3128	1.01
2009	8	2	36.8619	-104.8454	4.9594	2.466	0.72
2009	8	3	36.8569	-104.87	4.1445	1.7574	1.01
2009	8	3	36.8549	-104.8723	4.7396	2.1248	1.19
2009	8	3	36.855	-104.8726	8.6038	0.5137	2.63
2009	8	3	36.8554	-104.8728	5.0751	2.1113	1.24
2009	8	3	36.8551	-104.8708	6.6685	1.941	1.35
2009	8	3	36.8554	-104.8706	6.367	3.2059	1.06
2009	8	3	36.8311	-104.8601	7.8935	1.7574	1.8
2009	8	3	36.8818	-104.8384	5.7262	1.6913	1.19
2009	8	3	36.8299	-104.85	11.9311	2.1031	1.32
2009	8	3	36.8604	-104.87	7.445	1.0477	3.11
2009	8	4	36.8602	-104.8729	7.0017	2.6427	1.04
2009	8	4	36.8582	-104.8718	8.0593	0.5681	2.47
2009	8	4	36.8615	-104.8726	6.288	2.4698	0.92
2009	8	4	36.8347	-104.866	7.0835	3.5231	0.76

2009	8	4	36.8434	-104.8458	4.834	2.4007	1.01
2009	8	5	36.8513	-104.8497	4.009	1.9297	0.74
2009	8	6	36.8344	-104.8539	5.6799	2.69	1.28
2009	8	6	36.8521	-104.853	11.4969	4.5543	0.83
2009	8	6	36.8427	-104.8527	5.5326	2.9403	2.69
2009	8	6	36.8454	-104.8479	6.6192	4.1234	1.24
2009	8	6	36.8456	-104.8527	3.8402	2.2984	1.62
2009	8	6	36.8489	-104.8531	3.1453	2.3176	1.46
2009	8	6	36.8473	-104.8514	4.0346	2.486	1.5
2009	8	6	36.8482	-104.852	4.1052	1.8357	1.5
2009	8	6	36.8461	-104.8541	3.9565	1.6467	2.15
2009	8	6	36.8516	-104.8361	6.5071	3.4581	1.29
2009	8	6	36.845	-104.8558	10.0393	1.8088	1.84
2009	8	6	36.8439	-104.8544	8.5811	0.7328	2.68
2009	8	6	36.862	-104.8588	6.1513	2.775	1.16
2009	8	6	36.8402	-104.8463	5.8815	3.1215	1.27
2009	8	6	36.8368	-104.8384	8.1052	4.2343	1.24
2009	8	7	36.8572	-104.84	6.3544	2.7622	1.5
2009	8	7	36.8555	-104.8423	7.6934	1.2623	2.03
2009	8	8	36.8267	-104.8547	5.1714	3.3098	1.51
2009	8	8	36.8411	-104.8549	4.1254	1.9532	1.29
2009	8	8	36.8449	-104.8474	6.1926	2.6147	1.29
2009	8	9	36.8538	-104.8402	8.0188	1.4042	1.69
2009	8	9	36.8343	-104.8555	4.5657	1.7856	1.69
2009	8	10	36.8541	-104.8418	6.0232	1.7743	1.83
2009	8	10	36.8229	-104.8616	8.8584	3.355	1.1
2009	8	10	36.8254	-104.8616	10.6444	3.1826	1.07
2009	8	10	36.8224	-104.856	3.7663	2.3275	1.74
2009	8	11	36.8341	-104.8557	5.3405	2.3866	1.14
2009	8	11	36.8263	-104.8561	6.0172	2.2082	1.81
2009	8	11	36.8925	-104.8694	6.8346	3.666	-999
2009	8	11	36.8961	-104.8746	5.9272	2.361	1.05
2009	8	11	36.8932	-104.8749	4.256	1.8553	1.69
2009	8	11	36.8975	-104.8766	4.8105	2.1574	0.35
2009	8	11	36.8428	-104.8513	5.6398	2.2959	1.7
2009	8	11	36.9014	-104.872	4.8372	2.2036	0.98
2009	8	11	36.8942	-104.877	6.0009	2.4661	1.32
2009	8	11	36.8892	-104.8747	3.4119	2.6041	1.97
2009	8	12	36.8964	-104.8783	6.3973	2.4235	1.09
2009	8	12	36.8346	-104.8565	4.7306	1.7941	1.88

2009	8	12	36.8328	-104.8561	10.1274	4.0023	0.85
2009	8	12	36.89	-104.8725	4.5263	1.9484	1.16
2009	8	13	36.8329	-104.8571	6.8297	2.4536	1.08
2009	8	14	36.8315	-104.8566	9.8001	2.2244	1.66
2009	8	14	36.8327	-104.8557	5.4329	1.971	1.82
2009	8	14	36.8531	-104.8398	7.2987	3.7579	1.18
2009	8	14	36.8313	-104.8611	5.7401	2.6753	1.13
2009	8	14	36.8232	-104.8569	6.2167	3.4127	1.03
2009	8	14	36.834	-104.8561	8.7813	0.7114	2.49
2009	8	14	36.8309	-104.8536	9.1825	2.729	1.31
2009	8	14	36.8361	-104.2245	33.3126	3.7885	1.07
2009	8	14	36.8336	-104.8576	5.5129	2.6294	1.34
2009	8	14	36.84	-104.8341	5.6804	2.9926	2.35
2009	8	14	36.8329	-104.8603	5.0855	2.8085	1.36
2009	8	15	36.8233	-104.8582	8.333	4.5425	1.27
2009	8	15	36.8297	-104.8597	6.1756	3.5552	1.61
2009	8	15	36.8343	-104.3706	39.6909	2.021	0.99
2009	8	15	36.8373	-104.8549	7.8703	2.8613	1.39
2009	8	15	36.8799	-104.8441	10.1201	1.7763	1.51
2009	8	15	36.88	-104.8468	4.9295	2.4812	1.27
2009	8	16	36.8249	-104.855	10.7558	3.3395	1.18
2009	8	16	36.8329	-104.8591	7.6687	1.1564	2.27
2009	8	16	36.8334	-104.8555	5.1059	2.6744	1.27
2009	8	16	37.24	-105.0417	6.5836	2.8704	1.53
2009	8	16	36.8814	-104.8678	6.1011	2.6815	1.35
2009	8	16	36.8825	-104.8663	5.5953	2.5743	1.42
2009	8	17	36.8832	-104.8725	5.4102	2.4654	1.26
2009	8	17	37.2236	-104.3915	2.4013	1.1099	1.47
2009	8	17	36.9607	-104.8801	6.2802	3.1907	1.4
2009	8	18	36.8298	-104.836	5.5918	3.33	1.06
2009	8	19	36.8602	-104.8712	7.5099	0.7415	2.14
2009	8	19	36.8796	-104.8713	6.5027	2.8831	0.93
2009	8	19	36.8323	-104.8454	6.2994	3.5978	1.35
2009	8	19	36.8888	-104.8614	8.5552	3.0264	1.37
2009	8	20	36.8511	-104.8388	8.0032	2.9413	1.3
2009	8	21	36.8826	-104.8384	7.1262	1.8652	1.62
2009	8	21	36.8844	-104.8407	5.0129	2.3701	1.51
2009	8	21	36.8846	-104.8397	6.3206	3.1617	1.15
2009	8	21	36.9809	-104.9769	9.9046	0.8285	2.86
2009	8	21	36.8902	-104.8737	6.2259	2.6946	1.17

2009	8	21	36.9571	-104.8631	8.2532	3.0893	1.16
2009	8	22	37.0144	-104.9773	8.2155	3.6039	0.98
2009	8	23	37.0054	-104.9729	4.4644	2.3704	1.54
2009	8	23	36.852	-104.8392	6.5826	2.6048	1.04
2009	8	24	36.8856	-104.8724	3.7157	1.7195	1.74
2009	8	24	36.8632	-104.8693	4.1234	1.6624	1.77
2009	8	25	36.8545	-104.8374	6.3601	2.8561	1.41
2009	8	26	37.0128	-104.9773	4.6664	1.8642	1.77
2009	8	27	36.8969	-104.8741	4.7465	2.3773	1.14
2009	8	27	36.8374	-104.846	4.3523	1.8594	1.53
2009	8	27	37.2788	-104.9609	4.8097	2.3783	1.86
2009	8	27	36.8502	-104.8582	3.6726	3.2054	1.22
2009	8	27	36.8564	-104.8419	7.7279	1.9902	2.38
2009	8	27	36.8548	-104.8459	6.1963	2.8928	1.25
2009	8	27	37.2814	-104.9566	5.4125	2.7959	1.91
2009	8	27	36.8559	-104.8411	7.3641	1.2269	2.76
2009	8	28	37.2805	-104.9507	6.6928	3.2706	2.64
2009	8	28	36.8286	-104.86	4.9914	2.3321	1.44
2009	8	28	37.0126	-104.984	7.2927	2.9039	1.79
2009	8	29	36.8526	-104.8415	5.166	2.2705	1.35
2009	8	29	37.0072	-104.9841	8.2672	3.8538	1.43
2009	8	29	36.8895	-104.8663	5.9968	3.1816	0.75
2009	8	29	37.0214	-104.9761	4.6852	2.4103	1.5
2009	8	30	36.9678	-104.8561	13.1843	5.9866	1.21
2009	8	30	36.8845	-104.8731	4.7207	2.5347	1.98
2009	8	30	36.8844	-104.8741	6.5089	3.0473	1.68
2009	8	30	36.8872	-104.8829	4.7291	2.5414	-999
2009	8	31	36.8983	-104.8673	5.714	2.5201	1.41
2009	8	31	36.8827	-104.846	5.0596	3.0383	1.49
2009	8	31	36.896	-104.8661	5.1666	2.6482	1.25
2009	8	31	36.8911	-104.8849	7.5477	3.8153	-999
2009	9	1	36.8996	-104.8624	5.8744	3.4526	-999
2009	9	1	36.9932	-104.9738	4.5204	2.4194	1.11
2009	9	2	37.0022	-104.9717	5.3471	3.243	1.23
2009	9	2	37.017	-104.9818	4.8383	2.7419	1.5
2009	9	4	36.8812	-104.8467	4.8046	2.3336	1.38
2009	9	4	36.8711	-104.8729	7.7003	3.3025	1.47
2009	9	4	36.8694	-104.8702	7.7379	4.2993	0.85
2009	9	4	36.8726	-104.8699	10.6254	3.8894	0.99
2009	9	4	36.8713	-104.8699	6.7201	2.8943	1.01

2009	9	4	36.8723	-104.8715	5.4353	2.2879	1.48
2009	9	7	37.3484	-104.6374	4.3832	2.136	1.15
2009	9	8	36.8811	-104.8674	5.6079	3.1271	0.94
2009	9	8	36.8811	-104.8693	5.2293	1.8737	1.7
2009	9	8	36.8801	-104.8711	5.9111	2.261	1.92
2009	9	8	36.8804	-104.8687	7.7365	1.0778	2.16
2009	9	8	36.8801	-104.8709	5.5068	1.283	-999
2009	9	8	36.8801	-104.8709	4.9693	1.7014	-999
2009	9	8	36.8738	-104.8603	8.4524	3.702	0.86
2009	9	8	36.8751	-104.8635	4.4253	2.3757	1.03
2009	9	8	36.8739	-104.8603	8.3553	3.6569	-999
2009	9	8	36.8751	-104.8634	4.4521	2.4071	-999
2009	9	8	36.8801	-104.8709	4.988	1.6992	1.79
2009	9	8	36.8795	-104.8693	5.4341	2.442	1.41
2009	9	8	36.88	-104.8699	5.3893	2.3807	1.22
2009	9	8	36.8803	-104.8694	4.8302	2.2496	1.13
2009	9	8	36.8811	-104.8711	8.4545	0.7222	2.79
2009	9	9	36.8893	-104.8778	6.1975	2.9312	1.1
2009	9	9	36.8875	-104.875	6.7213	3.2877	1.19
2009	9	9	36.8498	-104.8492	4.9437	2.7775	-999
2009	9	10	36.9753	-104.8714	5.8951	2.7639	1.45
2009	9	10	37.0015	-104.9798	4.7602	2.3635	1.47
2009	9	11	36.8813	-104.8685	6.1797	2.4618	1.44
2009	9	12	37.0089	-104.9753	5.4951	2.5053	1.21
2009	9	12	37.0176	-104.9767	6.7167	1.8281	2.17
2009	9	12	37.0169	-104.9765	8.061	1.5939	2.49
2009	9	12	37.0071	-104.979	5.472	2.776	1.26
2008	8	9	36.9664	-104.8704	11.0181	2.5264	1.51
2009	9	13	37.0432	-105.023	5.9176	2.8171	1.67
2009	9	15	36.8465	-104.8623	7.8033	2.5739	1.63
2009	9	15	36.8856	-104.8616	8.4662	0.4489	2.99
2009	9	15	36.8874	-104.8604	5.1832	1.8461	1.43
2009	9	15	36.8891	-104.8625	6.0554	2.5098	1.48
2009	9	16	36.9263	-104.8708	7.2787	3.4651	-999
2009	9	1	36.856	-104.8528	4.4907	2.7326	1.5
2009	9	11	37.0416	-105.0201	5.2919	2.6421	1.51
2009	9	16	36.8486	-104.8719	8.6323	0.7006	2.78
2009	9	16	36.8802	-104.8756	4.3346	2.7197	-999
2009	9	17	37.1956	-104.7582	6.7291	2.9074	1.38
2009	9	17	36.8468	-104.8715	8.4062	0.6678	1.79

2009	9	17	36.865	-104.8682	7.6328	2.9173	1.22
2009	9	19	36.8505	-104.8541	4.6821	2.4501	1.08
2009	9	19	37.029	-104.9744	1.1372	0.573	3.71
2009	9	19	37.0328	-104.9728	5.0528	3.239	1.62
2009	9	19	37.0292	-104.9774	6.0493	2.7005	1.18
2009	9	20	37.0341	-104.973	6.6822	3.9692	1.98
2009	9	21	36.8746	-104.8727	12.5707	4.6521	1.02
2009	9	21	36.8866	-104.8623	7.513	0.9215	2.1
2009	9	22	36.8703	-104.8691	4.277	1.7764	1.9
2009	9	23	37.024	-104.9705	5.7557	3.1002	1.2
2009	9	24	37.0238	-104.9802	4.7138	2.1504	1.69
2009	9	25	36.8808	-104.8434	8.2423	3.7136	0.96
2009	9	25	36.8603	-104.8569	7.3999	1.2093	1.96
2009	9	26	36.8812	-104.846	6.2444	2.4974	1.09
2009	9	26	36.9498	-104.872	6.3197	2.7661	1.07
2009	9	26	36.7296	-104.9611	12.9242	1.8507	1.33
2009	9	26	36.7321	-104.9647	12.9724	1.6529	1.29
2009	9	27	36.8488	-104.8584	6.2639	2.6925	1.28
2009	9	27	36.7315	-104.9596	12.5699	2.175	1.49
2009	9	27	36.8812	-104.8385	4.2768	1.8624	1.05
2009	9	28	36.8981	-104.8519	5.4737	2.9554	1.33
2009	9	28	36.8993	-104.8532	4.1094	2.1936	1.44
2009	9	28	36.881	-104.8684	6.5914	2.7819	1.32
2009	9	28	36.8819	-104.8703	5.1678	1.8804	1.99
2009	9	28	36.7345	-104.9629	7.5576	2.7463	1.71
2009	9	28	36.8797	-104.8673	3.674	1.6938	1.08
2009	9	28	36.7333	-104.9625	7.157	3.1966	1.56
2009	9	28	36.7313	-104.9633	10.7486	3.2236	1.18
2009	9	29	36.8837	-104.8726	9.9012	3.704	0.95
2009	9	29	36.8845	-104.8751	5.5205	2.701	1.27
2009	9	29	37.0299	-104.9738	10.12	0.6985	3.46
2009	9	29	37.2233	-104.3933	1.9927	1.0638	1.32
2009	9	29	37.0349	-104.9683	1.187	0.147	3.74
2009	9	29	37.0446	-104.9735	5.4768	2.925	2.22
2009	9	30	37.0433	-104.9738	6.5963	3.0353	1.94
2009	9	30	36.8851	-104.8393	4.6418	2.1935	1.6
2009	9	30	36.7328	-104.9662	9.6812	4.4166	1.53
2009	10	1	36.8317	-104.8607	4.6501	2.456	0.95
2009	10	2	36.8818	-104.8566	5.9903	2.8758	1.11
2009	10	2	36.8823	-104.8607	4.7565	2.1871	1.29

2009	10	2	36.9778	-104.9793	5.8078	3.7272	1.4
2009	10	3	36.8595	-104.8696	5.4592	1.7431	1.6
2009	10	3	36.8603	-104.8698	5.7197	2.7348	1.22
2009	10	3	37.0284	-104.9674	6.5368	3.2542	3.75
2009	10	3	37.0305	-104.9718	5.7726	3.0014	1.58
2009	10	4	36.802	-105.0251	6.0167	2.4107	2.54
2009	10	4	36.8853	-104.872	8.6555	0.8664	2.64
2009	10	4	36.8868	-104.8731	4.763	2.4087	1.58
2009	10	5	36.8434	-104.8678	9.0147	0.6728	2.48
2009	10	5	36.8443	-104.8663	4.8974	2.1813	1.63
2009	10	5	37.0477	-104.9724	6.2158	3.3901	1.68
2009	10	5	37.0161	-104.9776	7.0603	2.2722	2.38
2009	10	5	36.8445	-104.8659	5.4221	2.4973	1.78
2009	10	5	37.0151	-104.9768	5.6915	2.7963	1.25
2009	10	5	37.0315	-104.97	6.2912	3.1074	1.58
2009	10	5	37.0109	-104.9766	5.0764	2.6687	1.44
2009	10	6	36.7332	-104.9621	8.8285	3.2995	1.61
2009	10	7	36.8078	-105.0175	9.1904	3.8866	1.38
2009	10	7	37.0206	-104.9784	5.7243	2.8944	1.64
2009	10	7	37.0231	-104.9781	5.5004	2.8044	1.26
2009	10	7	37.0224	-104.9783	3.907	1.8427	1.6
2009	10	7	37.0239	-104.9782	4.8965	2.6629	0.99
2009	10	7	37.0233	-104.979	3.777	1.8636	1.69
2009	10	8	37.3702	-104.6154	5.7547	1.4987	2
2009	10	8	37.0235	-104.9785	5.7456	2.9714	-999
2009	10	8	36.884	-104.8761	6.2453	2.9569	1.15
2009	10	9	36.9834	-104.9723	9.2063	4.2072	1.13
2009	10	10	36.8849	-104.8562	5.7664	2.4565	1.45
2008	8	10	36.842	-104.8457	5.2533	2.4337	1.37
2009	10	11	36.8845	-104.8816	5.3893	2.5755	1.4
2009	10	11	36.8911	-104.8717	3.9748	2.0191	1.32
2009	10	11	36.9668	-104.8742	7.7667	3.4217	0.76
2009	10	12	36.926	-104.8676	4.864	2.311	-999
2009	10	12	37.0195	-104.9769	6.0535	2.4786	1.35
2009	10	13	36.8914	-104.8712	6.5528	2.3851	1.45
2009	10	15	36.734	-104.9675	9.0612	3.8985	1.25
2009	10	15	36.8796	-104.8758	7.1462	1.6287	2.12
2009	10	16	36.8898	-104.8598	6.1292	1.8864	1.86
2009	10	16	36.7349	-104.9621	8.3756	2.6772	1.73
2009	10	16	37.0388	-104.9748	4.7275	2.9493	2.38

2009	10	16	37.041	-104.9722	5.989	2.0344	2.68
2009	10	16	36.9883	-104.9725	5.5527	3.0168	1.48
2009	10	16	36.8329	-104.8528	8.8944	2.7467	1.68
2009	10	17	37.2263	-104.3847	2.2176	1.1117	1.14
2009	10	17	37.0123	-104.9782	4.7137	2.3474	1.19
2009	10	18	36.8327	-104.8503	6.9221	3.3189	1.26
2009	10	18	37.0178	-104.9962	30.8157	1.3307	-999
2009	10	19	37.0412	-104.9705	4.3912	2.2346	1.62
2009	10	19	36.8902	-104.855	7.0697	3.1758	1.32
2009	10	20	36.8298	-105.0593	6.7886	3.8443	1.36
2009	10	20	36.8315	-105.0613	6.234	3.2763	1.46
2009	10	20	36.8268	-105.0549	6.9299	3.185	1.22
2009	10	20	36.7292	-104.9624	9.6501	4.7059	1.25
2009	10	21	36.8596	-104.8534	7.2939	3.1313	1.02
2009	10	22	36.8599	-104.8577	4.2719	2.1521	1.57
2009	10	22	36.829	-105.0624	7.3988	2.595	1.9
2008	8	10	36.8881	-104.8631	5.4894	2.2992	1.36
2009	10	22	36.9028	-104.8666	4.6108	2.4119	1.22
2009	10	23	36.8066	-105.0203	7.9711	2.461	1.67
2009	10	25	36.8361	-105.0641	5.6063	3.468	1.53
2009	10	26	36.8302	-105.0646	6.3293	3.4339	1.61
2009	10	26	36.8269	-105.0627	5.7921	3.22	1.54
2009	10	26	36.8287	-105.0625	5.6049	2.7275	1.7
2009	10	27	36.8214	-104.8578	7.757	4.0608	1.41
2009	10	28	36.8828	-104.8394	6.3706	2.671	-999
2009	10	29	37.0205	-104.9793	5.2707	2.4881	1.32
2009	10	29	37.0254	-104.9784	5.5536	2.6309	1.5
2009	10	29	37.0259	-104.9781	4.4706	2.7043	1.46
2009	10	29	37.026	-104.9792	3.878	1.9558	1.55
2009	10	29	37.0255	-104.9785	9.6737	0.7879	2.72
2009	10	29	37.026	-104.9786	9.0914	1.5787	2.43
2009	10	29	37.0282	-104.9768	5.6753	3.0587	1.39
2009	10	29	37.0267	-104.9777	9.6827	0.835	2.72
2009	10	29	37.0421	-104.9813	5.5859	3.0527	-999
2009	10	29	37.0248	-104.9791	4.4391	2.2648	1.49
2009	10	29	36.8505	-104.8582	6.8879	1.626	1.79
2009	10	29	36.8705	-104.8604	7.6154	3.4867	0.85
2009	10	30	36.8243	-104.8567	10.3044	5.1819	1.27
2009	10	30	37.0662	-105.0413	5.7935	2.9557	1.44
2009	10	30	37.0255	-104.9786	4.2739	2.0525	1.44

2009	10	30	36.8864	-104.8418	9.2995	4.7241	-999
2009	10	30	36.8519	-105.0292	7.8979	4.5456	-999
2009	10	31	36.8467	-104.8533	5.7286	3.1891	1.21
2009	10	31	36.9581	-104.8631	10.8217	2.006	1.66
2009	10	31	36.959	-104.8623	9.7266	3.2936	1.35
2009	11	1	36.8782	-104.8713	6.0929	2.8862	1
2009	11	1	36.8515	-104.8692	4.712	2.1916	1.47
2009	11	1	36.8514	-104.8734	5.0991	2.1113	1.69
2009	11	1	36.8505	-104.8693	7.8629	3.1319	-999
2009	11	1	36.8524	-104.8691	9.2078	2.6568	1.11
2009	11	1	36.8515	-104.8701	7.9665	2.608	1.28
2009	11	1	36.8515	-104.8711	6.3032	2.6554	1.51
2009	11	1	36.8514	-104.8713	8.6912	2.9062	1.59
2009	11	1	36.8244	-104.8592	9.5256	2.7445	1.56
2009	11	1	36.8238	-104.8586	10.067	2.5919	1.41
2009	11	1	36.8245	-104.8576	7.5344	3.0612	1.65
2009	11	1	36.8225	-104.8587	6.5274	3.0485	1.5
2009	11	1	36.8248	-104.8588	7.7576	2.8236	1.63
2009	11	1	36.8515	-104.8723	7.6257	1.3706	2.19
2009	11	2	36.8223	-104.8608	5.0385	2.611	1.88
2009	11	2	36.9612	-104.8535	11.0605	6.2622	0.27
2009	11	2	37.2207	-104.9533	5.1328	2.9348	1.25
2009	11	2	36.851	-104.87	6.7013	3.6657	-999
2009	11	2	36.8525	-104.8714	6.3459	2.6369	-999
2009	11	2	36.8209	-104.8603	4.4735	2.3497	1.67
2009	11	3	36.8255	-104.8586	6.5243	3.8277	1.48
2009	11	3	36.8517	-104.8714	5.3049	2.3448	1.59
2009	11	3	36.7302	-104.9637	6.1008	3.1984	1.41
2009	11	3	36.958	-104.8517	12.8606	3.9917	0.74
2009	11	4	36.9561	-104.8597	9.5908	2.2251	1.61
2009	11	4	37.037	-104.9708	5.2082	2.4338	1.67
2009	11	4	36.9589	-104.863	6.6674	3.0653	-999
2009	11	4	37.223	-104.3852	5.3899	0.9439	1.54
2009	11	4	36.9382	-104.8734	8.5406	1.7374	3.27
2009	11	5	36.8764	-104.8741	5.2718	2.8885	1.53
2009	11	5	36.9763	-104.9773	4.0229	1.9166	1.81
2009	11	8	36.8923	-104.8592	5.5058	2.1364	1.52
2009	11	9	36.9577	-104.8587	4.0121	1.9743	1.85
2009	11	9	36.9572	-104.8559	6.9129	3.4515	-999
2009	11	9	36.8541	-104.8683	9.0002	2.529	1.76

2009	11	11	36.9551	-104.8543	11.757	2.4557	1.57
2009	11	11	36.9638	-104.8645	8.5407	4.2285	1.12
2009	11	11	36.854	-104.8714	5.4588	2.5489	1.44
2009	11	11	37.2445	-104.6666	3.2954	1.3185	1.42
2009	11	11	36.855	-104.8694	5.4349	2.6112	1.72
2009	11	14	37.0117	-104.9797	5.4028	2.5634	2
2009	11	14	36.8189	-104.8574	11.8026	4.5188	-999
2009	11	14	36.8265	-104.8672	6.9706	3.3779	1.25
2009	11	16	36.8337	-105.0629	9.4471	1.9975	2.69
2009	11	16	36.9473	-104.8771	8.8877	4.2463	1.19
2009	11	16	36.9004	-104.8661	6.4768	2.4869	1.28
2009	11	16	36.8433	-105.0717	10.4066	3.363	2.06
2009	11	17	36.8821	-104.84	7.8732	2.7643	-999
2009	11	17	37.23	-104.6316	4.1418	1.8452	1.52
2009	11	17	36.8879	-104.872	6.988	2.7881	1.62
2009	11	17	36.8859	-104.8707	6.8318	3.468	1.44
2009	11	17	36.8816	-104.8765	5.9532	3.2533	1.46
2009	11	18	37.0679	-105.0427	5.8493	2.7332	1.16
2009	11	19	36.8913	-104.8869	5.324	2.9455	-999
2009	11	19	36.8876	-104.8786	4.0246	2.3958	1.43
2009	11	19	36.8881	-104.8764	4.8981	2.419	1.28
2009	11	19	36.8943	-104.8814	4.9464	2.8615	0.87
2009	11	19	36.8031	-105.0209	9.44	1.1271	3.22
2009	11	19	36.8873	-104.88	5.7376	2.8478	1.36
2009	11	19	36.8003	-105.0244	7.9585	2.9252	1.91
2009	11	20	36.8559	-104.8685	7.5463	3.1223	-999
2009	11	20	36.9607	-104.8669	9.9002	3.3884	1.2
2009	11	20	36.979	-104.9767	4.8594	2.6288	1.11
2009	11	20	36.8081	-105.0225	6.8024	3.014	2.33
2009	11	20	36.8073	-105.0227	10.0466	0.9485	3.85
2009	11	21	36.8444	-104.8633	9.216	3.0886	1.39
2009	11	21	36.8883	-104.8737	5.4184	2.5733	1.18
2009	11	21	37.2247	-104.6637	4.7635	1.591	1.67
2009	11	21	37.2272	-104.6421	7.7416	4.0227	1.22
2009	11	21	37.2258	-104.6614	4.4497	1.7532	1.65
2009	11	21	37.2221	-104.6659	4.6666	2.0201	1.47
2009	11	21	37.2316	-104.6432	7.3373	3.7059	1.13
2009	11	22	37.224	-104.6593	4.9489	1.8896	1.54
2009	11	22	37.2229	-104.6647	9.5077	3.8195	2.22
2009	11	22	37.2254	-104.663	4.4701	1.7479	2

2009	11	22	37.2254	-104.6611	4.396	1.922	1.6
2009	11	22	36.9774	-104.9882	6.8964	5.695	1.65
2009	11	22	37.2238	-104.6668	4.3428	2.0839	0.81
2009	11	22	37.2244	-104.6632	3.8546	1.5625	1.72
2009	11	23	37.2256	-104.6552	5.9047	3.1827	0.9
2009	11	23	37.2338	-104.3723	21.7956	0.7343	0.29
2009	11	24	36.7982	-105.0309	9.6096	3.6016	1.41
2009	11	24	36.8832	-104.837	8.486	3.7705	0.82
2009	11	25	36.8888	-104.8441	7.028	3.0108	1.23
2009	11	25	37.0405	-104.9708	5.1338	2.42	1.57
2009	11	25	37.211	-104.4552	4.7063	1.0525	1.01
2009	11	25	36.8056	-105.0328	9.3038	5.1021	1.34
2009	11	25	36.8022	-105.0322	18.1148	4.0544	1.15
2009	11	26	37.2107	-104.4568	4.9324	0.5437	1.64
2009	11	27	36.8823	-104.8705	8.794	3.2356	-999
2009	11	28	37.3117	-104.9291	5.952	3.3905	0.67
2009	11	28	36.8067	-105.016	8.7106	2.6005	1.69
2009	11	28	36.8825	-104.8453	7.7275	3.381	1.3
2009	11	28	36.8775	-104.8436	6.5125	1.9998	2.39
2009	11	29	36.8786	-104.8428	5.2529	2.637	-999
2009	11	29	36.877	-104.8392	7.8791	3.7277	-999
2009	11	29	36.8778	-104.8433	6.5257	1.9601	2.19
2009	11	29	36.8808	-104.8441	6.8033	3.3251	1.29
2009	11	29	36.8763	-104.8376	7.5261	3.8149	-999
2009	11	29	36.8795	-104.8443	7.0976	2.653	1.56
2009	11	29	36.8764	-104.8678	4.2434	2.0157	1.33
2009	11	29	36.8762	-104.8759	5.9771	3.4802	1.45
2009	11	29	36.8832	-104.8713	4.6303	2.3469	1.61
2009	11	29	36.8795	-104.8651	5.0967	2.7738	-999
2009	11	29	36.878	-104.8663	4.5557	2.3003	1.8
2009	11	29	36.8813	-104.8663	5.3405	3.0422	1.28
2009	11	29	36.8783	-104.8684	5.2034	2.3639	1.78
2009	11	29	37.0397	-105.0143	7.0278	3.2047	1.3
2009	11	30	37.2977	-104.6351	5.3293	1.8713	2.07
2009	11	30	37.0109	-104.9722	7.8527	3.4711	1.54
2009	11	30	36.878	-104.8448	7.2816	2.3635	1.2
2009	11	30	36.8776	-104.8415	8.45	2.2102	1.49
2009	11	17	36.8813	-104.8404	7.778	2.9112	-999
2009	12	1	36.8169	-104.858	8.712	3.6387	1.25
2009	12	1	36.8851	-104.8585	6.7941	3.5131	1.91

2009	12	1	36.9499	-104.8587	5.6831	2.6441	1.49
2009	12	2	37.3066	-104.9345	5.6987	2.976	-999
2009	12	3	36.8658	-104.8704	4.9732	2.2855	1.7
2009	12	3	36.8773	-104.8684	4.0458	2.0112	1.93
2009	12	3	36.8783	-104.8445	7.4721	2.9291	1.27
2009	12	4	36.8783	-104.842	7.3568	2.873	1.58
2009	12	4	36.9328	-104.8698	8.9336	2.7316	1.99
2009	12	5	36.8791	-104.8447	5.6499	2.5429	1.39
2009	12	5	36.9989	-104.9714	4.883	2.4115	1.04
2009	12	6	36.8758	-104.8386	7.6593	3.1487	-999
2009	12	6	36.954	-104.8666	5.2658	2.7281	-999
2009	12	8	36.8826	-104.8396	7.2432	2.8674	1.4
2009	12	9	36.8919	-104.8726	4.7897	2.6685	1.3
2009	12	10	37.3036	-104.9363	7.0233	3.6565	-999
2009	12	10	36.8848	-104.8709	5.8245	2.9009	-999
2009	12	10	36.8717	-104.8708	4.7806	1.905	2.08
2009	12	10	36.8698	-104.8684	5.4287	2.6428	-999
2009	12	11	36.9548	-104.8513	10.8217	5.1106	-999
2009	12	11	36.8704	-104.8732	7.8726	1.7854	1.5
2009	12	11	37.3745	-104.6079	4.4487	2.244	0.97
2009	12	11	36.8701	-104.8708	9.2064	0.739	3.56
2009	12	11	36.8741	-104.8697	8.3181	3.6535	2.14
2009	12	11	36.8696	-104.8666	6.2303	2.8792	1.46
2009	12	11	36.8683	-104.8703	4.4197	2.0468	1.3
2009	12	12	36.8671	-104.8676	4.9289	2.3642	-999
2009	12	13	36.8911	-104.8759	4.4733	2.2264	1.51
2009	12	23	37.0252	-105.0836	7.8186	5.8515	-999
2010	1	5	37.7946	-105.4893	14.2281	1.2318	1.57
2009	5	19	37.7307	-105.3773	6.9134	1.3928	1.31
2009	9	1	37.5658	-105.2973	10.0737	1.4395	1.2

Table 8. Barnhart's relocated earthquakes for the 2011 earthquake swarm [*Barnhart et al*., 2014]

Date[b]	OT1	Lon1	Lat1	OT2	Lon2	Lat2	Z (km)
2011/5/9	28:52.8	−104.783	37.021	28:51.2	−104.76534	37.06877	3[d]
2011/5/11	06:15.3	−104.665	37.1	06:13.2	−104.76775	37.05136	3[d]
2011/8/22	30:18.1	−104.8114	36.9751	30:17.1	−104.77892	37.05834	3[d]
2011/8/23	48:50.3	−104.7238	36.9226	48:48.7	−104.76071	37.01174	3[d]
2011/8/23[c]	46:17.8	−104.8722	37.0394	46:15.4	−104.75298	37.03811	3[d]
2011/8/23	12:18.3	−104.715	37.1222	12:58.6	−104.71761	37.12538	3[d]
2011/8/23	56:57.6	−104.6608	37.0849	56:55.9	−104.73306	37.09641	3[d]
2011/8/23	01:33.5	−104.7282	37.1493	01:31.9	−104.73334	37.11427	3[d]
2011/8/23	17:59.1	−104.7098	37.1266	17:56.2	−104.73158	37.10547	3[d]
2011/8/23	34:39.7	−104.7693	37.1155	34:37.3	−104.73845	37.09292	3[d]
2011/8/23	32:17.1	−104.6852	37.1633	32:15.7	−104.72594	37.14349	3[d]
2011/8/23	37:57.1	−104.7984	37.0082	37:54.4	−104.77573	37.00424	3[d]
2011/8/23	29:27.9	−104.8184	36.9205	29:29.6	−104.74202	37.08241	3[d]
2011/8/23	03:50.4	−104.7569	37.1376	03:17.9	−104.76328	37.03284	3[d]
2011/8/23	11:12.9	−104.8015	36.9967	11:10.6	−104.76907	37.03746	3[d]
2011/8/24	40:43.2	−104.7672	37.0886	40:42.5	−104.76219	37.05419	5.95
2011/8/24	07:49.4	−104.7354	37.1224	07:48.8	−104.7338	37.08096	5.31
2011/8/24	15:52.6	−104.7192	37.1589	15:51.7	−104.73122	37.0794	4.42
2011/8/24	39:48.4	−104.7278	37.122	39:47.1	−104.72931	37.09176	5.72
2011/8/25	44:35.8	−104.7601	37.0966	44:35.6	−104.74323	37.08858	4.94
2011/8/25	34:33.8	−104.7764	37.0235	34:34.1	−104.74538	37.05739	5.65

[a]OT1, Lon1, and Lat1 indicate origin time, longitude, and latitude from the NEIC/Hydra location. OT2, Lon2, and Lat2 indicate origin time, longitude, and latitude of the relocated event.
[b]Dates are formatted as yy/mm/dd.
[c]The 2011 Trinidad earthquake main shock.
[d]Fixed values of depth. Relative position between locations for each event are shown in Figure 3b. All depths are relative to mean sea level. The surface elevation in the Raton Basin near the 2011 Trinidad epicenter is ~2.1 km above sea level.

Table 9. Magnitude 3.8 > Earthquakes in Raton Basin from 1973 – 2011 [*Rubinstein et al.,* 2014]

Date (yyyy/mm/dd)	Time (hh:mm:ss.ss)	Latitude (°)*	Longitude (°)	Depth (km)	Magnitude[†]
1973/09/23	03:58:54.5	37.178	−104.61	1.05	4.2
2001/09/04[‡]	12:45:52.1	37.162	−104.65	1.45	4.0
2001/09/05[‡]	10:52:07.5	37.152	−104.66	2.65	4.5
2003/09/13	15:22:47.9	37.139	−104.88	2.99	3.8
2004/03/22[§]	12:09:54.9	36.852	−104.96	5.43	4.4
2004/08/01[§]	06:50:44.8	36.865	−105.01	2.41	**4.3**
2005/08/10[‖]	22:08:14.6	36.963	−104.83	2.77	4.1
2005/08/10[‖]	22:08:20.9	36.946	−104.84	5.95	**5.0**
2007/01/03	14:34:37.17	37.009	−104.911	5.17	**4.4**
2009/07/29	10:00:35.7	36.843	−104.83	13.33	**4.1**
2010/01/18	08:41:06.6	36.886	−104.83	10.04	**3.8**
2011/05/11	19:06:12.6	37.123	−104.69	1.1	**3.8**
2011/08/22[#]	23:30:18.1	37.019	−104.77	3.5	**4.7**
2011/08/23[#]	05:46:17.8	37.054	−104.76	3.5	**5.3**
2011/08/23[#]	14:11:13.0	37.048	−104.76	3.5	**4.0**
2011/09/13[#]	05:24:37.26	36.880	−104.869	3.58	4.0
2011/09/16	14:51:50.0	36.880	−104.88	2.25	**3.9**

*2σ location uncertainties are ±15 km for all events except the earthquakes on 22 and 23 August 2011.

[†]Magnitude is the authoritative magnitude in ComCat. Moment magnitudes (**M**) are indicated with the magnitude printed in boldface type. The other magnitudes are a combination of amplitude based measures: M_b, M_{bLg}, and M_L.

[‡]Cluster of M ≥4 earthquakes in 2001. These earthquakes are located close in space and time, such that they cannot be considered to be independent in space and time. As such, they are counted as an individual earthquake sequence in the statistical calculations.

[§]Cluster of M ≥4 earthquakes in 2004.

[‖]Cluster of M ≥4 earthquakes in 2005.

[#]Cluster of M ≥4 earthquakes in 2011.

Table 10. Earthquakes located with Meremonte's array from September 7 – October 15th [*Meremonte et al.*, 2002].

Earthquakes divided into 5 time periods:

Stations PT0, PD0, TK0, BH0, DK0, CKD, TKD installed

1. September 7–17, 2001
10 events

Station BUR installed

Station RG0 installed

2. September 18–24, 2001
16 events

Station VZ0 installed

Station MAD installed

3. Sept 24–Oct 1, 2001
3 events

4. October 2–8, 2001
6 events

Station VAL installed

5. October 9–15, 2001
4 events

DATE			TIME			LATITUDE		LONGITUDE		DEPTH	PREF.	RMS	GAP	PHASES		MIN	Q
YR	MO	DY	HR	MN	SEC	DEG	MIN	DEG	MIN	KM	MAG	SEC.	DEG	P	S	DIS	
1	9	10	18	56	1.12	37	7.70N	104	42.01W	4.7	3.4mb	0.05	117	7	7	7	B
1	9	12	3	52	0.63	37	8.73N	104	41.15W	3.8	0.0	0.03	135	5	5	9	D
1	9	13	6	46	12.98	37	8.75N	104	41.14W	3.7	0.0	0.04	136	7	7	6	C
1	9	13	11	22	14.97	37	8.70N	104	41.16W	2.7	2.8mb	0.03	135	7	7	6	A
1	9	13	11	22	29.48	37	8.77N	104	41.12W	3.3	0.0	0.03	136	7	7	6	D
1	9	13	11	38	5.63	37	8.48N	104	41.79W	1.7	0.0	0.03	131	5	5	9	A
1	9	13	16	39	5.48	37	8.71N	104	41.53W	4.4	3.0mb	0.05	135	7	7	6	B
1	9	14	19	19	2.50	37	7.76N	104	42.36W	1.1	0.0	0.06	118	5	5	9	A
1	9	14	22	22	54.54	37	7.85N	104	41.76W	6.0	0.0	0.03	91	6	6	6	B
1	9	17	12	33	47.79	37	9.14N	104	40.87W	4.4	0.0	0.03	93	6	6	4	B
1	9	19	6	58	52.87	37	8.59N	104	41.23W	4.4	0.0	0.02	133	5	5	6	C
1	9	19	8	16	52.83	37	6.92N	104	42.94W	4.1	0.0	0.02	154	5	5	4	B
1	9	19	20	19	9.41	37	9.04N	104	40.93W	3.1	0.0	0.03	141	6	6	7	D
1	9	19	20	21	52.53	37	7.95N	104	41.52W	6.0	0.0	0.04	122	6	6	5	A
1	9	20	2	47	6.96	37	7.89N	104	41.60W	5.9	0.0	0.04	121	6	6	5	A
1	9	21	3	17	5.12	37	7.53N	104	42.04W	5.6	0.0	0.04	115	6	6	4	A
1	9	21	19	10	59.76	37	7.25N	104	42.36W	5.8	3.4mb	0.04	110	8	8	4	A
1	9	21	19	14	46.87	37	7.13N	104	42.49W	5.0	0.0	0.03	161	5	5	4	A
1	9	21	19	39	13.14	37	6.98N	104	42.54W	4.9	2.8mb	0.05	106	7	7	4	A
1	9	21	19	49	23.67	37	8.31N	104	41.57W	4.6	0.0	0.02	128	5	5	5	B
1	9	21	20	9	23.40	37	7.08N	104	42.38W	6.1	0.0	0.06	108	6	6	4	A
1	9	21	20	36	1.86	37	7.21N	104	42.44W	5.0	0.0	0.04	109	6	6	4	A
1	9	22	2	11	12.33	37	7.18N	104	42.31W	5.5	0.0	0.05	109	6	6	4	A
1	9	22	7	5	43.85	37	7.06N	104	42.28W	6.0	0.0	0.04	108	6	6	4	B
1	9	23	5	2	12.75	37	7.51N	104	42.74W	3.8	0.0	0.04	113	6	6	5	B
1	9	23	7	38	49.92	37	8.07N	104	41.97W	5.1	0.0	0.05	124	5	5	5	B
1	9	25	16	22	35.60	37	7.37N	104	42.26W	4.7	0.0	0.04	112	7	7	1	A
1	9	27	2	56	48.24	37	7.93N	104	42.23W	2.9	0.0	0.05	75	10	10	1	A
1	9	27	21	2	18.59	37	9.41N	104	40.39W	3.4	0.0	0.01	264	5	5	3	B
1	10	5	0	51	52.32	37	8.67N	104	41.46W	2.7	0.0	0.06	75	8	8	1	A
1	10	6	18	56	30.73	37	9.20N	104	40.85W	3.7	0.0	0.03	144	7	7	3	A
1	10	6	23	8	55.35	37	8.95N	104	41.01W	3.5	0.0	0.03	86	11	11	2	A
1	10	7	0	22	0.58	37	8.99N	104	40.91W	3.5	0.0	0.02	140	7	7	3	A
1	10	7	2	42	22.15	37	9.08N	104	40.96W	3.4	0.0	0.03	142	7	7	2	A
1	10	7	2	53	21.06	37	8.76N	104	41.27W	3.5	0.0	0.02	205	6	6	2	A
1	10	9	1	27	59.02	37	7.30N	104	42.94W	2.9	0.0	0.05	89	7	7	2	A
1	10	11	7	41	46.01	37	8.60N	104	41.73W	2.7	0.0	0.04	197	5	5	2	A
1	10	12	13	47	8.97	37	7.65N	104	41.87W	5.9	0.0	0.03	117	8	8	1	A
1	10	15	10	24	16.59	37	7.57N	104	41.84W	5.8	0.0	0.04	116	7	7	1	A

Table 11. Modeled Parameters for different formations [Bohlen, 2013, COGCC, 2016, Robertson, 1988]

Modeled Formation(s)	Lithology	POROSITY	XYZ PERM	Wet Heat Conductivity (W/m-°C)	Specific Heat (J/kg-°C)	Pore Compressibility (1/Pa)	Pore Expansivity (1/°C)
Pierre Shale	Shale	0.095	4.69E-18	1.2-3	777	1.00E-10	2.70E-05
Niobrara	Limestone	0.09	9.87E-17	2-3.4	1000	1.11E-10	2.40E-05
Benton	Shale	0.11	4.93E-16	1.2-3	777	1.00E-10	2.70E-05
Dakota-Dockum	Sandstone	0.1	1.25E-14	1.5-4.2	930	1.43E-09	3.00E-05
Sangre De Cristo	Sandstone	0.06	1.06E-15	1.5-4.2	930	1.43E-09	3.00E-05
Basement	Granite, Gneiss, Schist	0.016	1.58E-18	2.4-3.8	1000	2.00E-11	2.40E-05

Table 12. Sampled temperatures at the storage tanks on the disposal well sites (Hal Mccartney, personal comm.).

Well	Test Date	Temperature °C
1	12/14/00	11.6
1	1/31/04	15.5
1	5/18/05	19.9
2	8/14/01	28
2	8/23/01	28.4
3	10/29/01	24.4
4	10/1/02	17.9
4	2/28/06	11.3
5	1/31/04	16.1
6	8/11/10	26.6
7	2/15/11	13.1
8	4/2/14	16.9
8	4/2/14	14.7

Results

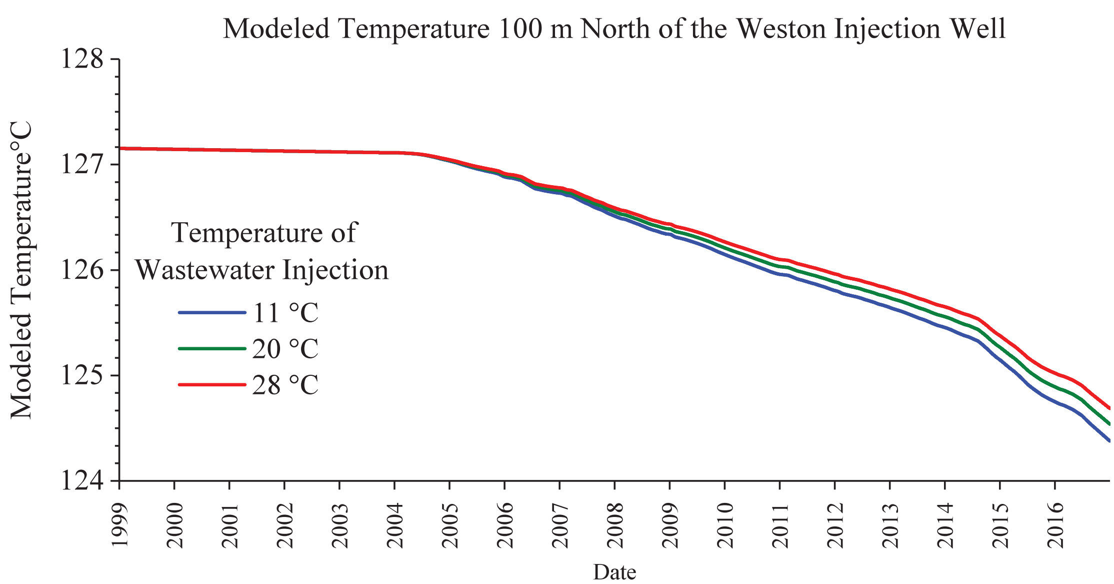

Figure 43. Sensitivity analysis for wastewater injection temperature for the Weston injection well

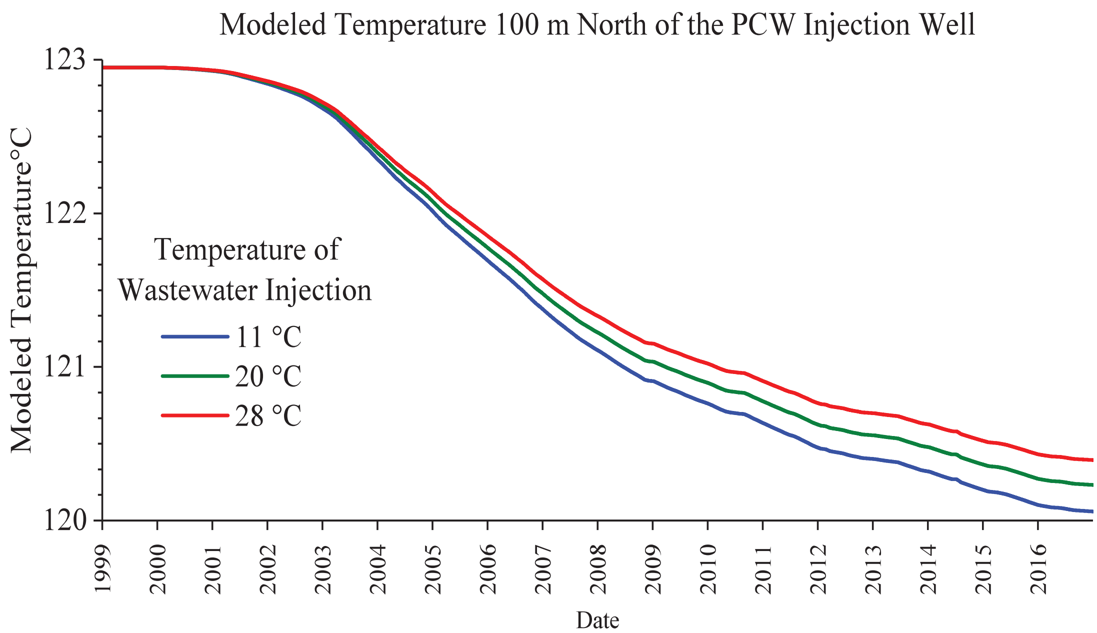

Figure 44. Sensitivity analysis for wastewater injection temperature for the PCW injection well

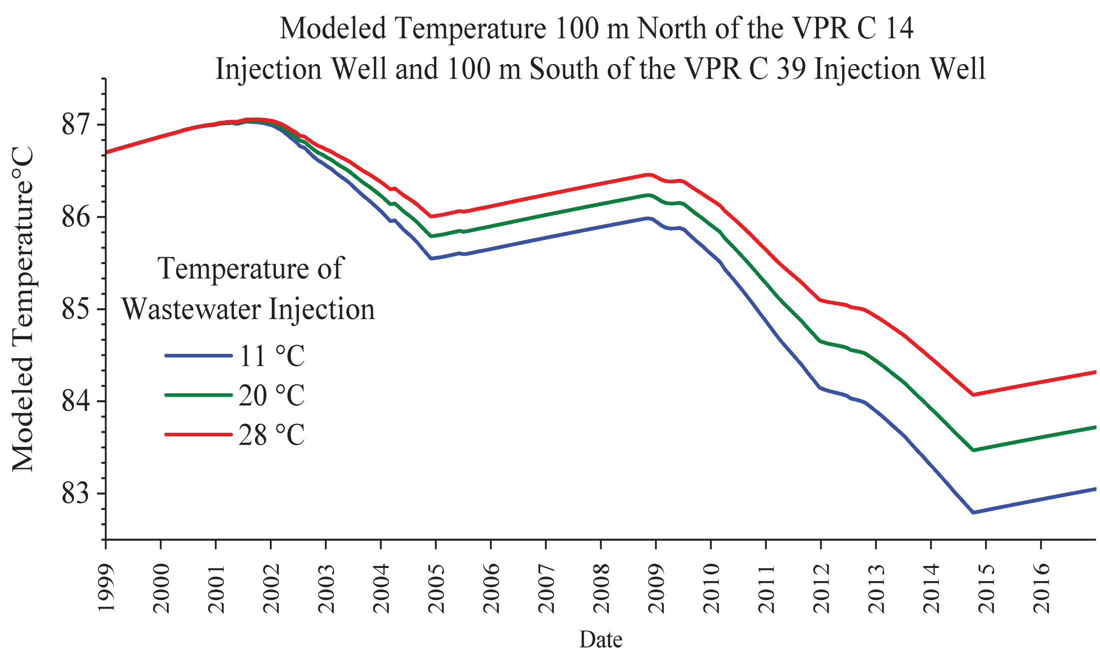

Figure 45. Sensitivity analysis for wastewater injection temperature for the VPR C 14 and 39 injection wells.